ISSN. 0377 - 2969
Vol. 49(3), September 2012

PROCEEDINGS
OF THE PAKISTAN ACADEMY OF SCIENCES

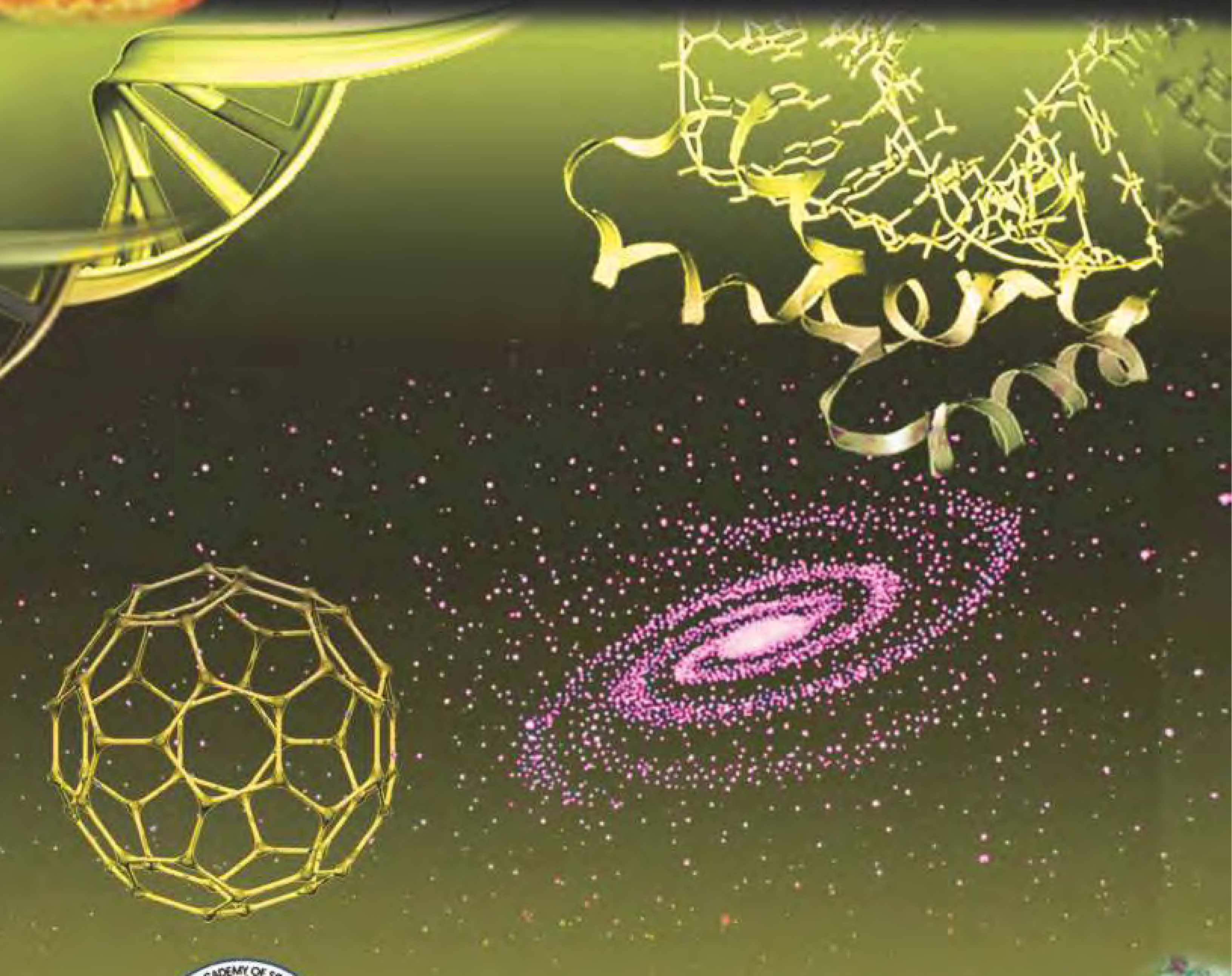

**Pakistan Academy of Sciences,
Islamabad, Pakistan**

PAKISTAN ACADEMY OF SCIENCES

Founded 1953

President:	Atta-ur-Rahman
Secretary General:	G.A. Miana
Treasurer:	Shahzad A. Mufti

Proceedings of the Pakistan Academy of Sciences, published since 1964, is quarterly journal of the Academy. It publishes original research papers and reviews in basic and applied sciences. All papers are peer reviewed. Authors are not required to be Fellows or Members of the Academy, or citizens of Pakistan.

Annual Subscription for 2012: Pakistan: Institutions, Rupees 2000/- ; Individuals, Rupees 1000/-
Other Countries: US$ 100.00 (includes air-lifted overseas delivery)

HEC Recognized, Category X; PM&DC Recognized

Published by **Pakistan Academy of Sciences**, 3 Constitution Avenue, G-5/2, Islamabad, Pakistan
Tel: 92-5 1-9207140 & 9215478; **Fax:** 92-51-9206770; **Website: www.paspk.org**

Printed at **PanGraphics (Pvt) Ltd.,** No. 1, I & T Centre, G-7/l, Islamabad, Pakistan
Tel: 92-51-2202272, 2202449 Fax: 92-51-2202450 E-mail: pangraph@isb.comsats.net.pk

Proceedings

OF THE PAKISTAN ACADEMY OF SCIENCES

CONTENTS

Volume 49, No. 3, September 2012 **Page**

Research Articles

Engineering Sciences

Green Processing of Coal to Liquid Fuels: Pakistan's Perspective 165
— *Zeeshan Nawaz, Naveed Ramzan, Saad Nawaz, Shahid Naveed and M. Bilal Khan*

Possibility of Control of Transition of Switching Arc Dc into Glowing 173
— *B. Miedzinski, G. Wisniewski, S.N. Kharin and H. Nouri*

Life Sciences

Taxonomic Study of Some *Cosmarium* Species from North-Eastern Areas of Pakistan 181
— *Waqar-ul-Haq, Zarina Ali, Masud-ul-Hasan and Mustafa Shameel*

A New Chewing Louse (Phthiraptera: Amblycera: Menoponidae) of *Anas platyrhynchos* (L.) from Karachi, Pakistan, having Parasitic Impact 187
— *Saima Naz and Syed A. Rizvi*

Physical Sciences

Hall Effects on Rayleigh-Stokes Problem for Heated Second Grade Fluid 193
— *Masud Ahmad and Muhammad Yaseen*

Exact and Numerical Solution for Fractional Differential Equation based on Neural Network 199
— *Hamid A. Jalab, Rabha W. Ibrahim, Shayma A. Murad and Samir B. Hadid*

Demographic Dependency of Aging Process in Bangladesh 209
— *M.Taj Uddin, M. Nazrul Islam and Ahmed Kabir*

New Class of Harmonic p-Valent Functions of Complex Order 219
— *M. K. Aouf, A. A. Shamandy, A.O. Mostafa and A. K. Wagdy*

Stability for Univalent Solutions of Complex Fractional Differential Equations 227
— *Rabha W. Ibrahim*

Instructions for Authors 223

Submission of manuscripts: Manuscripts should be submitted as E-mail attachment or on CD. Authors should consult the ***Instructions for Authors*** at the end of this issue and Website: www.paspk.org.

Proceedings of the Pakistan Academy of Sciences 49 (3): 165–172 (2012)

ISSN: 0377 - 2969

Pakistan Academy of Sciences

Original Article

Green Processing of Coal to Liquid Fuels: Pakistan's Perspective

Zeeshan Nawaz[1,3*], Naveed Ramzan[1], Saad Nawaz[2], Shahid Naveed[1], M. Bilal Khan[3]

[1]Gasification Research Laboratory, Department of Chemical Engineering,
University of Engineering & Technology, Lahore, Pakistan
[2]School of Mechanical Manufacturing & Automation-7,
Beijing University of Aeronautics & Astronautics, Beijing, China
[3]Center of Energy Systems, National University of Science & Technology, Islamabad, Pakistan

Abstract: The role of energy supplies in economic prosperity and environmental quality is one of the most important challenges in Pakistan. The continuing upward trend in crude oil prices in the world and heavy reliance on petroleum and its derivatives in daily life makes the economy vulnerable to critical stress. Therefore, the energy security has gained increasing importance. In Pakistan, only the transportation sector consumes one-third of petroleum derived fuels while other consumers include electric power generation and a number of petrochemical products. The use of oxygenates (fuel additives), olefins (petrochemicals), etc. are becoming popular. The recent discoveries of coal reserves and its pronounced scope in the energy sector in the wake of new technologies have led to its green processing and effective utilization. The challenge of efficient utilization and green processing of coal at manageable cost is of interest to researchers. It is through the Coal to Liquid (CTL) technology that coal is converted to valuable liquid hydrocarbons. The two step process, i.e., gasification, followed by its conversion to liquid fuel by Gas-to-Liquid (GTL) technology is a proven strategy, commonly known as Fischer–Tropsch synthesis (FTS) process. Significant improvement of scope in this technology through improved catalysts and process conditions is of interest. Underground Coal Gasification (UCG) is an attractive option for GTL technology for economic gains. Preliminary studies have already been conducted in the country. The prospective use of CTL and GTL fuels technologies in Pakistan has been reviewed in this paper.

Keywords: Coal, green processing, GTL, CTL, Fischer–Tropsch synthesis, gasification

1. INTRODUCTION

The world fuel reserves are estimated as: crude oil, 5775 Quads (Q); gas 5137 Q; and coal 30100 Q [1]. The overwhelming energy security as coal is appreciated by industry and it is believed that this status may not change in the forth coming era. The possibility of using coal as a source of syngas production for liquid fuels and petrochemicals is obvious [2, 3]. Pakistan is amongst the country having significantly high coal reserves, but unfortunately the coal has not been used extensively as energy source. Primarily this is due to lack of infrastructure, investment in modern coal mining and processing technology. Pakistan's total coal reserves are approximately 185 billion tones, while the economic coal deposit is restricted to Paleocene and Eocene rock sequences [4]. At present the country faces serious energy crises and its future demand is growing at a rate of 7.5 % per annum. To the future requirements of the country with indigenous resources, domestic exploration is expected to be intensified. Currently, the attention is focused for development and utilization of Thar coalfield, one of the world's largest lignite deposits (approximately 175 billion tones) spread over more than 9,000 sq km [4, 5].

A feasibility study on coal gasification has been undertaken and the gasification of coal was found feasible. The importance of coal as an industrial fuel and its role in a wide range of industrial applications are well known in the industry. Coal is used as boiler fuel for the supply of steam the to process plants in paper, chemical, electrical and food processing industries. It is also used for direct

Received, March 2012; Accepted, September 2012
*Corresponding author: Zeeshan Nawaz; Email: engr.dr.zeeshan@gmail.com

firing in the manufacturing of cement, bricks, pipes, glass tanks, and metal smelting. Another effective technology for power generation from lignite coal is Circulating Fluidized Bed (CFB), where coal mixed with limestone is burned in a fluidized bed [6]. The sulfur in the coal is absorbed by the calcium carbonate, and the emissions are free from sulfur oxides [7].

Continuous increase in the prices of gas and oil have severely affected the energy prices. Underground coal gasification, a means to generate coal gas economically, is known to have the potential for power generation and production of other high value chemical products such as diesel, gasoline, olefins, methanol, and ammonia. The technology of UGC is available for both horizontal and inclined coal beds. The mathenated synthesis gas (known as SNG) can be blended with natural gas and transported through pipelines.

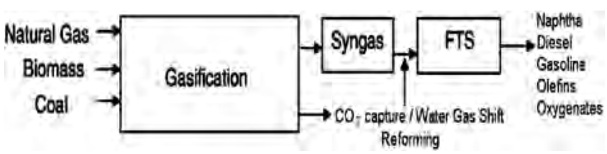

Fig. 1. CTL/GTL process.

The importance of coal as an industrial fuel and its role in a wide range of industrial applications are well known. In this paper we will highlight green processing of coal to energy and explore the space for more valuable products. Indirect use of coal processing to liquid fuels proceeds in two steps: (i) coal gasification; and (ii) conversion of the gas (called syngas) to liquid fuels (Fig. 1). A variety of CTL/GTL technologies for converting coal feedstock into liquid fuels exists, the most popular being Fisher Tropsch process. Generally the steps involved are: (i) feedstock preparation; (ii) gasification; (iii) syngas clean-up; (iv) compression; (v) mathenation; and (vi) conversion into liquid fuel in a reactor. Germany in the Second World War and South Africa at present have used this technology extensively. Recently, interest has aroused to make use of this technology all over the world. Qatar is about to produce about 394,000 barrels of GTL products per day and will become prominent figure in the world in GTL. A list of Qatar's GTL ventures is shown in Table 1 [8]. It is expected that the total GTL production in the world shall reach 1–2 million bpd by 2015 [9].

Table 1. GTL joint venture projects in Qatar.

Project Installer	Full Capacity (bpd)
ConocoPhillips	160,000
Pearl(Shell)	140,000
ExxonMobil	154,000
QP/Sasol Chevron	130,000
Marathon	120,000
Oryx	100,000

Source: Culligan [8].

2. COAL GASIFICATION

Coal and natural gas as source of syngas have been extensively studied [10]. Coal gasification is the most capital intensive part (~40%) of a CTL process. Therefore, selection of gasification method and its design has considerable impact on overall utilization of coal. Partial oxidation (catalytic/non-catalytic), steam-reforming, auto-thermal reforming, compound reforming, underground gasification and ceramic membrane reforming are known gasification techniques. A simplified coal gasification process is shown in Fig. 2. Steam reforming, partial oxidation or a combination of both oxygen blown Auto-Thermal Reforming (ATR) were the potential technologies for CTL/GTL [11–14]. Coal is prepared by milling, grinding and drying operations and then fed to the gasifier where it reacts with steam and an oxidant agent, in this case, pure oxygen, to generate a mixture of gases (mainly CO, H_2 and, CO_2). In steam reforming, a multi-tubular fixed bed catalytic reactors produce high H_2/CO ratio of syngas ranging from 3 to 5. The main reforming reactions are

$$CH_4 + H_2O = CO + 3H_2; \Delta H^0_{298K} = 205.92\text{kJ/mol}$$

$$CH_4 + CO_2 = 2CO + 2H_2; \Delta H^0_{298K} = 247.32\text{kJ/mol}$$

Partial oxidation is simple but suffers from soot formation and high outlet temperature, i.e., 1500°C.

$$CH_4 + 1/2O_2 = CO + 2H_2; \Delta H^0_{298K} = -35.25\text{kJ/mol}$$

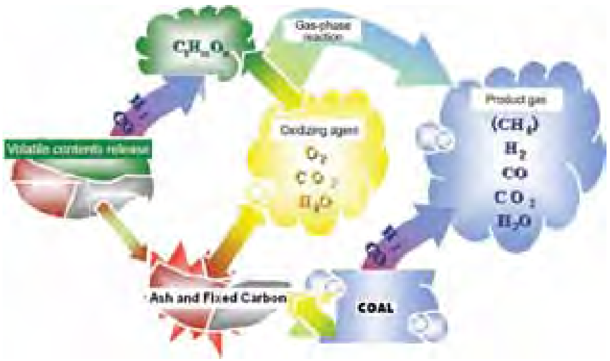

Fig. 2. Overview of coal gasification process.

In the auto-thermal reforming process, both partial oxidation and steam reforming are integrated in reactor and higher pressure syngas is obtained. In ATR process large volume of CO_2 is produced. In compound reforming both early-stage steam reforming reaction and the late-stage automatic-thermal reforming reaction take place in separate reactors and finally high-pressure gas is obtained. Catalytic Partial Oxidation (CPOX) on membranes is known to be the most economical technology as combustion is employed.

Gasifier designs are characterized as: wet or dry feed, air or oxygen blown, reactor flow direction and the gas cooling process. High temperature, entrained flow design gasifiers produce by-products like slag while lower temperature design produces ash. The majority of successful coal gasification processes have been achieved using pressure at 20–70 bar, entrained flow, and slagging gasifiers operating temperatures is about 1400^{o}C [13]. Most advanced gasifiers with lower methane and CO_2 content are the Shell Gasifier, PRENFLO, and E-Gasifier, etc. Benefits of entrained flow designs are clean, tar-free syngas, high operation temperatures, inert slag separation, high oxygen consumption, etc.

Nitrogen is especially undesirable when the syngas produced is intended for FT synthesis as it increases the volume of gas to be compressed; hence, Air Separation Unit (ASU) is critical. At present cryogenic distillation for oxygen-nitrogen separation is the only commercially proven technology for large scale systems. Apart from the reduced size of the gasifier and downstream equipment, other advantages associated to an oxygen-blown gasifier are: (a) the volume of gas produced is reduced; correspondingly, the sensible heat loss from the gasifier is reduced; (b) the gasifier can be operated economically at higher pressures; and (c) the heat-exchangers for the recovery of the sensible heat from the syngas are thus smaller.

During gasification, the sulfur is converted to H_2S or carbonyl sulfide (COS). One of the main concerns in this system is the removal of hydrogen sulfide, carbonyl sulfide, particulate matter, carbon dioxide, and hydrogen chloride. For most syngas contaminants the critical aspect of filtering out these undesirables is the volatility of various components. The maintenance of temperature is of concern. The catalyst poisoning concerns have led to limit the concentration limits of FT reactors to 1 ppm for particulates and 10 ppb for sulfur compounds. Bio-desulphurization of coal is also an option to avoid the sulfur contaminations [15]. The necessary step in acid gas clean-up is to convert the COS into H_2S and CO_2 by COS hydrolysis. The H_2S and CO_2 get absorbed from gas stream through an absorber where the Selexol solvent before the FT reactor.

The coal production, transportation, and utilization processes have impact on the environment in terms of dust, ash, CO_2, NO_x, SO_x, etc. Therefore, green processing to minimize the harmful impact coal utilization on the environment is attractive for rapid commercialization. Numerical simulation of gasification processes is a very effective tool to predict the characteristics of pilot to full scale production unit and allows optimization. There is, however, a significant issue of variation in coal characteristics, even if the coal has come from the same coal mine.

3. SYNGAS TO LIQUID FUELS

The syngas generated from gasifier is sent to a Fischer Tropsch (FT) synthesis reactor after cleaning. The reactor having various metal based patented catalyst (e.g. Fe, Ga, Ni, Cr, Co, Mo, Mg, Pt, Ru, Re, etc.), produces liquid fuel through water-gas shift reaction. The conversion of hydrocarbons into liquid fuels in FT reactors proceeds via surface polymerization reactions over a catalyst. Syngas components get adsorbed on the catalyst surface to form monomer and water. The FT reactions that lead to the formation of synthetic liquid fluids are given below, where the H_2/CO ratio is reaction dependent and is between 2–3.

Main Reactions:

Paraffins $(2n+1)H_2 + nCO \rightarrow C_nH_{2n+2} + nH_2O$

Olefins $2nH_2 + nCO \rightarrow C_nH_{2n} + nH_2O$

Water gas shift reaction $CO + H_2O \rightleftarrows CO_2 + H_2$

Side reactions:

Alcohols $2nH_2 + nCO \rightarrow C_nH_{2n+2}O + (n-1)H_2O$

Boudouard reaction $2CO \rightarrow C + CO_2$

3.1. Fischer-Tropsch (FT) Reactors

The selection of reactor and their design for FT synthesis is based on temperature and hydrodynamics of catalyst [16]. In this exothermic reaction large amount of heat is generated and effective heat removal manages carbon deposition and subsequent deactivation of the catalyst. The temperature, pressure at the FT reactors and type of active metals in catalyst will determine the final product distribution. Higher temperatures generally favor the formation of smaller chains hydrocarbons and lower temperature favors the formation of higher molecular weight products. High performance for high temperature FT reactions for the production of gasoline are entrained fluidized bed reactor with riser coolers {such as Sasol's Synthol reactor [17]}, and the fixed fluidized-bed reactor with internal cooling coils (used at Carthage-Hydrocol plant, Texas [18]). In order to produce middle distillates or olefins the most feasible options are fixed bed tubular reactors (Sasol fixed bed tubular design is known as ARGE), dual bed and slurry bubble columns. The alternative to the fixed bed is a slurry bubble column which has been introduced in market by Sasol, Exxon and Rentech [19]. In these three phase reactors, solid catalyst is suspended in a liquid phase, often well mixed FT wax with syngas is in slurry phase [19]. The slurry phase reactor has therefore better catalyst dispersion and results in a higher single pass conversion compared to the ARGE reactor. Both types of reactors have some limitations; in fixed bed the catalyst is poisoned near the gas inlet while in slurry column attrition and continuous separation between the catalysts-liquid is a problem [19].

3.2. FT Catalysts

Most of Group VIII transition metal oxide catalysts are generally capable of CO hydrogenation; for example Ruthenium based catalyst has highest activity and selectivity for producing high molecular weight products [20], but is expensive. Nickel has a good activity but promote methane formation and its stability is also an issue. Iron is the most commonly used catalyst for FT process, although produces unwanted CO_2 [21, 22]. Generally, Fe catalysts are good for water gas shift reaction, therefore, needs a separate WGS reactor. Cobalt-based catalysts shows low selectivity for WGS reaction, therefore, it is only suitable for a syngas of high H_2/CO ratio and used as separate WGS reactor prior to the FT synthesis reactor. Active metal supports in the catalysts also plays vital role in controlling FT reactions and their important features are higher surface area, hydrothermal stability, active metal dispersion, shape selectivity effect, etc.

The product distribution in F-T synthesis reaction proceeds as explained by Anderson-Schulz-Flory polymerization model [23].

$$\log \frac{m_p}{P} = \log(\ln^2 \alpha) + P \log \alpha$$

m_p is weight fraction of each carbon number fraction

P is carbon number

α is the probability of chain growth

According to above model the maximum production of C_2-C_4 hydrocarbons is about 56% of the total yield. Most of the syngas to olefins conversion catalysts are either mixed oxides or carbonyls derives on different supports. Nickel-palladium, Zn/Cr, Fe/Co, and cobalt-cerium oxides with number of supports and promoters, prepared using a co-precipitation procedure were studied as catalysts for the direct conversion of syngas to light olefins. The higher Co percentage (around 80%) relative to Ce (i.e. around 20%) in the catalyst's proposed optimum in activity and selectivity with H_2/CO molar feed ratios 2/1. The yield and selectivity of lower olefins in direct conversion route is still far from optimum and has scope for R&D in the development of robust catalyst.

4. SYNGAS TO LIQUID FUEL TECHNOLOGIES

The technologies for converting coal to gaseous and liquid fuels are in commercial use as well as improvement through R&D activity. These technologies provide an opportunity to reduce dependence on crude based feedstock. Various syngas production technologies include partial oxidation (catalytic/non-catalytic), steam reforming, auto-thermal reforming, compound reforming ceramic membrane reforming, etc. There is significant room for development and optimization. One of the most economical technology in this reference is considered to be oxygen blown auto-thermal reforming (ATR) process. It has been commercialized by Haldor Topsøe [21]. In this case the process is operated at 0.6 steam to carbon (S/C) ratio. Recently, syngas to light olefins concept was introduced and in future, there is a huge potential for syngas to spatiality chemicals. Extensive experimentally study, construction of pilot/demonstration scale plants and operation of commercial plants makes GTL a mature technology. Many well-known companies have large-scale plant operating experience like ExxonMobil in GTL, Sasol, Shell, IFP, BP, Syntroleum, Rentech and Conoco [22]. A brief of the new developments are summarized here.

Sasol a South African company founded in 1950 is well known due to coal driven syngas to liquid fuels. In 1951, Sasol construction first production facility 'Sasol-I' on German Fischer-Tropsch technology began in Sasolburg, and started production in 1955. Coal based Sasol/Lurgi fixed-bed dry bottom gasifiers at Sasolburg and Secunda. This syngas is fed to Sasol FTS plant having designed capacity around 135,000 bpd. Recently, Sasol start integrated their FT technology with Haldor Topsoe auto-thermal reforming technology. Sasol has developed several types of Fischer-Tropsch technologies as listed below:

(a) High Temperature Fischer-Tropsch (HTFT) reactors:
   1) Synthol-Circulating Fluidized Bed (SCFB) reactor (Synthol)
   2) The Sasol Advanced Synthol (SAS) reactor

(b) Low Temperature Fischer-Tropsch (LTFT) Reactors:
   1) Multi-Tubular Fixed Bed (MTFB) reactor
   2) Slurry Phase (SP) reactor

Mossgas (Pvt) Ltd., is a South African government-owned company, introduced three step production process to synthetic diesels: (i) syngas by steam reforming of natural gas; (ii) high temperature FTS (Sasol technology) to form an olefinic synthetic distillate, synthol light oil (SLO); and (iii) Mossgas process convert lighter olefinic gasses to distillate (COD). In this process olefins are oligomerized over COD-catalyst to form high quality diesel fuel, kerosene, gasoline components, liquid petroleum gas (LPG) and a range of anhydrous alcohols. The 22,500 bpd sulfur-free and eco-friendly fuel is produced by Mossgas.

Royal Dutch Shell introduced a state-of-the-art proprietary GTL process - Shell Middle Distillate Synthesis (SMDS). In 1973, it started research on a modified low-temperature Fischer-Tropsch (F-T) process, leading to the development of the Shell Middle Distillate Synthesis (SMDS) route and first commercialized in Shell's Bintulu plant in Malaysia in 1993. This plant has the capacity to convert 100 million standard cubic feet per day (MMSCFD) of natural gas into 12,500 bpd of middle distillates (gasoil, kerosene, naphtha) and specialty products. In 1997, an explosion took place in the air separation unit (ASU) and damaged the GTL facility. The facility was rebuilt and started production again in 2000. Shell had a good experience in development of low temperature FTS catalyst and its use in the Shell proprietary multi-tubular reactor. It has been claimed that the catalyst has higher yield and selectivity of 90% for desirable middle distillate products. After getting operational and scale-up experience at Bintulu and breakthrough in the low-temperature FTS catalyst development, Shell signed agreements with Qatar Petroleum in 2003 to build the world's largest GTL plant in Ras Laffan, Qatar is likely to produce 140,000 bpd of products primarily naphtha and transport fuel.

Syntroleum, an Australia GTL process design company is working since 1980s. A highly active cobalt-based FTS catalysts for air fed auto-thermal reactor syngas conversion in a multi-tubular fixed-bed reactor or/and slurry reactor has been developed. An 11,500 bpd plant to convert natural gas into ultra-clean specialty products, such as lubricants, industrial fluids and paraffin's, as well as synthetic transportation fuels was installed at Sweetwater Australia. Syntroleum has grown significantly and now has nine commercial GTL projects worldwide with six in Qatar as joint ventures with major international oil companies [24].

ExxonMobil was created by Exxon's 1999 after acquisition of Mobil. Exxon has invested heavily in research to develop its "Advanced Gas Conversion technologies" and build 200 bbl/day GTL three step pilot plant in Baton-Rouge, USA, in 1995-96. Catalytic partial oxidation using fluidized bed reactor for conversion of synthesis gas by slurry phase (F-T) reactor and fixed bed hydro-isomerization. Exxon claims its proprietary process has high productivity and economic benefits. The products of Exxon's GTL process are clear, colorless, biodegradable, very-clean burning liquids with low odor, free of Sulphur, Nitrogen, Aromatics and other impurities; they are ideal feeds for petrochemical and refining applications. Recently, Syntroleum executed an agreement with ExxonMobil that grants it a worldwide license under "ExxonMobil's GTL" patents to produce fuels from natural gas and coal [25].

Chevron is engaged in design and engineering for Nigeria GTL facility, which is likely to convert natural gas into synthetic crude oil. Chevron also signed 50/50 joint venture with Sasol for Sasol's F/T technology and Chevron's Iso-cracking technology offers a unique combination of world class technologies to establish GTL [op.cit.]. Rentech GTL Technology, Colorado, USA has developed F-T process in 1985, using slurry reactor and precipitated iron catalyst to convert synthesis gas produced from range of feed stocks into clean, sulfur-free, and aromatic-free alternative fuels [op. cit.]. Rentech GTL Technology has unique features in its technology in terms of formulation of catalyst and reactor configuration.

Conoco Philips initiated a GTL research and development program in 1997 and began operation of a 400 bbl/day GTL in a demonstration plant in Ponca City, Oklahoma in 2003. They design a number of catalysts for said process. Conoco's proprietary catalysts to be used in synthesis and Fischer-Tropsch processes are known to be unique. Lurgi of Germany founded in 1897, recently builds the largest three-train coal gasification to olefins (syngas to methanol to propylene to polypropylene) plant in China. Previously they have wide experience in Methanol-to-Olefins (MTO) and/or Methanol-to-Propylene (MTP). IFP France is also in the process of piloting a GTL plant.

5. GTL CHALLENGES IN PAKISTAN

The design and development of CTL/GTL plants of commercial scale is very complex and challenging especially as R&D is lacking along with engineering fabrication and related potential in Pakistan. At the moment there is no piloting experience in these technologies and their catalyst development. Recently the Government of Pakistan has shown keen interest in developing these technologies in the wake of acute energy short supply and shortage indigenizes the resources. In this regards, Department of Chemical Engineering, University of Engineering & Technology (UET), Lahore and Center of Energy Systems, National University of Science and Technology (NUST), Islamabad have joined hands to promote these technologies. Initially, UET-built pilot scale gasification facilities, including down draft, cross draft, circulating fluidized bed gasification and underground coal gasification. Simulation and modeling studies have also been undertaken. On the other hand, NUST is pursuing piloting GTL process and integrated catalyst development. In order to address the challenges, international collaboration has been established in South African, UK and Germany. The other major challenge is to integrate internal utilities, like high grade energy users in reformer, oxygen/steam generator, product-workup fired heaters and recycle compressors. Increasing capacity of single-train brings more issues as ASU capacity, compressors, reduction of steam to carbon (S:C) ratio leads to further challenges in burner and reactor design, controlled catalytic partial oxidation, etc.

The art of process design and optimization of coal technologies should be addressed with the state of minimum entropy production in several process units. These studies gave insight into the design with more or less fixed boundary conditions. One of the important questions in such chemical processes is: how does the yield in the reactor affect the downstream units and energy efficiency? (e.g., composition, flow rate of the recycle streams, separation equipments, compressors, etc.) Optimum synthesis of a GTL technology is complicated due to many degrees of freedoms in a highly constrained design space. In a confined design space of equipments and operation, the selection of alternative syngas technologies, different types of Fisher-Tropsch catalysts and reactors, choice of air separation units, compressors, sulfur removal, heat integration options and a range of operational conditions. The state of art computational modeling expertise is being developed to enable the design of sophisticated GTL process design where economic performance should be aligned with carbon and energy efficiencies. Coal-to liquid process is a promising choice to convert coal to syngas and then to synthetic liquid fuels. In the second step, the green GTL synthetic fuel produced from synthesis gas ($CO+H_2$) through FTS (Fischer–Tropsch synthesis) retains extremely low sulfur and aromatic compounds using Fe- or Co-based catalysts, and reduces emissions of carbon monoxide, nitrogen oxides, etc.

6. CONCLUSIONS

To ease out the energy crisis situation in Pakistan, it is inevitable to focus on the development of synthetic fuel from coal in a manner that it does not deteriorate the environment. Rapidly expanding population and infrastructure in the country will inevitably lead to increase the fuel consumption for transportation, energy generation and petrochemical products. To meet future energy requirements of the country, Pakistan has to explore the unused coal reserves through CTL/GTL technologies. Both of these are well developed and proven technologies and offer an important option for producing FTS liquids, oxygenates, fuel additives and chemicals. Different strategies to convert coal to liquid fuels and commercial GTL activities have been discussed. Mega GTL plants with large capacities can be commercialized with ASU and slurry bed reactors having cobalt-based catalyst. Moreover, utilities requirement for CTL/GTL depends upon the train capacity of the unit, like heat integration, heat removal from the syngas and FTS units. Thus, in today's coa- rich Pakistan, GTL technology may be favored and catalyst R&D must be focused.

7. REFERENCES

1. Meyer, E.G. The wrong fuel (letter to editor). *Chem. Eng. News* 6 (Nov. 24, 2003).
2. Levenspeil, O. What will come after petroleum? *Ind. Eng. Chem. Res.* 44 (14): 5073–5078 (2005).
3. Heng, H.C., & S. Idrus. The future of gas-to-liquids as a gas monetization option. *J. Nat. Gas Chem.* 13: 63–70 (2004).
4. PPIB. Pakistan's Thar Coal Power Generation Potential. Private Power and Infrastructure Board (PPIB), Ministry of Water & Power, Government of Pakistan (July 2008).
5. Malik, A., S. Naveed, & Z. Nawaz. Suitability of multistage enthalpy extraction technology for power plants in Pakistan. *Journal of the Energy. Institute, UK* 80 149-152 (2007).
6. Pathan M.I., Z. Nawaz & N.A. Sheikh. Frragmentation investigation of Lakhra coal (Pakistan) in fluidized bed technology. *Mehran University Research Journal of Engineering & Technology* 25: 157-162 (2006).
7. Chen, Q. & H. Wang. Clean processing and utilization of coal energy. *Chinese Journal of Process Engineering* 6 (3): 507-511.
8. Culligan, M. *Natural Gas.* Fifth Doha Gas Conference, Feb 28–March 3, 2005, Qatar, International Energy Outlook, p. 37–48. Report # DOE/EIA-0484 (2005).
9. Keshav. T.R. & S. Basu. Gas-to-liquid technologies: India's perspective. *Fuel Processing Technology* 88: 493–500 (2007).
10. Couch, G.R. *Coal to Liquids.* IEA Clean Coal Centre, London (2008).
11. Bowen, B.H., & I.W. Marty. Coal Gasification and Fischer-Tropsch, In: *CCTR Basic Files #1.* Energy Center at Discovery Park, Purdue University, West Lafayette, IN, USA (2006).
12. Nawaz, Z., T. Xiaoping, Q. Zhang, W. Dezheng. & F. Wei. A highly selective Pt-Sn/SAPO-34 catalyst for propane dehydrogenation to propylene. *Catalysis Communications* 10 1925-1930 (2009).
13. Higman, C. & M.V.D. Burgt. *Gasification, 2nd ed.* Gulf Professional Pub./Elsevier Science, Amsterdam; XVI, 435 (2008).
14. Probstein, R.F., & R.E. Hicks. S*ynthetic Fuels.* McGraw-Hill Book Company (1982).
15. Nawaz, Z., S. Naveed, N.A. Sheikh, & A. Ali. Bio-desulphurization of Lakhra coal by effective microorganisms (EM) technology. *Journal of Chemical Society of Pakistan* 28: 611-619 (2006).

16. Steynberg, A.P. Introduction to Fischer-Tropsch technology. *Fischer-Tropsch Technology* 152: 1-63 (2004).
17. Fox, J.M. F-T Reactor selection. *Catalysis Letters* 7(1-4): 281-292 (1991).
18. Davis, B.H. Overview of reactors for liquid phase Fischer-Tropsch synthesis. *Catalysis Today* 71(3-4): 249-300 (2002).
19. Jager, B. Developments in Fischer-Tropsch technology. *Natural Gas Conversion* 107: 219-224 (1997).
20. Henriciolive, G., & S. Olive. F-T Synthesis – Molecular weight distribution of primary products and reaction mechanisim. *Angewandte Chemie* (*International Edition, in English)* 15(3): 136-141 (1976).
21. P.K. Bakkerud. Update on synthesis gas production for GTL. *Catal. Today* 106: 30–33 (2005).
22. Fleisch, T.H., R.A. Sills, & M.D. Riscoe. Emergence of the gas-to-liquids industry: A review of global GTL developments. *J. Nat. Gas Chem.* 11: 1–14 (2002).
23. Henrici-Olive, G. & S. Olive. The Fischer-Tropsch Synthesis: Molecular weight distribution of primary products and reaction mechanism. *Angew. Chem., Int. Ed. Engl.* 15: 136-141 (1976).
24. FACTS. *Gas Databook I.* Asia-Pacific Natural Gas and LNG, Honolulu, HI, USA. p. 87 (2005).
25. Al-Shalchi, W. *Gas to Liquid Technologies (GLT).* Baghdad (2006).

Proceedings of the Pakistan Academy of Sciences 49 (3): 173–180 (2012)

ISSN: 0377 - 2969

Pakistan Academy of Sciences

Original Article

Possibility of Control of Transition of Switching Arc Dc into Glowing

B. Miedziński[1], G. Wiśniewski[1], S.N. Kharin[2*] and H. Nouri [3]

[1]Institute of Electrical Power Engineering,
Wrocław University of Technology, Wroclaw, Poland
[2]Kazakh-British Technical University, Almaty, Kazakhstan
School of Electrical & Computer Engineering,
[3]University of the West of England, Bristol, UK

Abstract: This paper presents and discusses results of investigations of arc to glow transformation phenomenon at contact opening, under dc inductive loads of low power (≤ 10 J) and low voltage (≤ 250 V). The proportion in duration of arcing and glowing is investigated in dependence on current and voltage value, contact material properties, gas quenching medium and its pressure. The transition phenomenon is analysed by means of fast photography and emission spectroscopy. On the basis of investigated results the conclusions about the possibility of control of the arc to glow transformation for practical use in electrical control switching devices are formulated.

1. INTRODUCTION

Arc to glow transformation is found to appear also at contact opening for specified load conditions, particularly under heavy inductive loads of low power (≤ 10 J) and low voltage (≤ 250 V) dc, which is the most onerous category of utilization (DC-13) [1]. This phenomenon appears to be a real advantage for reliable operation of a switch device due to significant reduction of contact surface erosion. Moreover, switching in circuits can be over-voltages suppressed. The transformation from glow to arc discharge is a well-known phenomenon [2-6].

However, the inverse transformation from arc to glow discharge is a little-studied and recognized process. At present, no theory exists, which can explain the physically based and mathematically described mechanism of arc-to-glow transformation. This results from a complexity of the problem due to the fact that in a given arc, a number of mechanisms co-exist with one more prominent than the others, but where a dynamic change in contact environment can lead to a shift in their relative magnitudes so that a different mechanism becomes dominant.

The essential problem before mathematical modelling is to find conditions, criteria and optimal choice of interdependent parameters (material and gas properties, current, voltage, circuit time constant, pressure, opening velocity etc) providing arc instability and controlled arc-to-glow transformation. Therefore, respective investigations were carried out both at atmospheric conditions as well as in a hermetic chamber filled with pure argon or with $N_2 + H_2$ (5%) mixture at normal and decreased pressure (from 100 kP up to about 10 kPa). On the basis of the measuring results conclusions about possibility of control of the switching arc to glowing are formulated.

2. EXPERIMENTAL INVESTIGATIONS

2.1. Testing Procedure

Investigations were carried out in a special testing system controlled by a PC and equipped with a

Received, June 2012; Accepted, September 2012
*Corresponding author: S.N. Kharin; Email: staskharin@yahoo.com

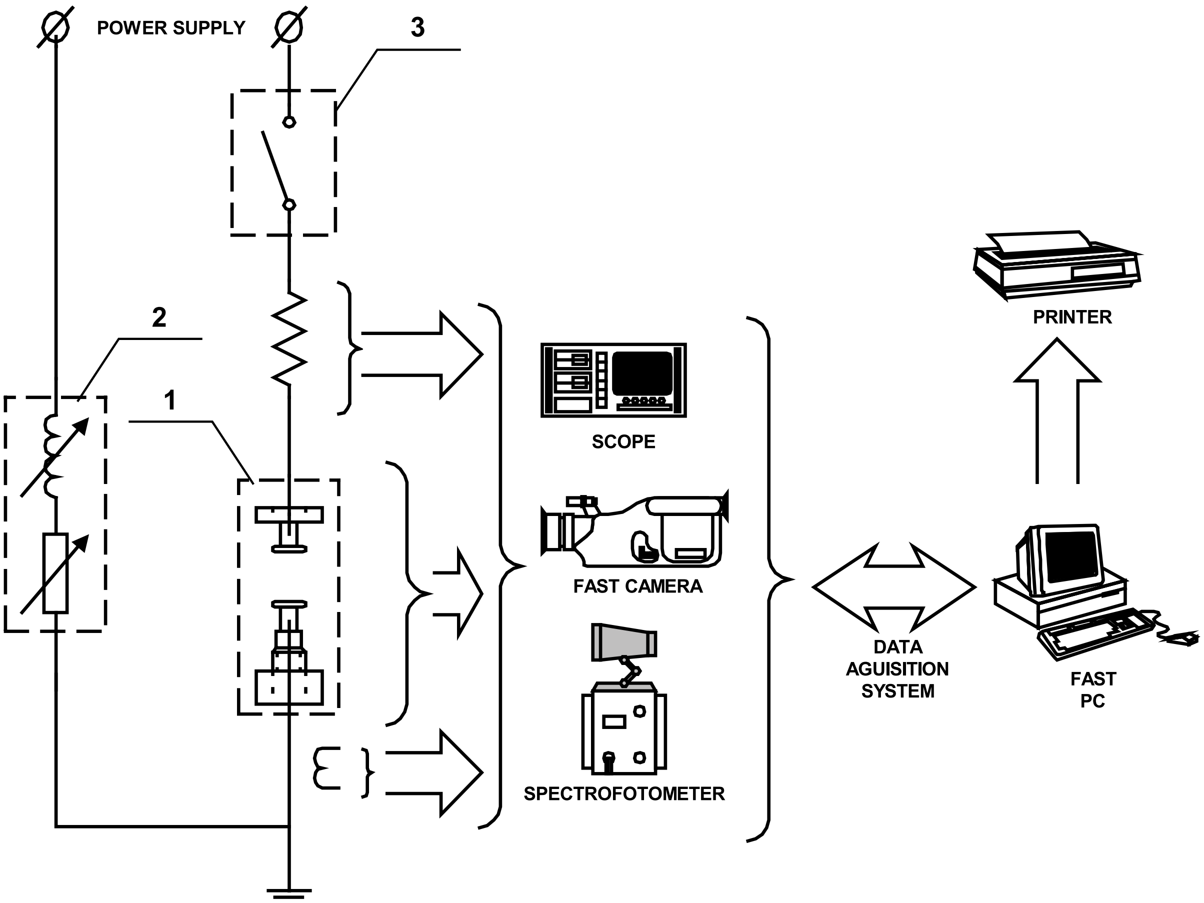

Fig. 1. Schematic set-up of the test apparatus (1-dismountable chamber stand, 2-load to be adjusted, 3-auxiliary protection switch).

dismountable hermetic chamber with a contact system inside as in Fig. 1 [7]. As a gaseous medium, both air, pure argon and $N_2 + H_2$ (5%) mixture were used. Plain round contacts (of 5 mm in diameter and 1 mm in thickness) made of both refractory and non-refractory fine material (W, Mo, Ni, Ti, Ta), selected fine power tungsten-copper sinters (with some additives like Co 2%, TiAl 1%) and vapour deposited copper molybdenum compositions were tested with a medium opening velocity, ranging from 0.04 m/s up to about 0.4 m/s, at contact force up to 40 N. To complete the study of the arc to glow transformation by fast photography (2200 frames per second) and radiation spectra measurements, the contact gap value is enlarged up to 7 mm. The contact set is located vertically with movable cathode at the bottom [8]. Due to the principle of the operation of the fiber-optics spectrometer applied, which is able to analyze the spectrum only as a resultant radiation within 200 ms, the inductive load to be switched is selected to produce the DC arc discharge and/or the glowing as an independent phenomena. The spectrum detected is limited to a visible range, from 300 nm up to about 750 nm due to the transparency of a fibre waveguide. The investigations are performed for currents in the range of 0.5-3 A at voltage from 48V to 250V and at a circuit time constant varied from 10 ms up to 40 ms (discharge energy ≤ 10 J). The current, voltage, discharge power and the contact gap length variation were recorded. To reduce the influence of surface contaminations as much as possible, the contacts were preliminary, mechanically and chemically cleaned and subjected to operation under load before testing. Mean values and predicted ranges with a 95 percent level of confidence are calculated for ten samples of each contact material.

3. RESULTS AND DISCUSSION

3.1. Contact Material Effect

The investigated results have indicated that contact material is a key factor. However, the arc-glow transition may occur for both refractory and non-refractory different materials, under specified conditions of operation but some materials like silver and its compositions are useless here, since the glow transition is almost unattainable. The observation of consecutive switching under identical conditions shows some variation in general appearance. For identical conditions arc to glow transformations are never exactly the same, but they are similar. The reason for this is that some of the mechanisms depend on the probability of various events and therefore, the arc to glow transformation is not completely determined, but is subject to the laws of probability.

The glow discharge at contact opening is found to arise most easily when fine nickel is applied. It can be attainable even at the beginning of contact

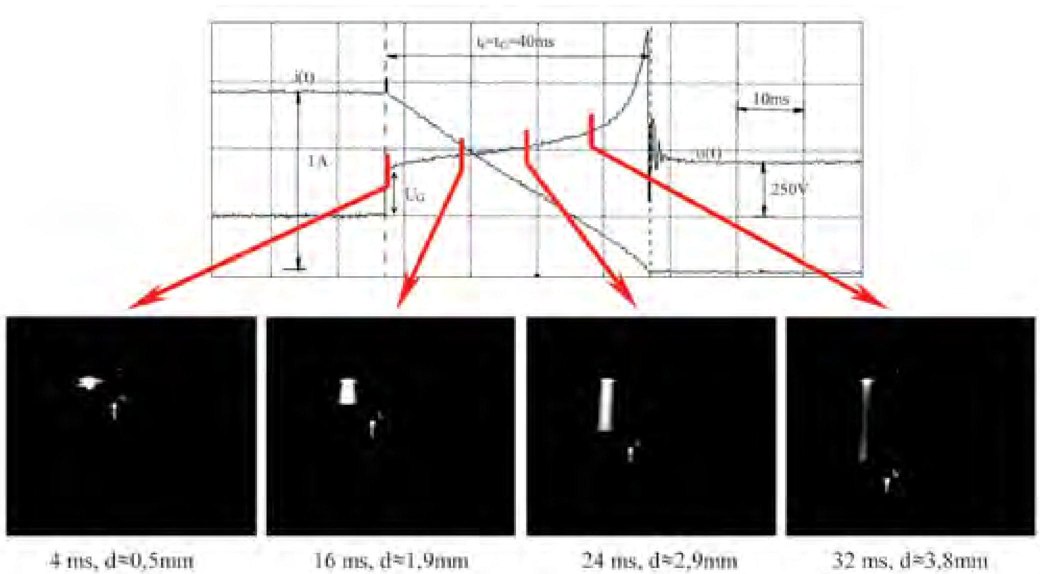

Fig. 2. Glow discharge triggered at the beginning of the contact separation when brake inductive load DC (250 V, 1 A, 40 ms) in air (~ 100 kPa) with contacts made of fine nickel. (t_t, t_G – total and glowing time respectively, U_G – glow voltage).

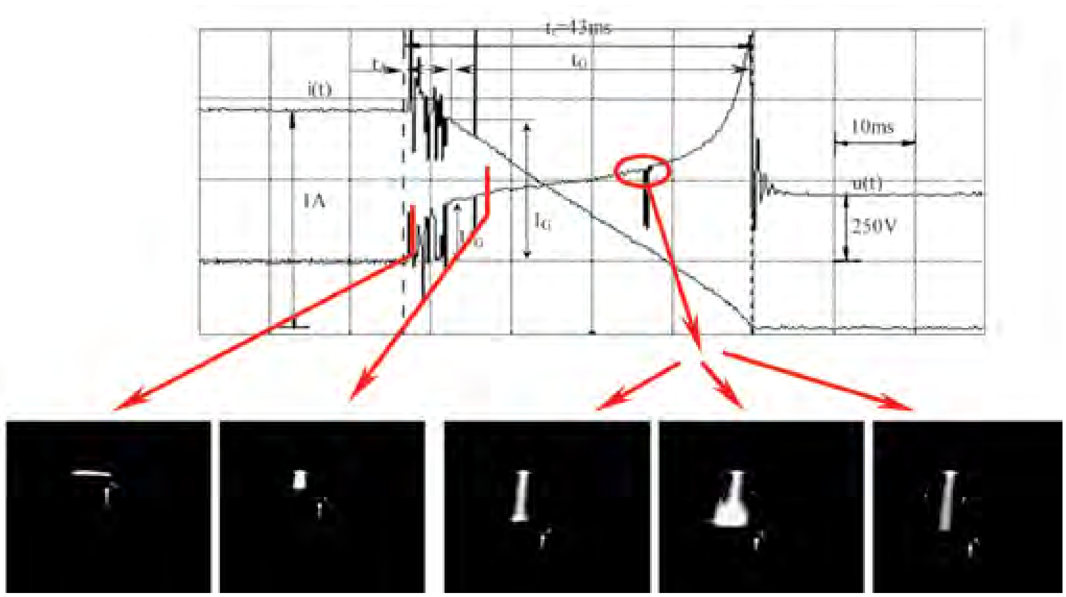

Fig. 3. The unstable arc to glow transition when use the nickel contacts (250 V, 1 A, 40 ms, air ~ 100 kPa) (t_t t_{ARC}, t_G – total, arcing and glow discharge time respectively, U_g – glow voltage, I_G – arc to glow transformation current value).

displacement (at the moment of bridge evaporation or protrusions explosion) as illustrated in Fig. 2. As a result, the discharge energy within the contact area is dissipated at a much higher voltage level (U_g about 300V) and for current decreasing almost linearly with time. Therefore, both contact erosion and switching over-voltage values are reduced significantly. However, the glowing is usually generated due to transition from very unstable arc discharge (short arc, showering arc) which can be compared from Fig. 3 and Fig. 4. In these cases the discharge tends to lead to occasional arcing due to explosive erosion from the cathode (see 30 ms for gap ≈ 3.6 mm in Fig. 3). This is related to a sudden change of the cathode surface conditions and associated reinforced emission, which confirm the major role of this electrode. For the contacts made of refractory materials like tungsten or molybdenum the arc to glow transformation can also be obtained. However, the extensive unstable arcing can be seen even for relatively low current values being broken as demonstrated in Fig. 4. Since the arc appearance for tungsten and molybdenum contacts does not vary significantly in pure argon (as a quenching medium), the increased oxidation of the contact surface in air at an elevated temperature does not

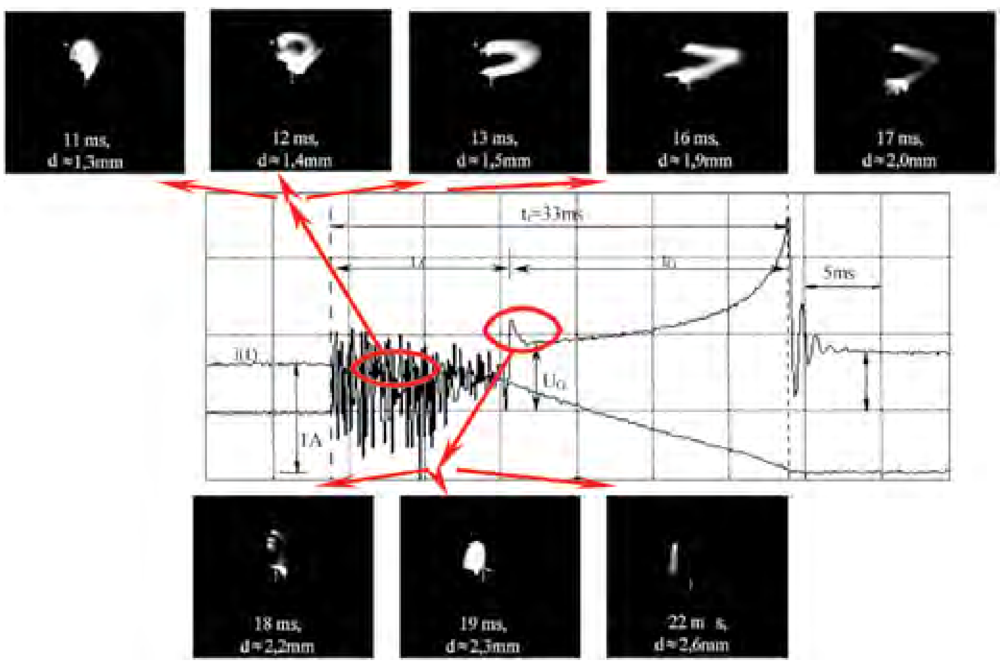

Fig. 4. Development of the electrical discharge when use contacts made of fine molybdenum (250, 0.5 A, 40 ms, in air under 100 kPa).

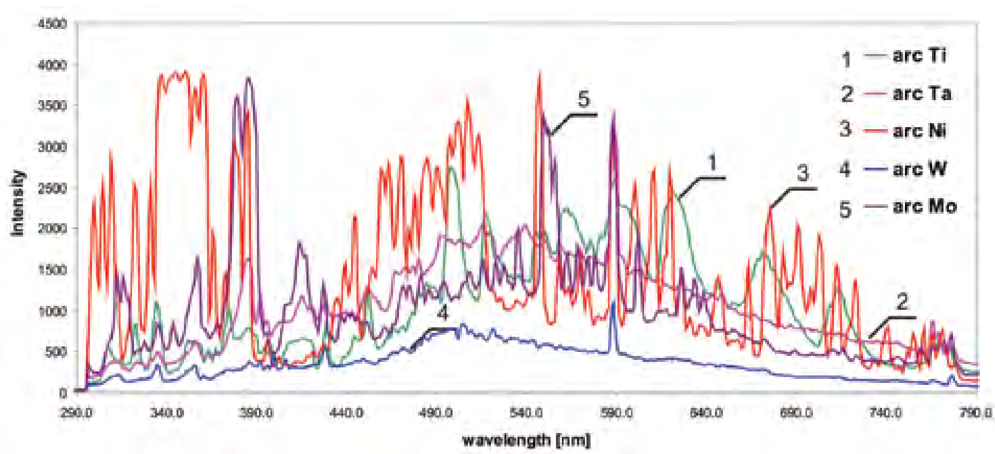

Fig. 5. Radiation spectrum of breaking arc in air under normal pressure for contacts made of different fine materials (Ti, Ta, Ni, W, Mo).

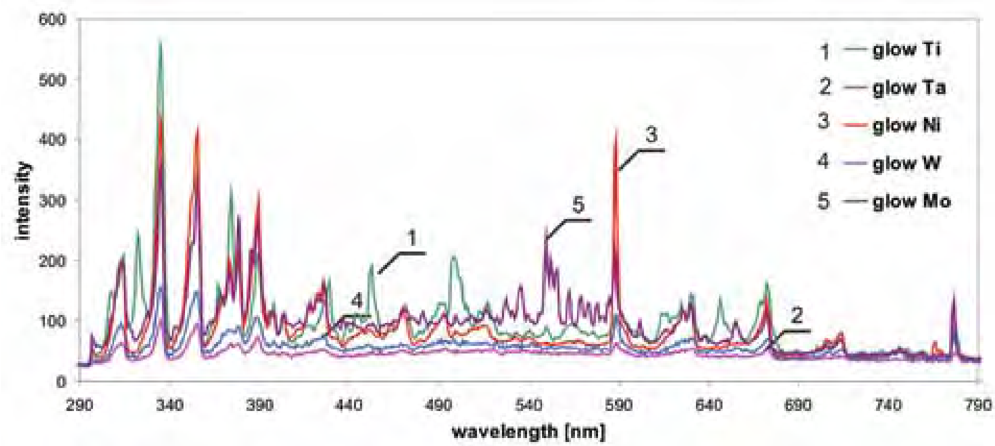

Fig. 6. Radiation spectrum for glowing discharge at contact opening in air for different fine contact materials (Ti, Ta, Ni, W, Mo).

seem to be a major stimulating factor. Besides, it is worth noting that just at the transition moment, the anodic spot may split into a few separate parts (see three spots delete at 18 ms in Fig. 4). It appears that the diffused anodic arc or multi-spot glowing confirms the importance of the anode as well and complexity of the problem. It should also be noted that the arc to glow transition can be initiated at a current (I_G) higher than so called 'minimum arcing' current values (I_{cr}) for the applied contact materials [3]. This is particularly visible for fine nickel where ratio I_G/I_{cr} value can reach up to about 2.5. The fine copper, likewise silver and its compositions are found useless as a contact material under DC heavy inductive loads, since the electric discharge within the contact gap area is usually dominated by a stable electric arc. However, for copper-molybdenum condensed materials, with the increase of the molybdenum content (under the test up to about 14%) the arc to glow transition is visible, but with a small portion of glow duration.

The measuring results of the radiation spectra during electrical discharges at contact opening confirm the arc to glow transition phenomenon. The contribution of gaseous elements (when operated in air) in arc radiation intensity is about 60% which indicates the existence of both metallic and gaseous arc phases (Fig. 5). Intensity of the glowing radiation is about 10-times lower and exhibits an identical picture, independently of the contact material what can be compared from Fig. 6. The contribution of the electrodes elements under glowing, which is about 14%, results most probably from the fact that the metallic vapours inject into the gap area at the moment of bridge or protrusion explosion.

3.2. Velocity and Contact Gap Effect

The arc to glow transition, which occurs under inductive load DC in a gaseous medium does not exhibit a strong dependence neither on contact opening velocity (under the range investigated) or on gap length. Note that maximum velocity up to about 0.4 m/s is selected due to the compliance and damping of bellows anticipated for use in a real model of hermetic compact auxiliary switch operating, according to DC-13 category of utilization. The glow discharge can be reached almost immediately after contact separation (contact gap ≤ 0.1 mm) or after short arcing (contact gap ≤ 2.5 mm) so the discharge phenomena are greatly affected by the electrodes and their neighbouring contraction regions. Therefore, the arc to glow transformation seems little dependent on contact gap length. However, it is interesting to note that the rate of voltage at glow stage for AgCdO contacts is found positive in the range of opening velocity up to about 0.4 m/s, while in the range from 0.5 m/s to 0.75 m/s it becomes negative [9]. For higher (> 0.5 m/s) opening velocity it is also observed that both velocity at contact separation as well as variation of acceleration can be important for the control of arc-to-glow transition.

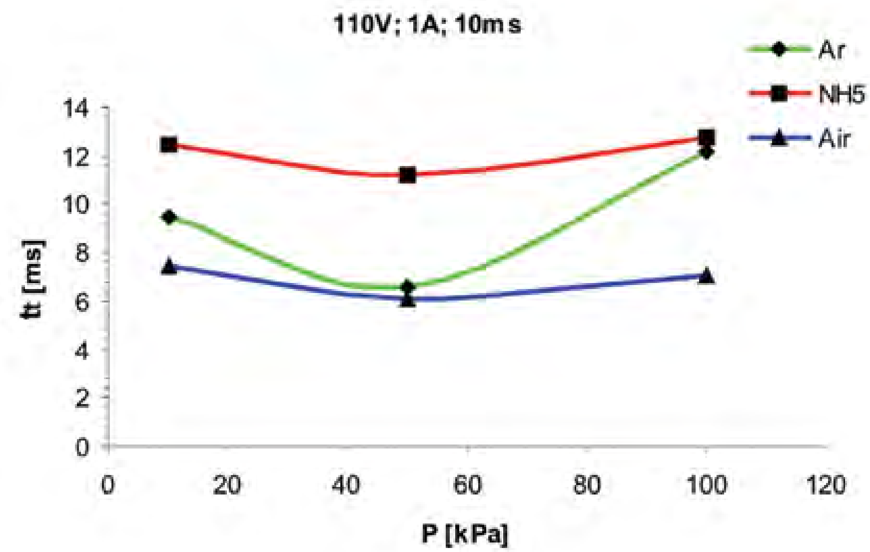

7a

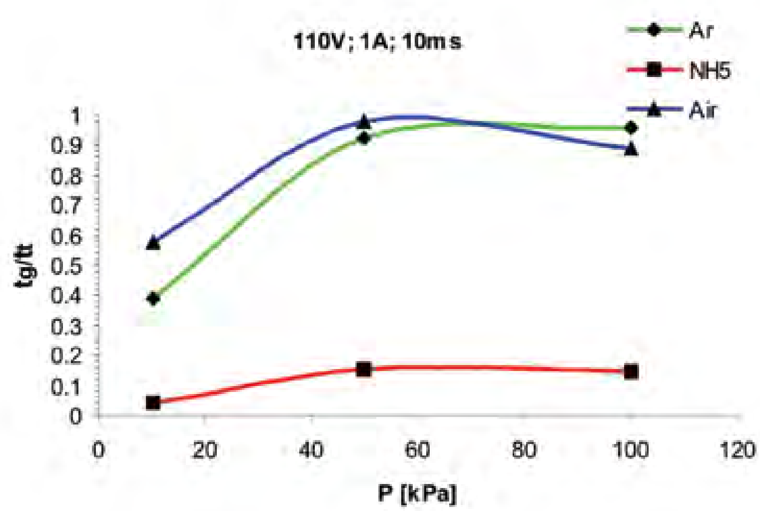

7b

Fig. 7. Variation of the discharge time (t_t) and the portion of the glow duration (t_G/t_t) versus pressure (P) when interrupt inductive load DC (110 V, 1A, 10 ms) in selected gaseous mediums (air, argon, nitrogen-hydrogen 5% mixture) with contacts made of the fine nickel.

3.3. Load and Environment Effect

For the given stored circuit inductive energy (circuit time constant) the total discharge time (t_t) was found to be almost independent on the quenching medium pressure particularly for air and nitrogen-hydrogen (5%) mixture. However, when pure argon is applied it is reduced visibly at about 50 kPa when use contacts made of the fine nickel. (see Fig. 7a). With point of view of the effective arc to glow transformation the reduction of the pressure below 50kPa is not desirable what for investigated mediums can be compared from Fig. 7b. It is also worth to note that in argon the glow duration is extending due to a much lower glowing voltage (U_G) value [9]. On the contrary, when the air is replaced with N_2+H_2 (5%) gaseous mixture, the results under both normal and decreased pressure appear unsatisfactory due to the generation of high stability arc discharge [9]. The total discharge time t_t as well as the portion of the glow duration is also enhanced by the increased supply voltage what for different contact material is illustrated in Fig. 8.

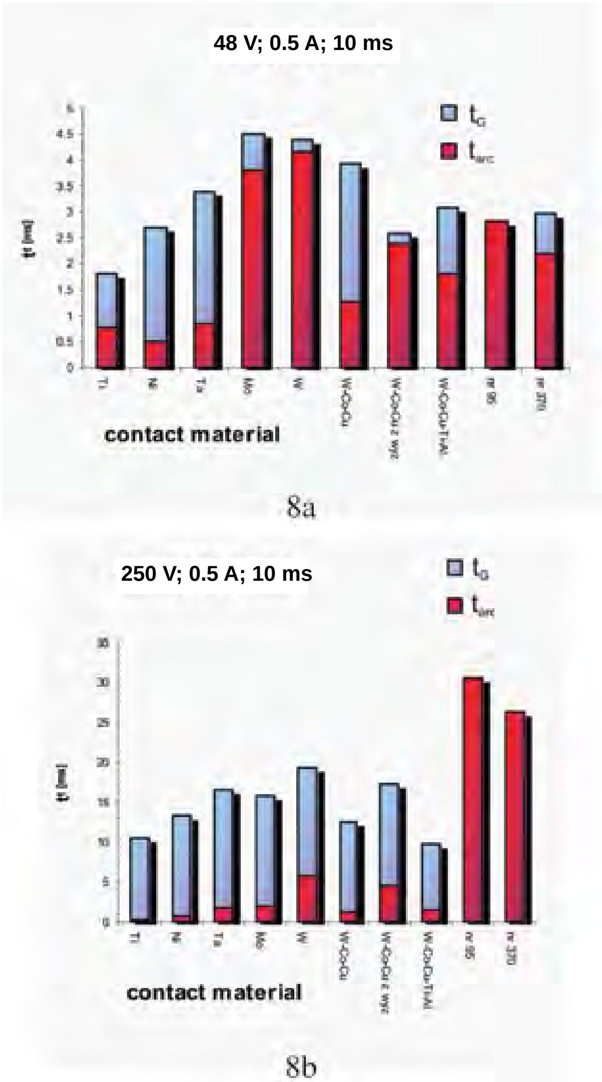

Fig. 8. Comparison of total discharge time (t_t) and portion of the glow duration (t_G) for tested contact materials when interrupt inductive load DC (0.5A, 10 ms) at different voltage value (48 V and 250 V) in air under normal pressure (~100 kPa).

It is found that for almost each material applied there is a certain value of gas pressure under which the arc is easily transformed. The best results are obtained for the fine nickel contacts when use either pure argon or with air (as a quenching medium) under pressures around 50-100 kPa. However, titanium seems to be promising as well particularly as dopant for fine powder sinters (Fig. 8) [10-11]. The superiority of fine nickel as a contact material over tungsten concerning the arc to glow transition, particularly for increasing current is visible in Fig. 9.

The portion of the glow duration here, is the highest under the same conditions of operation which reduces surface erosion significantly. The surface topography inspection, as well as a microstructure

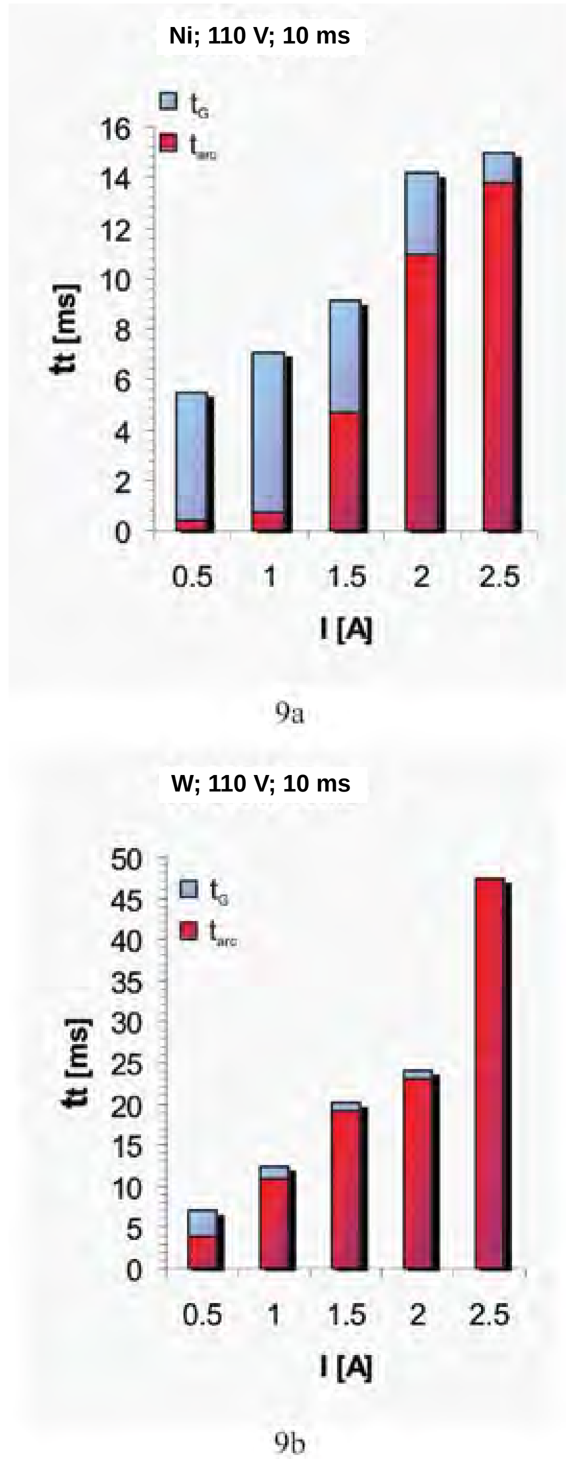

Fig. 9. Comparison of total discharge time (t_t) and portion of the glow duration (t_G) for nickel and tungsten as contact materials when interrupt inductive load DC (110 V, 10 ms) at different current value in air under normal pressure (~100 kPa).

analysis, indicates that in a case when the arc-glow transition occurs easily the erosion is less extensive.

4. CONCLUSION

Arc to glow transition appears at contact opening for specified conditions of operation and is an advantageous phenomenon resulting in the decrease of contact surface erosion and switching over-voltages.

- Neither materials of the highest melting and boiling points (like tungsten) or of the lowest (like fine copper, silver and their compositions) are found to be useful. The best results were obtained for fine nickel in air or in pure argon under pressures around 50-100 kPa.
- The duration of the glow stage increased with increasing supplied voltage and circuit time constant and became maximum at a certain value of the ambient pressure, depending on gas and contact material.
- Opening velocity and acceleration are important for the control of arc to glow transition. However, at low velocity it seems to be little dependent on contact gap length. The rate of glow voltage was positive for low opening velocity and negative for high opening velocity.
- However, the arc to glow transition can be obtained for any low voltage, and low power switch, operating even in air, but it is particularly recommended for auxiliary hermetic switches of compact structure, in which effects such as oxidation, contamination etc can be neglected.

5. REFERENCES

1. Miedzinski, B., A. Szymanski, G. Wisniewski, & A. Grodzinski *Transformation of Low Power Arc to Glowing under Inductive Load DC.* Proc. Int. Conf. on Switching Arc Phenomena SAP. Lodz, 17-20 Sept. 2001, p. 117-120 (2001).
2. Llewellyn-Jones, F. *The Glow Discharge and an Introduction to Plasma Physics.* Methuen Co., London (1966).
3. Holm, R. *Electric Contacts. Theory and Applications.* Springer-Verlag, Berlin (2000).
4. Slade, P. *Electrical Contacts. Principles and Applications.* Marcel Dekker, Basel, Switzerland (1999).
5. Browne, T.E. *Circuit Interruption. Theory and Design.* Marcel Dekker (1984).
6. Mills, C.W. The Mechanism of the Showering Arc. *IEEE Transaction on Parts, Hybrids and Packaging* 5: 47-55 (1969).
7. Bąkowski, P., B. Miedzinski, S. Szkolka & H. Poniewierski. *System for Material Testing of Hermetic Switches.* Proc. SAP-93 Conf, Lodz, p. 301-304 (1993).
8. Miedzinski, B., G. Wisniewski, W. Okraszewski, H. Nouri & S. Kharin. *Analysis of Arc to Glow Transition using Fast Photography.* Proc. 52nd Int. Relay Conf., Oak Brook, Ill, p. 8.1-8.5 (2004).
9. Kharin, S.N., H. Nouri, B. Miedzinski & G. Wisniewski *Transient Phenomena of Arc to Glow Discharge Transformation at Contact Opening.* Proc. 21st ICEC Zurich, Switzerland, p. 425-431 (2002).
10. Nouri, H., B. Miedzinski, S.N. Kharin & G. Wisniewski. *Analysis and Investigations of Arc to Glow Discharge Transformation under DC Inductive Loads.* MIAG No 8/439, p.7-22 (2007).
11. Miedzinski, B., A. Szymanski, G. Wisniewski & A. Grodzinski. *The Influence of Contact Materials on Arc to Glow Transformation.* Proc. 49th Int. Relay Conf. Oak Brook, Ill, 23-25.04. p. 3.1-3.6 (2001).

Proceedings of the Pakistan Academy of Sciences 49 (3): 181–186 (2012)

ISSN: 0377 - 2969

Pakistan Academy of Sciences

Original Article

Taxonomic Study of Some *Cosmarium* Species from North-Eastern Areas of Pakistan

Waqar-ul-Haq[1], Zarina Ali[1]*, Masud-ul-Hasan[2] and Mustafa Shameel[3]

[1]Department of Botany, Federal Urdu University of Arts, Science & Technology, Gulshan-e-Iqbal Campus, Karachi-75300
[2]Department of Botany, Govt. College University, Katchehri Road, Lahore-54000
[3]Department of Botany, University of Karachi, Karachi-75270, Pakistan

Abstract: Ten species of the placoderm desmid, *Cosmarium* Corda *ex* Ralfs (phylum Volvophycota Shameel) were collected from various freshwater habitats in Azad Kashmir as well as provinces of Punjab and Khyber Pakhtoonkhwa of Pakistan during April 2004 and December 2006. They were taxonomically investigated and described. They appeared in winter, occurred predominantly in spring and summer, and disappeared in the autumn. Out of these, *C. ctenoideum, C. formulosum* Hoff *in* Nordstedt and *C. garrolense* Roy *et* Bisset are being reported for the first time from Pakistan.

Keywords*:* Freshwater algae, Volvophycota, desmids, *Cosmarium*, taxonomy, cytology, reproduction

1. INTRODUCTION

Cosmarium Corda *ex* Ralfs is a very common genus of placoderm desmids (family Desmidiaceae, order Desmidiales, class Desmidophyceae, phylum Volvophycota [1, 2]. It grows luxuriantly in freshwater habitats of Pakistan. Its 41 species were collected from different places in the north-eastern areas of Pakistan, out of which 31 species have been described earlier [3, 4]. The present investigation is a continuation of such studies, where 10 species were taxonomically evaluated and described.

2. MATERIALS AND METHODS

The material was collected from various freshwater habitats at Gujranwala, Jauharabad, Jhang, Lahore, Pasroor, Sheikhupura and Sialkot districts of the Punjab Province, Attock and Swat in the province of Khyber Pakhtoonkhwa as well as Chenari and Neelam Valleies of Azad Kashmir during April 2004 and December 2006. The methods used for its collection, preservation, microscopic examination and preparation of drawings were the same as have been described earlier [5]. The specimens were identified up to species level with the help of authentic literature [6-30]. The voucher specimens are kept in the Phycology & Phycochemistry Lab. (Room No. 18), MAH Qadri Biological Research Centre, University of Karachi, where this research work was carried out.

3. RESULTS AND DISCUSSION

From collected material ten species of the genus *Cosmarium* Corda 1839: 242 *ex* Ralfs 1848: 91 were identified. Their microscopic examination revealed the following taxonomic characters, on the basis of which they may be distinguished as follows:

Received, September 2011; Accepted, September 2012
*Corresponding author: Zarina Ali; Email: zarinaali2006@gmail.com

1. Cells more than 51 µm long 2
   Cells less than 51 µm long 3
2. Cell-wall smooth .... *C. galeritum* (*3*)
   Cell-wall otherwise.. 4
3. Cells up to 20 µm broad 5
   Cells more than 20 µm broad 6
4. Cells up to 42 µm broad ..... *C. formulosum* (*2*)
   Cells up to 46 µm broad.......................... *C. margaritiferum* (*10*)
5. Semi cells sub-circular .... *C. imressulum* (*8*)
   Semi cells oblongo-elliptic .... *C. leave* (*9*)
6. Width of isthmus more than 10 µm .... *C. hammeri* (*7*)
   Width of isthmus up to 10 µm........................ 7
7. Cells more than 24 µm broad .... *C. garrolense* (*4*)
   Cells up to 24 µm broad 8
8. Semi cells truncate-pyramidal................................ *C. granatum* (*6*)
   Semi cells otherwise....................................... 9
9. Cell surface undulate and flattened at apices.......... *C. gibberulum* (*5*)
   Cell surface otherwise .... *C. ctenoideum* (*1*)

1. *C. ctenoideum*

General Characters: Cells 26.4-28.0 µm long and 22-24 µm broad, isthmus 4-5 µm wide; cell-walls punctuate; semi-cells trapezoid in each cell, rare in medium (Fig. 1).

Locality: Lahore District: Ghulam Colony Village (22-6-2005).

Geographical Distribution: Worldwide.

Remarks: Specimens were collected in summer from rice fields. This is the first report of its occurrence in Pakistan.

2. *C. formulosum* Hoff *in* Nordstedt 1888: 194

References: Sherwood 2004: 10, ŠŤastný 2009: 143 [28-29].

General Characters: Cells 51-52 µm long and 40-42 µm broad; isthmus 13-14 µm wide; cell-walls dentate; ends are not clear (Fig. 2).

Locality: Khyber Paktoonkhwa: Swat, Utrod river side in Kalam (13-8-2005).

Geographical Distribution: U. S. A., Denmark, Poland and Czech Rep.

Remarks: Collected during summer from the side of Utrod River. This is the first report of its occurrence in Pakistan.

3. *C. galeritum* Nordstedt 1870: 209

Synonymy: *Cosmarium pyramidatum* Brébisson *in* Bernard 1808: 107, *C. pyramidatum* Brébisson f. *subgranatum* Klebs 1879: 31.

References: Krieger & Gerloff 1962: 107, Duthie & Ostrofsky 1975: 262, Bando *et al.* 1989: 16, Masud-ul-Hasan & Yunus 1989: 114, Sahin & Akar 2007: 1824, ŠŤastný 2010: 12 [7, 9, 14, 21, 26, 30].

General Characters: Cells 51-53 µm long and 42-50 µm broad, isthmus 14-18 µm; cells of moderate size, slightly longer than broad; deeply constricted, sinus narrowly linear with a dilated extremity; semi-cells pyramidal trapesiform, apex narrowly truncate and generally slightly convex; basal angle rounded, cell outline broadly elliptic; ends flat, side rounded; cell-walls smooth; chloroplast axial, each with two pyrenoids (Fig. 3).

Localities: Sheikhupura District: Mureedke and Narang Mundi (5-9-2005); Khyber Paktoonkhwa: Swat, Utrod river sides in Kalam (13-8-2005).

Geographical Distribution: Worldwide.

Remarks: Specimens were collected during summer and autumn from ponds and rice fields mixed with other free-floating algae.

4. *C. garrolense* Roy *et* Bisset 1894: 101

Synonymy: *Cosmarium alpinum* (Raciborski) De Toni var. *helveticum* Schmidle 1894: 89, *C. alpinum* (Raciborski) De Toni var. *garrolense* (Roy *et* Bisset) Schmidle 1897: 66, *C. latere-undatum* Roy *et* Bisset 1894: 101.

References: Krieger & Gerloff 1962: 43, Sahin & Akar 2005: 60, ŠŤastný 2010: 13 [1, 26, 30].

General Characters: Cells slightly longer than broad; semi-cells hemispherical in shape; flattened at the apex, lateral undulations are five or six; length 29-38 µm and width 23-29 µm; width of isthmus 7-10 µm (Fig. 4).

Localities: Lahore District: Ghulam Colony Village (18-7-2005); Pasroor District: Mutaike-Raypootan Village (4-3-2006).

Geographical Distribution: England, Germany, Switzerland, Turkey, Afghanistan and Brazil.

Remarks: Collected in spring and summer from stagnant water ponds and rice fields. This is the first report of its occurrence in Pakistan.

5. *C. gibberulum* Lütkemüller

References: Masud-ul-Hasan & Zeb-un-Nisa 1986: 242, Leghari *et al.* 2002: 76, ŠŤastný 2010: 13 [18, 19, 30].

General Characters: Cell surface undulate; flattened at apices; chloroplast one in each semi-cell, each with a pyrenoid; cell length 27-32 µm and breadth 20-24 µm, isthmus 1-9 µm broad (Fig. 5).

Localities: Azad Kashmir: Chenari (28-4-2004), Neelam Valley (5-4-2005).

Geographical Distribution: Czech Rep., Afghanistan and Pakistan.

Remarks: Collected in spring from river sides and stagnant water ponds.

6. *C. granatum* Brébisson *in* Ralfs 1848: 96

Synonymy: *Didymidium granatum* (Brébisson) Reinsch 1867: 109, *Euastrum granatum* (Brébisson) Gay 1884: 59, *Cosmarium pseudogranatum* Nordstedt *in* Gutwinski 1891: 47, *C. sexangulare* Lundell f. *minima* Nordstedt *in* Bohlin 1901: 70.

References: Krieger & Gerloff 1962: 111, Islam 1970: 924, Masud-ul-Hasan & Zeb-un-Nisa 1986: 242, Gontcharov *et al.* 2001: 99, Kopp 2006: 123, Gul *et al.* 2008: 201, Rai *et al.* 2008: 61, Sarim *et al*, 2008: 39, ŠŤastný 2009: 143 [10, 11, 13, 14, 17, 19, 23, 27, 29].

General Characters: Cells 1-1 ½ times as long as broad, semi-cells truncate pyramidal; chloroplast one in each semi-cell with a pyrenoid; cell length 26-31 µm and breadth 19-23 µm, isthmus 4.9-7.0 µm wide; cell-walls smooth (Fig. 6).

Localities: Lahore District: Ghulam Colony Village (18-7-2004), Mari Village (23-7-2005); Sialkot District: Sambraal Road near Ravi Marals (6-4-2005); Azad Kashmir: Chenari (28-4-2006), Neelam Valley (15-12-2006).

Geographical Distribution: Worldwide: U.S.A., England, Germany, Switzerland, Czech Rep., South Amrica, India, Pakistan and Afghanistan.

Remarks: Collected in winter, spring and summer from paddy fields, stagnant water ponds and river sides.

7. *C. hammeri* Reinsch 1867: 115

Synonymy: *Euastrum hammeri* (Reinsch 1867) Cohn 1879: 250.

References: Krieger & Gerloff 1962: 57, Gontcharov *et al.* 2001: 99, Husna *et al.* 2008: 106 [10, 12, 14].

General Characters: Cells about median size, deeply constricted; sinus narrowly linear, with a dilated extremity; semi-cells acrate-pyramidal from a broad wavy base, angle rounded; cell-wall smooth wavy at apices; length of semi-cells 37-38 µm and width 20-21 µm; width of isthmus 13.5-14.5 µm (Fig. 7).

Locality: Lahore District: Fountain of Shalimar Garden (20-5-2005).

Geographical Distribution: Cosmopolitan, all over the world.

Remarks: Collected in spring from fountain water (tempertature 39.6 ºC and pH 7).

8. *C. impressulum* Elfving 1881: 13

Synonymy: *Cosmarium meneghinii* Brébisson f. *latiuscula* Jacobsen 1876: 197, *C. meneghinii* Brébisson f. *octangularis* Wille 1879: 43, *C. meneghinii* var. *simplicissimum* Wille 1880: 30, *Euastrum impressulum* Gay 1884: 61, *C. meneghinii* f. *reinschii* Istvanfi 1886: 237, *C. crenulatum* (Nägeli) Schmidle 1893: 96, *C. crenulatum* (Nägeli) Schmidle var. *reinschii* (Istvanfi) Schmidle 1893: 96, *C. transiens* Gay f. *minor* Gutwinski 1909: 458, *C. undulatum* Corda var. *crenulatum* (Nägeli) Wittrock *in* Krieger 1932: 190, *C. undulatum* Corda f. *minima* Cosandey 1934: 451, *C. repandum*

Nordstedt f. *minor* Irénée-Marie 1938: 178.

References: Krieger & Gerloff 1965: 133, Islam 1970: 924, Masud-ul-Hasan & Batool 1987: 353, Masud-ul-Hasan & Yunus 1989: 114, Leghari *et al.*, 2002: 76, Novakovskaya & Patova 2008: 839, Rai *et al.* 2008: 61, Sterlyagova 2008: 917 [13, 15, 18, 20-23].

General Characters: Cells rather small, deeply constricted, sinus narrowly linear with slightly dialated apex; semi-cells sub-circular, margin regularly and markely undulate, sometimes almost crenate; crenation two at the apex and two on each side of convex sides; cell-wall punctate; chloroplast axile with a central pyrenoid. Overall cell shape irregularly polygonal; semi-cells with a rounded perimeter of about eight small straight edges or undulation; length of cells is 20-30 µm and width is 15-20 µm; isthmus 3.4-9.0 µm broad (Fig. 8).

Localities: Gujranwala: Nandipur (4-4-2004); Jhang District: near Riwaz Chund Bridge, Chenab (22-1-2005); Lahore District: Ghulam Colony Village (18-7-2005); Sheikhupura District: Mureedke and Narang Mundi (12-9-2006); Khyber Paktoonkhwa: Attock (12-1-2005).

Geographical Distribution: U. S. A. Canada, Europe, Pakistan and Afghanistan.

Remarks: Collected from paddy fields, river water, canal side ponds and stagnant ponds mixed with other free-floating algae.

9. *C. leave* Rabenhorst 1868: 161

Synonymy: *Cosmarium leiodermum* (Gay) Hansgirg 1888: 194, *C. gerstenbergim* Richter f. *typica* Richter 1895: 23, *C. gerstenbergim* Richter f. *subreniformis* Richter 1895: 23, *C. leiodermum* (Gay) Hansgirg var. *maius* Gutwinski 1898: 145, *C. leiodermum* (Gay) Hansgirg f. *maior* Borge 1901: 24, *C. granatum* Brébisson var. *subgranatum* Nordstedt f. *crassa* Roller 1925: 147, *C. meneghinii* f. *octangularis* Wille.

References: Krieger & Gerloff 1969: 259, Ahmed *et al.* 1983: 426, Bando *et al.* 1989: 16, Kitner *et al.* 2004: 49, Sahin & Akar 2007: 1824, Celewicz-Gołdyn & Kuczyńska-Kippen 2008: 17, Husna *et al.* 2008: 106 [6-8, 12, 16, 24, 25].

General Characters: Cells small, very deeply constricted; sinus narrowly linear with dilated apex, depressive at apex; semi-cells oblongo-elliptic, with basal angles slightly rounded; apex narrowly truncate and retuse; cell-walls smooth, chloroplast axile with a central pyrenoid, rare in median; length of semi-cell is 25.5-26.5 µm and width 19-20 µm; width of isthmus 13-14 µm (Fig. 9).

Locality: Lahore District: Fountain of Shalimar Garden (20-4-2005).

Geographical Distribution: Cosmopoliton, found all over the world.

Remarks: Collected from fountain water of historical place (temprature 35.1 ºC and pH 7).

10. *C. margaritiferum* Meneghini *ex* Ralfs 1848: 100

Synonymy:*Cosmarium confusum* var. *regularis* Nordstedt.

References: Masud-ul-Hasan & Zeb-un-Nisa 1986: 243, Gul *et al.* 2008: 202, ŠŤastný 2009: 143 [11, 19, 29].

General Characters: Cell-wall punctate and granulated; semi-cells pyramidal truncate, basal and upper angles rounded; sides slightly convex, apex broad and straight; sinus deep, narrowly linear, dialated at the extremity; chloroplasts two in a semi-cell, each with a pyrenoid; cell length 49-58 µm and breadth 39-46 µm; isthmus 13-17 µm wide (Fig. 10).

Localities: Jauharabad (16-2-2005); Sialkot District: Ravi Marala Link, Sambraal Road (6-4-2005); Azad Kashmir: Chenari (28-4-2006).

Geographical Distribution: U. S. A., Denmark, Poland, Czech Rep., Pakistan and New Zealand.

Remarks: Collected from three different places from stagnant water pools.

The collected species of *Cosmarium* were observed to appear in the winter season; they occurred predominantly in spring and summer, and gradually disappeared in the autumn.

4 CONCLUSIONS

The species were identified mainly on the basis of cellular morphology and cell dimensions, but future

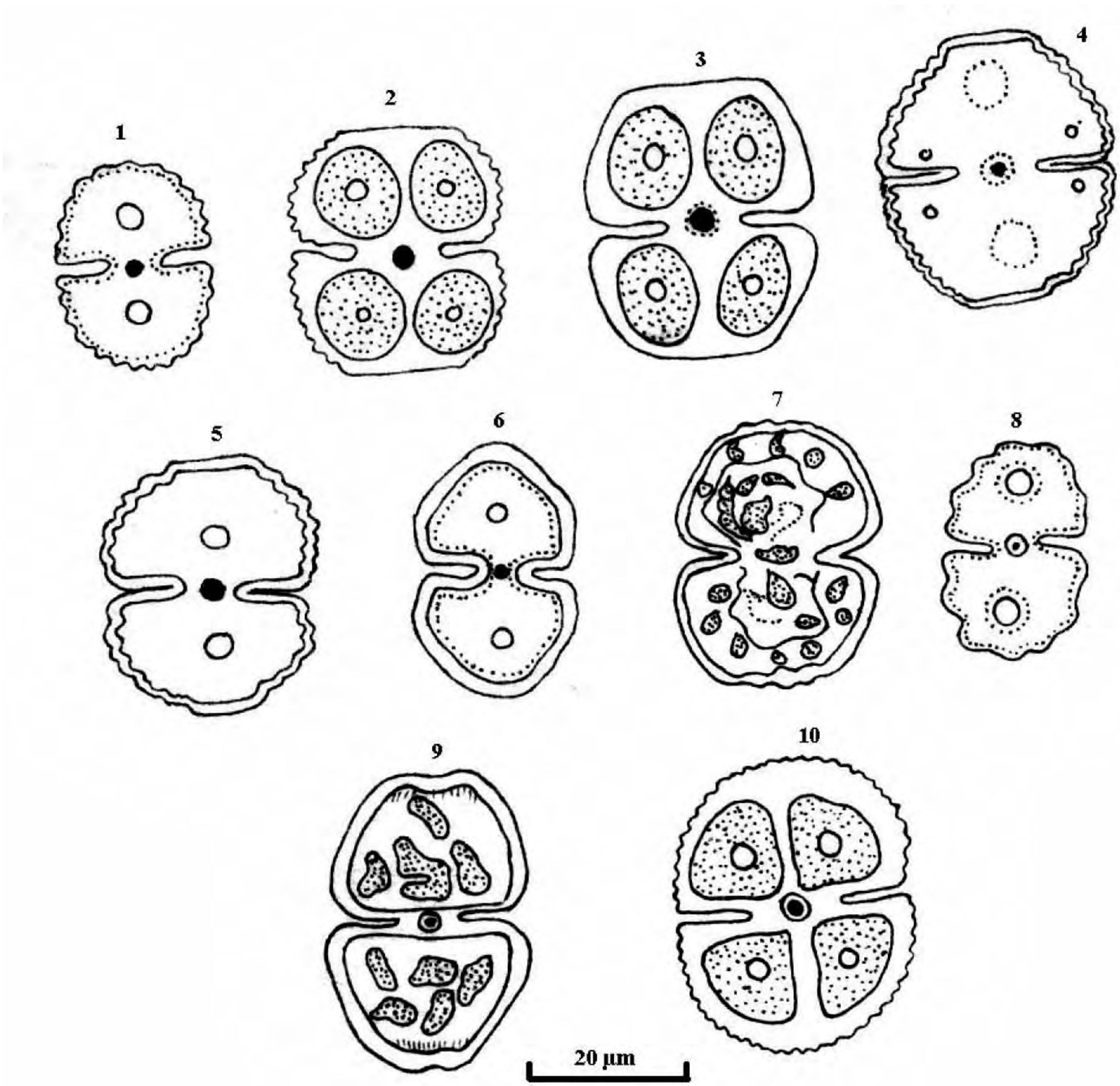

Fig. 1-10. Species of *Cosmarium* from Pakistan: **1.** *C. ctenoideum,* **2.** *C. formulosum*, **3.** C. *galeritum,* **4.** *C. garrolense*, **5.** *C. gibberulum*, **6.** *C. granatum,* **7.** *C. hammeri*, **8.** *C. impressu*lum, **9.** *C. leave*, **10.** *C. margaritiferum*.

studies, like molecular analysis using *rbc*L and mitochondrial *COX*3 genes as molecular markers ,may confirm their identification. The investigated species appeared in winter, occurred predominantly in spring and summer, and gradually disappeared during autumn. The frequency of their occurrence during autumn season was extremely low. This may be attributed to poor availability of nutrients which are usually exhausted up to the end of summer season by blooming algae. This tendency was repeatedly observed over three years.

5. REFERENCES

1. Shameel, M. An approach to the classification of algae in the new millennium. *Pakistan Journal of Marine Biology* 7: 233-250 (2001).
2. Shameel, M. Change of divisional nomenclature in the Shameelian classification of algae. *International Journal of Phycology & Phycochemistry* 4: 225-232 (2008).
3. Waqar-ul-Haq, Z. Ali, Masud-ul-Hasan & M. Shameel. Taxonomic study on ten species of *Cosmarium* Corda (Desmidophyceae Shameel) from north-eastern areas of Pakistan. *International*

Journal of Phycology & Phycochemistry 6: 107-114 (2010).

4. Waqar-ul-Haq, Z. Ali, Masud-ul-Hasan & M. Shameel. Taxonomic study of ten more species of *Cosmarium* from north-eastern areas of Pakistan. *Pakistan Journal of Botany* 43: (in press).
5. Waqar-ul-Haq, Z. Ali, Masud-ul-Hasan & M. Shameel. Taxonomic study of the family Scenedesmaceae (Volvocophyta Shameel) in certain north-eastern areas of Pakistan. *Proceedings Pakistan Academy of Sciences* 45: 23-30 (2007).
6. Ahmed, J., M. Begum & S. Begum. Survey and cultivation of freshwater algae from Karachi and its Suburbs. *Bibliotheca Phycologia* 66: 389-445 (1983).
7. Bando, T., T. Nakano & M. Watanabe. The desmid flora of Kathmandu, Nepal. *Bulletin of the National Science Museum,* Tokyo, Ser B, 15: 1-25 (1989).
8. Celewicz-Gołdyn, S. & N. Kuczyńska-Kippen. Spatial distribution of Phytoplankton communities in a small water body. *Botanika-Steciana* 12: 15-21 (2008).
9. Duthie, H. C. & M. L. Ostrofsky. Freshwater algae from Western Labrador: II. Chlorophyta and Euglenophyta. *Nowa Hedwigia* 24: 253-268 (1975).
10. Gontcharov, A. A., M. Watanabe & M. M. Watanabe. Contribution to the desmid flora of Papua New Guinea II. *Bulletin of the National. Science Museum,* Tokyo, Ser. B 27: 93-107 (2001).
11. Gul, R., Z. Ali, Masud-ul-Hasan & M. Shameel. Taxonomic study of some microalgae from Sialkot, Pakistan. *International Journal of Phycology & Phycochemistry* 4: 57-64 (2008).
12. Husna, B., Z. Ali, Masud-ul-Hasan & M. Shameel. Taxonomic study of Volvocophyta Shameel from fountain water of Lahore, Pakistan. *International Journal of Phycology & Phycochemistry* 4: 99-110 (2008).
13. Islam, A.K.M.N. Contributions to the knowledge of desmids of East Pakistan, Part I. *Nowa Hedwigia* 20: 903-983 (1970).
14. Krieger, W. & J. Gerloff. *Die Gattung Cosmarium.* Vol. 1, Verlag J. Cramer, Weinheim (1962).
15. Krieger, W. & J. Gerloff. *Die Gattung Cosmarium.* Vol. 2, Verlag J. Cramer, Weinheim (1965).
16. Krieger, W. & J. Gerloff. *Die Gattung Cosmarium.* Vols. 3 & 4, Verlag J. Cramer, Weinheim (1969).
17. Kopp, R. Phytoplankton of the Zámecký Pond: Fytoplankton Zámeckého Rybníka. *Czech Phycology Olomouc* 6: 111-125 (2006).
18. Leghari, M. K., M. Y. Leghari & M. Shah. Ecological study of algal flora of Korang Nalla of Rawal Dam, Islamabad. *Biologia* 48: 65-80 (2002).
19. Masud-ul-Hasan & Zeb-un-Nisa. Taxonomic studies of the freshwater algae from Azad Jammu and Kashmir. *Biologia* 32: 229-256 (1986).
20. Masud-ul-Hasan. & I. Batool. A taxonomic study of some freshwater algae from Attock and Sargodha districts. *Biologia* 33: 345-366 (1987).
21. Masud-ul-Hasan. & A. Yunus. An addition to the algal flora of Lahore. *Biologia* 35: 99-131 (1989).
22. Novakovskaya, V. I. & E. N. Patova. Green algae in spruce forests in the north-east of European Russia. *Biologia Bratislava* 63: 836-842 (2008).
23. Rai, S. K., B. R. Subba & K. P. Limbu. Freshwater algae from running stream of Gajurmukhi VDC, Ilam, Nepal. *Our Nature* 6: 80-81 (2008).
24. Kitner, M., A. Poulíčková, R. Novotný & M. Hájek. Desmids (Zygnematophyceae) of the spring fens of a part of West Carpathians: Kràsivky Prameništ' čàsti zapadních karpat. *Czech Phycology Olomouc* 4: 43-61 (2004).
25. Sahin, B. & B. Akar. Epipelic and epilithic algae of Küçükgöl lake (Gümüşhane-Turkey). *Turkish Journal of Botany* 29: 57-63 (2005).
26. Sahin, B. & B. Akar. The desmid flora of some high mountain lakes of the Turkish eastern Black Sea region. *Pakistan Journal of Botany* 39: 1817-1832 (2007).
27. Sarim, F. M., Khair-un-Nisa & N. Afzal. Some freshwater algae of Tarbela Dam, Pakistan. *Pakistan Journal of Plant Sciences,* 14, 35-39 (2008).
28. Sherwood, A. R. Bibliographic checklist of the nonmarine algae of the Hawaiian Island. *Museum Occasional Papers* 80: 1-23 (2004).
29. ŠŤastný, J. The desmids of the swamp nature reserve (north Bohemia, Czech Republic) and a small neighbouring bog: Species composition and ecological condition of both sites. *Fottea* 9: 135-148 (2009).
30. ŠŤastný, J. Desmids (Conjugatophyceae, Viridiplantae) from the Czech Republic: New and rare taxa, distribution, ecology. *Fottea* 10: 1-74 (2010).

Proceedings of the Pakistan Academy of Sciences 49 (3): 187–192 (2012)

ISSN: 0377 - 2969

Pakistan Academy of Sciences

Original Article

A New Chewing Louse (Phthiraptera: Amblycera: Menoponidae) of *Anas platyrhynchos* (L.) from Karachi, Pakistan, having Parasitic Impact

Saima Naz* and Syed A. Rizvi

Department of Zoology, University of Karachi, Karachi-75270. Pakistan

Abstract: A new species of the genus *Holomenopon* Eichler (Phthirpatera: Amblycera: Menoponidae) has been described on the Common Duck, *Anas platyrhynchos* (L.), with special reference to its chaetotaxy and male, female genitalia. It has been compared with its closest species, *H. leucoxanthum* (Burmeister), on the same host. It is the first record of this genus from Karachi, Pakistan. The prevalence of the new species has been discussed, which is 4.8-37.3% and 9.2-35.9% in male and female ducks, respectively,. The intensity of infestation has also been recorded, that is 27.9-88.2% in two different localities of Karachi, Pakistan. The holotype and paratype are deposited in Natural History Museum, Department of Zoology, University of Karachi, Karachi, Pakistan.

Keywords: *Holomenopon*, new species, common duck, prevalence, intensity, Pakistan

1. INTRODUCTION

The genus *Holomenopon* Eichler [1] is a common but specific ecto-parasite of duck in Pakistan. It is represented by 16 species, and found on 81 species of Anatids (Anseriformes: Anatidae) worldwide. It is the host-specific genus and all its species have been recorded on family Anatidae only [2, 3].

The common duck, *Anas platyrhynchos* (L.) accommodates seven species of Mallophaga (Phthiraptera) throughout the world, *viz. Anaticola crassicornis* (Scopoli), *Anatoecus dentatus* (Scopoli), *A. icterodes* (Nitzsch), *Holomenopon leucoxanthum* (Burmeister), *H. maxbeieri* Eichler, *H. transvaalense* (Bedford) and *Trinoton querquedulae* (L.). Ansari [4] reported only two species, *Anaticola crassicornis* and *Anatoecus dentatus*, from *Anas platyrhynchos* from Lyallpur (now Faisalabad), but no chewing louse species of the common duck has yet been reported from Karachi [4-10].

It is the first record of the genus *Holomenopon* on *Anas platyrhynchos* from Karachi, Pakistan.

2. MATERIALS AND METHODS

The Common Duck has been observed for its lice species at two localities of Karachi (i.e., Safari Park, Gulshan Iqbal Town and Qaide Azam Park, Bin Qasim Town). Overall, about 780 specimens of lice have been collected from 15 birds.

The chewing lice were collected by using the pyrethroid sprayed in feathers of the bird, kept on a white paper sheet in the small cage. After 10 to 15 minutes, lice were shed off the bird by sprinkling the wings and feathers on to the sheet. They were preserved in 85% EtOH solution, mounted in Canada balsam by the standard method and microscopic investigations were undertaken by using the latest literature.

Illustrations and dimensions were made by using micro ocular graticule in light microscope and photographs were made by using Nikon P7000 digital camera through stereomicroscope, at 100x for whole mount and 400 x for terminalia and male genitalia. Measurements are given in millimeters (mm). Holotype and Paratypes were deposited in

Received, May 2012; Accepted, September 2012

*Corresponding author: Saima Naz; Email: dr.symanaz@gmail.com

Natural History Museum, University of Karachi (NHMUK).

Abbreviations used in this manuscript are: TL for total length, HL for head length, POW for preocular width, TW for temporal width, PL for prothorax length, PW for prothorax width, ML for metathorax length, MW for metathorax width, AL for abdominal length, GL for genitalia length and GW for genitalia width at the anterior end of parameres.

3. RESULTS

3.1 Holomenopon fatemae sp.n. (Fig. 1-13)

Type Host: *Anas platyrhynchos* (L.)

Dimensions: (♂: n=3, ♀: n=4) TL: ♂ 1.47 (1.475–1.482), ♀ 1.82 (1.772–1.885); HL ♂ 0.27 (0.269–0.286), ♀ 0.307 (0.286–0.338); POW ♂ 0.46 (0.429–0.50), ♀ 0.408 (0.403–0.416); TW ♂ 0.56 (0.55–0.58), ♀ 0.58 (0.57–0.59); PL ♂ 0.21 (0.201–0.213), ♀ 0.236 (0.215–0.26); PW ♂ 0.438 (0.43–0.443), ♀ 0.463 (0.455–0.468); ML ♂ 0.14 (0.115–0.156), ♀ 0.16 (0.155–0.169); MW ♂ 0.48 (0.472–0.507), ♀ 0.537 (0.527–0.546); AL ♂ 0.85 (0.845–0.855), ♀ 1.2(1.10–1.28).

3.1.1. Head (Fig. 1-7)

Anterior margin evenly rounded dilated posteriorly; dorso–lateral margin straight; DHS 9 very long and marginal; DHS 8, 10 and 11 short but 11 very much shorter; DHS 14–16 together in a line; DHS 17 widely separated from sensilla *d*, DHS 23 short, in temporal region, near to seta 22; hypopharynx developed; subocular seta longest; maxillary palpi (Fig. 5) short; antennal groove short and shallow; antennae (Fig. 6) short, with small, rounded flagellomere II, bearing two subterminal setae and terminal disc at very lateral side; gular plate (Fig. 7) rounded, sculptured with scaly texture, posterior gular setae very long (0.15-0.17).

Fig. 1-2: *Holomenopon fatemae* sp.n. 1 Male, 2 Female.

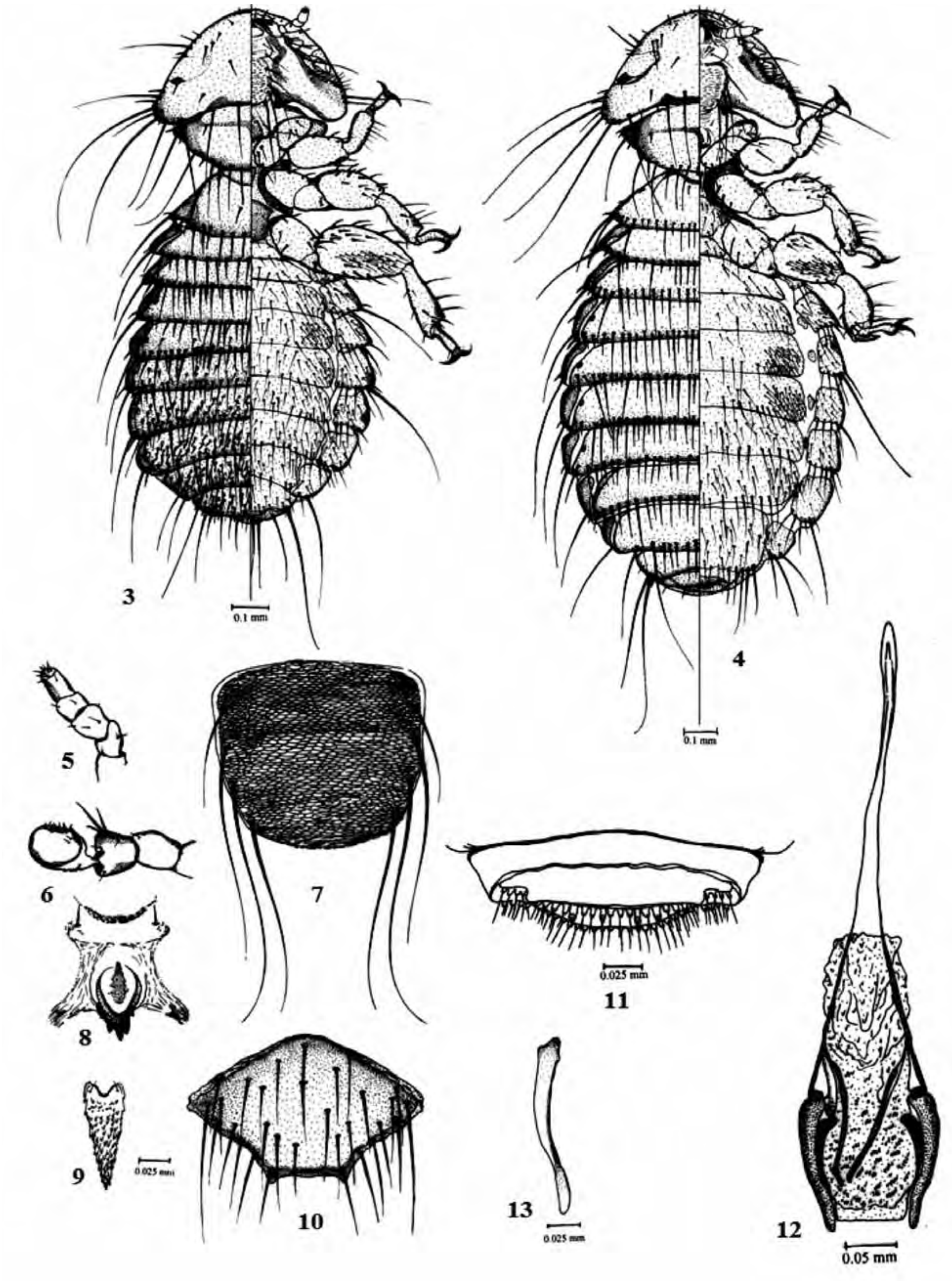

Fig. 3-13: *Holomenopon fatemae* sp.n. 3. Male, 4. Female, 5. Maxillary Palp, 6. Antenna, 7. Gular Plate, 8. Prosternal Plate, 9. Mesosternal Plate, 10. Metasternal Plate, 11. Female Vulval Margin, 12. Male Genitalia, 13. Paramere enlarged.

31.2. Thorax (Fig. 1-4, 8-10)

Pronotal anterior seta 2 evident in female; pronotal marginal setae 1, 2, 4, 6, 8 short and setae 3, 5, 7, 9, 10 long in female; pronotal marginal setae 1, 3, 5 short and setae 2, 4, 6-9 long in male; prosternal plate (Fig. 8) weakly sclerotized, roughly triangular, anteriorly membranous, bearing two anterior fine setae, posterior margin well sclerotized, with three–four dentations, lateral margins weakly developed; mesonotum very short; mesosternal plate (Fig. 9) elongated, characteristically speculated, with anterior margin shallow concave and one pair of microsetae at antero-ateral corners; metanotum large, two anteri?r metanotal setae present; posterior marginal metanotal setae 1, 4, 5 short and setae 2, 3, 6–10 long in male; marginal metanotal setae 1, 4, 5, 7–9, 11 shorter and 2, 3, 6, 10, 12–14 long in female; metasternal plate (Fig. 10) squat, large, bearing twenty nine thick, long and fine setae; coax I laterally expanded, bearing five posterior setae and four anterior setae; trochanter II and III with three microsensillae on each; femur III bears a large brush of spiniform microsetae; euplantula III dilated.

3.1.3. Abdomen (Fig. 1–4)

Male Abdomen: Shorter than female abdomen; tergites I–VII more or less equal in width, tergite VIII shorter; tergal marginal setae alternately long and short, in single row on tergites I–VIII: 20, 30, 30, 33, 31, 34, 20 and 16 respectively; anterior tergal setae densely present on tergites VI–VIII only; sternite I well developed, bears few setae at posterior; strnites III and VI with very thin setal brushes, sternites IV and V with relatively thick setal brushes; sternal chaetotaxy as on strnites I–VII: 9, 12, 14, 22, 30, 58 and 50 respectively; sternites usually separated from pleurites by a very small pleuro–steal sclerite.

3.1.4. Male Terminalia

Tergite IX larger than very short tergite X; tergite IX bearing thirty three scattered setae, two pairs of lateral setae, one long and one short, nine alternately short and long marginal setae at posterior margin present; sternite VIII separated from subgenital plate; anal margin with six normal fine posterior marginal setae and two very long latero–posterior setae.

3.1.5. Female Abdomen

Broad and oblong; anterior tergal setae usually absent; tergal marginal setae on tergites I–VIII: 24, 28, 31, 36, 34, 29, 28 and 14 respectively; sternites with irregularly scattered thin fine setae; sternite IV and V with thick setal brushes; sternal marginal setae on sternite I–VII: 9, 22–25, 47, 16, 27, 66–68 and 70 respectively; pleuro–sternal sclerites relatively larger than male; pleurites with six–seven fine posterior marginal setae.

3.1.6. Female Terminalia

Tergite IX larger with trapezoidal shape, without anterior and marginal setae; two pairs of long to very long lateral setae present (0.335 inner seta and 0.455 outer seta); dorso–posterior margin with six very short microsetae; subgenital plate wide and large (Fig. 4), with wavy posterior margin, bearing five pairs of long fine latero–posterior setae and thirty nine–forty median to posterior scattered, short fine setae; anal margin (Fig. 11) oval, narrow; anterior fringe of anal margin bearing four a–typical setae among the twenty two normal setae, attached on hyaline base and thirty similar setae in posterior margin.

3.1.7. Male Genitalia (Fig. 12–13)

Dimensions: GL: 0.63 (0.630–0.640); GW 0.14 (0.141–0.142).

Basal apodeme elongated, narrow to tapering anteriorly into blade like end; parameres (Fig. 12) elongated, measure 0.1425 (0.140–0.145), rod like, broader anteriorly, slightly curved posteriorly, reaching behind the posterior margin of endomere; endomeral plate narrower, with posterior margin very straight; genital sac with very minute fine spicules; genital sclerites two elongated, narrow, rods, more or less V–shaped, in median to posterior position, measuring 0.12–0.125.

3.1.8. Material Examined

HOLOTYPE: 1♂, on *Anas platyrhynchos*, niche:

Table 1. Number of chewing louse, *Holomenopon fatemae* sp. n., its prevalence and mean intensity on common Ducks, *Anas platyrhynchos* (L.), in Karachi, Pakistan.

Locality	**Ducks Examined**				**No. of lice collected from total ducks**	**Prevalence (%)**		**Mean Intensity**
	Male ducks	No. of lice	Female ducks	No. of lice		**Male ducks**	**Female ducks**	
Qaid Azam Park, Bin Qasim Town, Karachi	A1	12	A5	29	251	4.78	11.55	27.88
	A2	24	A6	23		9.56	9.16	
	A3	13	A7	37		5.18	14.74	
	A4	28	A8	41		11.16	16.33	
			A9	44			17.53	
	Total Lice	77	TotalLice	174		100	100	
Safari Park, Gulshan Iqbal Town Karachi	A10	77	A13	102	529	35.48	32.69	88.16
	A11	81	A14	98		37.33	31.41	
	A12	59	A15	112		27.19	35.90	
	Total Lice	217	Total Lice	312		100	100	

wing and ramp feathers; Karachi, Pakistan; 02-I-2007; leg. S. Naz. PARATYPE: 3♂, 3♀, on *Anas platyrhynchos*, same data.

3.1.9. Etymology

This new species of the genus *Holomenopon* has been given the name in the credit of first author's daughter, Fatema Naaz.

4. REMARKS AND DISCUSSIONS

The *Holomenopon fatemae* sp.n. is closely related to the *H. leucoxanthum* on the basis of some specific characters, which lay this species in the *leucoxanthum* group of the genus. It resembles in the characters given by Price [2], including female anal fringe with at least four a-typical setae; without mid–dorsal setae adjacent to sensilla *d*; TW less than 0.7; mesosternal and metasternal plates are almost similar as in Price [2: Fig 7, 8]; posterior postmental setae always long; metanotum with two anterior setae; male genital sclerites have similar shape in both species [2, 11]. But the present species can easily be separated from *H. leucoxanthum* by having shape of anal opening and arrangement of anal setae with base more protruded in *H. fatemae*, number of metasternal setae fifteen–twenty five in *H. leucoxanthum* and twenty nine–thirty one in *H. fatemae*.

The male genitalia are also clearly variable in having more extended endomeral plate, with posterior margin slightly concave; parameres more broader and expanded antero–laterally and more narrow posteriorly; genital sac sclerite anteriorly curved, shorter (0.1–0.125) in *H. leucoxanthum*, whereas in *H. fatemae*, the genital sclerite more expanded anteriorly, longer (0.13–0.135); endomeral plate less expanded, with even corners and clearly straight posterior margin; parameres spatulate anteriorly and slightly narrow mid–anteriorly, posteriorly curved inward outside, as described above.

Besides the above characteristic differences the present species is successfully grown up on the host, *Anas platyrhynchos* in the region, and designated as a new species of the genus *Holomenopon.*

During the present study, 15 birds were examined at two localities of Karachi, infested with total of 780 specimens (251 and 529 respectively) of *Holomenopon fatemae* sp.n. (Tab. 1). These ducks were examined in two very different localities of Karachi region, Safari Park at Gulshan Iqbal Town and Qaid Azam Park at Bin Qasim Town.

In Qaid Azam Park, male ducks (n=4) harbor 77 lice. Their infestation with maximum number of lice was recorded 28 and minimum infestation was recorded 12, with the prevalence ranges from 4.78–11.16%. The female ducks (n=5) were more infested (174 lice) than their males, with maximum 44 and minimum 23 lice per bird. Their prevalence ranges 9.16–17.53%, showed low rate of infestation.

In Safari Park, 6 ducks examined for their lice with total Male ducks (n=3) harbor 217 lice specimens and found maximum infestation was 81 (37.33% prevalence) and minimum infestation was 59 (27.19% prevalence). In this locality, female ducks (n=3) were again highly infested (312 specimens of lice), with maximum 112 and minimum 98 lice. Their prevalence ranges 31.41–35.90% that showed medium rate of infestation on these quite healthy ducks, *Anas platyrhynchos.* However, in this group of ducks, the common duck louse *H. leucoxanthum* (Burmeister) was also recorded in few numbers (5–9) on only two birds from Safari Park, Gulshan Iqbal Town, Karachi.

The mean intensity of parasitism in ducks of both localities ranging 27.88–88.16, and prevalence on male and female ducks ranging 4.78–37.33 % and 9.16–35.90 % respectively.

Overall infestation of both *H. leucoxanthum* and *H. fatemae* and their parasitic intensity found very low to medium in the region, hence no significant parasitic effect showed in ducks [10, 12, 13].

5. REFERENCES

1. Eichler, W. Zur Klassifikation der lauskerfe (Phthiraptera Haeckel: Rhynchophthirina, Mallophaga und Anoplura). *Archiv f¸r Naturgeschichte* 10(3): 345-398 (1941).
2. Price, R.D. A review of the genus *Holomenopon* (Mallophaga: Menoponidae) from the Anseriformes*; Annals of the Entomological Society of America* 64(3): 633-646 (1971).
3. Price, R.D., D.H. Clayton, R.A. Hellenthal, K.P. Johnson & R.L. Palma, The chewing lice: world checklist and biological overview. *Illinois Natural History Survey,* Special Publication 24: 1–105+X (2003).
4. Ansari, M.A.R. Mallophaga (Ischnocera) infesting birds in the Punjab (India). *Proceedings of the National Institution of Science, India* 13(6): 253-303 (1947).
5. Ansari, M.A.R. Studies on the Amblyceran Mallophaga infesting birds in Pakistan. *Proceedings of the 7th Pakistan Scientific Conference, Agriculture, Bahawalpur, Pakistan,* pp. 51–57 (1955).
6. Ansari, M.A.R. Some new Ischnoceran Mallophaga in the Zoological Survey Department, Karachi. *Pakistan Journal of Scientific Research* 8(1): 10-22 (1956 a).
7. Ansari, M.A.R. Description of some new Amblyceran Mallophaga from the Zoological Survey Department, Karachi. *Pakistan Journal of Scientific Research*8(2): 57-61 (1956 b).
8. Ansari, M.A.R. Studies on the Ischnoceran Mallophaga infesting birds in Pakistan*. Proceedings of the 7thPakistan Scientific Conference, Biology, Bahawalpur, Pakistan* 42: 42-62 (1957).
9. Lakshminarayana, K.V. A synoptic list of Mallophaga *sens. lat.* (Phthiraptera: Insecta) from India and adjacent countries together with host and regional indices. *Records of the Zoological Survey, India* 75: 39-201 (1979).
10. Naz, S., S.A. Rizvi & O. Sychra, *Anaticola crassicornis* (Phthiraptera: Ischnocera: Philopteridae) on wild geese from Pakistan; *Zootaxa* 2659: 60-66 (2010).
11. Burmeister, H.C.C. Mallophaga. 418-443, In: *Handbuch der Entomologie* 2(1): Berlin: Enslin (1838).
12. Broderson, D., A.G. Canaris, & J.R. Bristol, Parasites of waterfowl from Southwest Texas: II. The shoveler, *Anas clypeata. Journal of Wildlife Diseases* 13: 435-439 (1977).
13. Canaris, A.G., A.C. Mena, & J.R. Bristol, Parasites of waterfowl from Southwest Texas. III. The green-winged teal, *Anas crecca. Journal of Wildlife Diseases* 17: 57-64 (1981).

Proceedings of the Pakistan Academy of Sciences 49 (3):193–198 (2012)

ISSN: 0377 - 2969

Pakistan Academy of Sciences

Original Article

Hall Effects on Rayleigh-Stokes Problem for Heated Second Grade Fluid

Masud Ahmad* and Muhammad Yaseen

Department of Mathematics, University of Sargodha,
Sargodha, Pakistan

Abstract: The aim of the present paper is to discuss the influence of Hall current on the flows of second grade fluid. Two illustrative examples have been considered (i) Stokes first problem for heated flat plate (ii) The Raleigh-Stokes problem for a heated edge. Expressions for velocity and temperature distributions are obtained. The results for hydrodynamic fluid can be obtained as the limiting cases.

PACS Code 47.85.-g

Keywords: Heated plate and edge, Hall effect, second grade fluid, Fourier Sine transform

1. INTRODUCTION

Recently, the Rayleigh Stokes problem for a flat plate and an edge has acquired a special status. The solution of Stokes first problem for a Newtonian fluid is obtained employing similarity transformations in [1, 2]. But for the same problem in second grade fluid such similarity transformations are not useful [3]. In general, the governing equations of second grade fluid are one order higher than the Navier-Stokes equation and to obtain an analytic solution is not so easy. Also for a unique solution one needs an extra condition. For the detail of this issue, I may refer the readers to the references [4-7]. In study [8] Bandelli et al. discussed the Stokes first problem using Laplace transformation treatment. It is shown that the resulting solution does not satisfy the initial condition. Fetecau and Zierep [9] removed this difficulty by using Fourier Sine transform technique. Christov and Christov [10] have given comments on [9] by showing that solution of [9] is incorrect and have given the correct solution. Heat transfer analysis on the unidirectional flows of a second grade fluid is examined by Bandelli [11]. In continuation Fetecau and Fetecau [12,13] analyzed the temperature distribution in second grade and Maxwell fluids for laminar flow on a heated flat plate and in a heated edge. The purpose of the present investigation is to extend the analysis of reference [12] for Hall effects. The corresponding results of Newtonian fluid can be recovered by choosing $\alpha = 0$. In absence of Hall effects, the results can be obtained by letting $\boldsymbol{B}_0 = 0$.

2. BASIC EQUATIONS

For second grade fluid the Cauchy stress tensor $\boldsymbol{T}$ is

$$T = -pI + \mu A_1 + \alpha_1 A_2 + \alpha_2 A_1^2, \tag{1}$$

where p is the scalar pressure, $\boldsymbol{I}$ is the identity tensor, μ is the coefficient of viscosity, $\alpha_i \ (i = 1, 2)$ are the material parameters of second grade fluid and $\boldsymbol{A}_i \ (i = 1, 2)$ are the first two Rivlin-Ericksen tensors defined through

$$A_1 = (grad\, V) + (grad\, V)^T \tag{2}$$

$$A_2 = \frac{d\mathrm{A}_1}{dt} + A_1 (grad V) + (grad V)^T A_1 \tag{3}$$

Received, November 2011; Accepted, September 2012
*Corresponding author: Masud Ahmad, E-mail: amasud112@yahoo.com

in which t is the time. The issue regarding the signs of α_1 and α_2 is controversy. For detailed analysis relevant to this issue, one may refer the readers to the references [14, 15]. The equations governing the MHD flow of heated fluid are:
Continuity equation:

$$div V = 0. \tag{4}$$

Equation of motion:

$$\rho \frac{dV}{dt} = div T + (J \times B). \tag{5}$$

Energy equation:

$$\rho \frac{de}{dt} = T.(grad V) - div q + \rho r. \tag{6}$$

Maxwell equations:

$$div B = 0, \qquad Curl B = \mu_m J, \qquad Curl E = -\frac{\partial B}{\partial t}. \tag{7}$$

Generalized Ohm's law:

$$J + \frac{w_e \tau_e}{B_0}(J \times B) = \sigma(E + V \times B). \tag{8}$$

In above equations J is the current density, $B(=B_0 + b)$ is the total magnetic field, B_0 is the applied magnetic field, b is the induced magnetic field, σ is the electrical conductivity of the fluid, E is the electric field, μ_m is the magnetic permeability, $\frac{d}{dt}$ is the material derivative, $e(=c\theta)$ is the internal energy, ρ is the fluid density, c is the specific heat, θ is the temperature, $q(= -grad\theta)$ is the heat flux vector, r is the radial heating, w_e and τ_e are the cyclotron frequency and collision time of electron respectively. It is assumed that $E = 0$ and $b = 0$. Further $w_e\tau_e \approx O(1)$ and $w_i\tau_i << 1$ (where w_i and τ_i are cyclotron frequency and collision time for ions respectively). Under the aforementioned assumptions, Eq (5) becomes

$$\frac{dV}{dt} = \frac{1}{\rho} div T - \frac{\sigma B_0^2 (1 + i\phi) V}{\rho(1 + \phi^2)}, \tag{9}$$

where $\phi = w_e \tau_e$ is the Hall parameter.

3. THE FIRST PROBLEM OF STOKES FOR A HEATED FLAT PLATE WITH HALL CURRENT

Let a second grade fluid, at rest, fill the space above an infinitely extended plate in (y, z)-plane. When time $t = 0^+$, the plate starts suddenly to slide, in its own plane, with velocity V. Let T(t) and f(x) denote the temperature of the plate for $t \geq 0$ and the temperature of the fluid at the moment $t = 0$. The velocity and temperature fields are

$$V = v(x,t)\hat{j}, \qquad \theta = \theta(x,t). \tag{10}$$

where $\hat{j}$ is a unit vector in the y-direction. The continuity equation (4) is identically satisfied. Furthermore, Equations (6) and (9) give

$$(\upsilon + \alpha \frac{\partial}{\partial t}) \frac{\partial^2 v(x,t)}{\partial x^2} - \frac{\sigma B_0^2 (1 + i\phi) v(x,t)}{\rho(1 + \phi^2)} = \frac{\partial v(x,t)}{\partial t}, \qquad x > 0, \quad t > 0, \tag{11}$$

$$\beta \frac{\partial^2 \theta(x,t)}{\partial x^2} + g(x,t) = \frac{\partial \theta(x,t)}{\partial t}, \qquad x > 0, \quad t > 0, \tag{12}$$

where $\upsilon = \mu / \rho$ is the kinematic viscosity,

$$\alpha = \frac{\alpha_1}{\rho}, \quad \beta = \frac{k}{\rho c}$$

$$g(x,t) = (\frac{\upsilon}{c}) \left[\frac{\partial v(x,t)}{\partial x} \right]^2 + \frac{r(x,t)}{\rho c}.$$

The relevant initial and boundary conditions are

$$v(x,0) = 0, \quad x > 0, \quad v(0,t) = V(t), \quad t > 0, \tag{13}$$

$$\theta(x,0) = f(x), \quad x > 0; \quad \theta(0,t) = T(t), \quad t \geq 0, \tag{14}$$

$$v(x,t), \quad \frac{\partial v(x,t)}{\partial x}, \quad \theta(x,t), \quad \frac{\partial \theta(x,t)}{\partial x} \to 0 \quad as \quad x \to \infty. \tag{15}$$

By Fourier Sine transform, the solution for v is

$$v(x,t)=\frac{2}{\pi}\int_0^\infty \frac{\upsilon\xi(1+\phi^2)}{\left\{\sigma B_0^2(1+i\phi)+\upsilon\xi^2(1+\phi^2)\right\}}$$

$$\left[V(t)-V(0)\exp\left\{-\frac{\left\{\sigma B_0^2(1+i\phi)+\upsilon\xi^2(1+\phi^2)\right\}}{(1+\phi^2)(1+\alpha\xi^2)}t\right\}\right]\sin\xi x d\xi$$

$$-\frac{2}{\pi}\int_0^\infty\left[\begin{array}{l}\dfrac{\xi\left\{\upsilon(1+\phi^2)-\alpha\sigma B_0^2(1+i\phi)\right\}}{(1+\alpha\xi^2)\left\{\sigma B_0^2(1+i\phi)+\upsilon\xi^2(1+\phi^2)\right\}}\\ \displaystyle\int_0^t V'(\tau)\exp\left\{-\frac{\left\{\sigma B_0^2(1+i\phi)+\upsilon\xi^2(1+\phi^2)\right\}}{(1+\phi^2)(1+\alpha\xi^2)}(t-\tau)\right\}d\tau\end{array}\right]$$

$$\sin\xi x d\xi. \tag{16}$$

If the plate moves with constant velocity *V*, then $V'(\tau)=0$ and the above equation simplifies to:

$$v(x,t)=\frac{2}{\pi}\int_0^\infty \frac{\upsilon\xi(1+\phi^2)}{\left\{\sigma B_0^2(1+i\phi)+\upsilon\xi^2(1+\phi^2)\right\}}$$

$$\left[V(t)-V(0)\exp\left\{-\frac{\left\{\sigma B_0^2(1+i\phi)+\upsilon\xi^2(1+\phi^2)\right\}}{(1+\phi^2)(1+\alpha\xi^2)}t\right\}\right]\sin\xi x d\xi. \tag{17}$$

For B_0 = 0, we get the results of reference [12] as

$$v(x,t)=V\left[1-\frac{2}{\pi}\int_0^\infty \exp\left\{\frac{-\upsilon\xi^2}{1+\alpha\xi^2}t\right\}\frac{\sin\xi x}{\xi}d\xi\right]. \tag{18}$$

When $\alpha\to 0$ the above equation yields

$$v(x,t)=V\left[1-Erf\left(\frac{x}{2\sqrt{\upsilon t}}\right)\right], \tag{19}$$

where Erf (x) is the error function of Guass. Employing the same methodology as for v we obtain

$$\theta(x,t)=T\left[1-Erf\left(\frac{x}{2\sqrt{\beta t}}\right)\right]$$

$$+\int_0^t T'(\tau)\left[1-Erf\left(\frac{x}{2\sqrt{\beta(t-\tau)}}\right)\right]d\tau+$$

$$\sqrt{\frac{2}{\pi}}\int_0^\infty \exp(-\beta\xi^2 t)\sin(x\xi)$$

$$\left[f_s(\xi)+\int_0^t g_s(\xi,\tau)\exp(\beta\xi^2\tau)d\tau\right]d\xi, \tag{20}$$

$$T=\lim_{t\to 0}T(t)$$

At rest, the temperature distribution is the same in presence of Hall currents as for a second grade fluid and for a Newtonian one. Further if the radiant heating $r(x,t)$ is negligible quantity the relation (20) takes the same form as in [12], i.e.,

$$\theta(x,t)=T\left[1-Erf\left(\frac{x}{2\sqrt{\beta t}}\right)\right]$$

$$+\int_0^t T'(\tau)\left[1-Erf\left(\frac{x}{2\sqrt{\beta(t-\tau)}}\right)\right]d\tau+$$

$$\sqrt{\frac{2}{\pi}}\int_0^\infty \sin(x\xi)f_s(\xi)\exp(-\beta\xi^2 t)d\xi. \tag{21}$$

From the above results we see that, if $t\to\infty$, then $\theta(x,t)\to T(\infty)$.

Moreover, if the initial temperature of the fluid is zero and the plate is kept to the constant temperature T, Eq. (21) gives

$$\theta(x,t)=T\left[1-Erf\left(\frac{x}{2\sqrt{\beta t}}\right)\right], \tag{22}$$

and $\theta(x,t)\to T \quad as \quad t\to\infty.$

4. THE RAYLEIGH-STOKES PROBLEM FOR HEATED EDGE WITH HALL CURRENT

Consider a second grade fluid at rest occupying the space of the first dial of rectangular edge (x ≥ 0, $-\infty<y<\infty,\ z\geq 0)$. For t = 0^+, the extended edge is impulsively brought to the constant speed V. The walls of the edge have temperature $T(t)$. The velocity and temperature fields are

$$\boldsymbol{V}=v(x,z,t)\hat{\boldsymbol{j}}, \tag{23}$$

$$\theta=\theta(x,z,t).$$

Equations (6) and (9) here are of the following forms:

$$\left(\nu+\alpha\frac{\partial}{\partial t}\right)\left(\frac{\partial^2}{\partial x^2}+\frac{\partial^2}{\partial z^2}\right)v(x,z,t)$$

$$-\frac{\sigma B_0^2(1+i\phi)}{\rho(1+\phi^2)}v(x,z,t)=\frac{\partial}{\partial t}v(x,z,t), \tag{24}$$

$$x>0,\quad z>0,\quad t>0,$$

$$\beta\left[\left(\frac{\partial^2}{\partial x^2}+\frac{\partial^2}{\partial z^2}\right)\theta(x,z,t)\right] \tag{25}$$

$$+g(x,z,t)=\frac{\partial}{\partial t}\theta(x,z,t),$$

$$x>0,\quad z>0,\quad t>0,$$

where

$$g(x,t)=\left(\frac{v}{c}\right)\left\{\begin{array}{l}\left[\dfrac{\partial v(x,z,t)}{\partial x}\right]^2\\ +\left[\dfrac{\partial v(x,z,t)}{\partial z}\right]^2\end{array}\right\}+\frac{r(x,z,t)}{\rho c}.$$

The corresponding initial and boundary conditions are

$$v(x,z,0)=0,\quad x>0,\quad z>0,$$

$$v(0,z,t)=v(x,0,t)=V,\qquad t>0, \tag{26}$$

$$\theta(x,z,0)=f(x,z),\quad x>0;\quad z>0;$$

$$\theta(0,z,t)=\theta(x,0,t)=T(t),\quad t\geq 0, \tag{27}$$

where the function $f(x,z)$ represents the temperature distribution of the fluid at the moment t = 0. Moreover, $v(x,z,t)$, $\theta(x,z,t)$ and their partial derivatives with respect to x and z have to tend to zero as $x^2+z^2\to\infty$.

Following the same method of solution as in section 3, we obtain

$$v(x,z,t)=\frac{4}{\pi^2}\int_0^\infty\int_0^\infty\frac{\upsilon(\xi^2+\eta^2)(1+\phi^2)}{\eta\xi\left\{\sigma B_0^2(1+i\phi)+\upsilon(\xi^2+\eta^2)(1+\varphi^2)\right\}}\times$$

$$\left[V(t)-V(0)\exp\left[-\left\{\frac{\left\{\sigma B_0^2(1+i\phi)+\upsilon(\xi^2+\eta^2)(1+\varphi^2)\right\}}{(1+\phi^2)\left\{1+\alpha(\xi^2+\eta^2)\right\}}t\right\}\right]\right]\times$$

$$\sin\xi x\sin\eta z\,d\xi d\eta+\frac{4}{\pi^2}\int_0^\infty\int_0^\infty\frac{(\xi^2+\eta^2)}{\eta\xi\left\{1+\alpha(\xi^2+\eta^2)\right\}}\times$$

$$\left[\begin{array}{l}\dfrac{\alpha\sigma B_0^2(1+i\phi)-\mu(1+\varphi^2)}{\sigma B_0^2(1+i\phi)+\mu(\xi^2+\eta^2)(1+\varphi^2)}\\ \displaystyle\int_0^t V'(\tau)\exp\left[-\frac{\left\{\sigma B_0^2(1+i\phi)+\upsilon(\xi^2+\eta^2)(1+\varphi^2)\right\}}{(1+\phi^2)\left\{1+\alpha(\xi^2+\eta^2)\right\}}(t-\tau)\right]d\tau\end{array}\right]\times$$

$$\sin\xi x\sin\eta z\,d\xi d\eta. \tag{28}$$

When plate has constant velocity *V*, then $V'(\tau)=0$ and the above equation reduces to

$$v(x,z,t)=\frac{4}{\pi^2}$$

$$\int_0^\infty\int_0^\infty\frac{\mu(\xi^2+\eta^2)(1+\phi^2)}{\eta\xi\left\{\sigma B_0^2(1+i\phi)+\mu(\xi^2+\eta^2)(1+\varphi^2)\right\}}\times$$

$$\left[V(t)-V\exp\left[-\left\{\frac{\left\{\sigma B_0^2(1+i\phi)+\mu(\xi^2+\eta^2)(1+\varphi^2)\right\}}{\rho(1+\phi^2)\left\{1+\alpha(\xi^2+\eta^2)\right\}}t\right\}\right]\right]\times$$

$$\sin\xi x\sin\eta z\,d\xi d\eta. \tag{29}$$

For B_0 = 0 above equation reduces to the result of [12].

$$v(x,z,t)=V\left[1-\frac{4}{\pi^2}\int_0^\infty\int_0^\infty\frac{\sin\xi x}{\xi}\times\frac{\sin\eta z}{\eta}\times\exp\left[-\frac{\nu(\xi^2+\eta^2)}{1+\alpha(\xi^2+\eta^2)}d\xi d\eta\right]\right]. \tag{30}$$

The expression of temperature is

$$\theta(x,z,t)=T\left[1-Erf\left(\frac{x}{2\sqrt{\beta t}}\right)Erf\left(\frac{z}{2\sqrt{\beta t}}\right)\right]$$

$$+\int_0^t T'(\tau)\left[1-Erf\left(\frac{x}{2\sqrt{\beta(t-\tau)}}\right)Erf\left(\frac{z}{2\sqrt{\beta(t-\tau)}}\right)\right]d\tau$$

$$+\frac{2}{\pi}\int_0^\infty\int_0^\infty\exp\left\{-\beta(\xi^2+\eta^2)\right\}\sin(x\xi)\sin(z\eta)$$

$$\left[f_s(\xi,\eta)+\int_0^t g_s(\xi,\eta,\tau)\times e\,\mathrm{xp}\left\{\beta(\xi^2+\eta^2)\tau\right\}d\tau\right]d\xi d\eta. \tag{31}$$

in which $f_s(\xi,\eta)$ *and* $g_s(\xi,\eta,t)$ are the double Fourier sine transforms of the functions $f(x,z)$ *and* $g(x,z,t)$ with respect to the variables x and z. When $\alpha\to 0$, relations (30) and (31) reduce again to those resulting from the Navier-Stokes fluids. Thus, we recover the universal profile of velocity [2].

$$v(x,z,t)=V\left[1-Erf\left(\frac{x}{2\sqrt{\nu t}}\right)Erf\left(\frac{z}{2\sqrt{\nu t}}\right)\right], \tag{32}$$

in which only similarity variables $x/\sqrt{\nu t}$ *and* $z/\sqrt{\nu t}$ occur. For $z \to \infty$, $v(x,z,t)$ goes to $v(x,t)$ given by (19). The expression for $\theta(x,z,t)$ is

$$\theta(x,z,t) = T\left[1 - Erf\left(\frac{x}{2\sqrt{\beta t}}\right)Erf\left(\frac{z}{2\sqrt{\beta t}}\right)\right] + \int_0^t T'(\tau)\left[1 - Erf\left(\frac{x}{2\sqrt{\beta(t-\tau)}}\right)Erf\left(\frac{z}{2\sqrt{\beta(t-\tau)}}\right)\right]d\tau, \quad (33)$$

which for $z \to \infty$ goes to

$$\theta(x,z,t) = T\left[1 - Erf\left(\frac{x}{2\sqrt{\beta t}}\right)\right] + \int_0^t T'(\tau)\left[1 - Erf\left(\frac{x}{2\sqrt{\beta(t-\tau)}}\right)\right]d\tau. \quad (34)$$

If the edge is maintained to the constant temperature T, Eq. (33) takes the form

$$\theta(x,z,t) = T\left[1 - Erf\left(\frac{x}{2\sqrt{\beta t}}\right)Erf\left(\frac{z}{2\sqrt{\beta t}}\right)\right], \quad (35)$$

and $\theta(x,z,t) \to T$ *as* $t \to \infty$.

5. CONCLUSIONS

In this paper, the exact solutions for laminar flow of an electrically conducting non-Newtonian fluid are obtained. The velocity field and the temperature distribution in a second grade fluid on heated flat plate and on a heated edge in the presence of Hall current are determined. These solutions are obtained using simple and double Fourier sine transforms and presented as a sum of steady state and transient solutions. For large values of time, when transient disappear, these solutions reduce to steady-state solutions. Direct calculations show that $\theta(x,t)$ and $\theta(x,z,t)$ of Eqs. (20) and (31) as well $v(x,t)$ and $v(x,z,t)$ of Eqs. (16) and (30) satisfy the corresponding partial differential equations together with the initial and boundary conditions.

Putting B_0 = 0 in Eqs. (17) and (29), we obtain the results of [12]. If we put $\alpha \to 0$ in (17), (20), (30) and (31), we find corresponding solutions for the Navier-Stokes fluid. In a fluid at rest the temperature distribution is the same whether it is second grade or not. If the radiant heating is negligible $\theta(x,t)$ and $\theta(x,z,t)$ become $T(\infty)$ *as* $t \to \infty$ or T if the plate and the edge are maintained to the constant temperature. The corresponding results in absence of Hall current can be obtained by choosing B_0 = 0.

6. REFERENCES

1 Zierep, J. *Similarity Laws and Modeling.* Marcel Dekker, New York (1971).

2 Zierep, J. Das Rayleigh-Stokes problem fur die Ecke. *Acta Mechanica* 34: 161-165 (1979).

3 Tiepel, I. The impulsive motion of a flat plate in a viscoelastic fluid. *Acta Mechanica* 39: 277-279 (1981).

4 Rajagopal, K.R. & A.S. Gupta. An exact solution for the flow of a non-Newtonian fluid past an infinite porous plate. *Mechanica* 19: 1948-1954 (1984).

5 Rajagopal, K. R. On the creeping flow of the second-order fluid. Journal of Non-Newtonian. *Fluid Mechanics* 15**:** 239-246 (1984).

6 Rajagopal, K.R. & N.P. Kaloni. *Some Remarks on Boundary Conditions for Flows of Fluids of the Differential Type.* Proceedings of Canadian Applied Mathematics Society, Barnaby, Canada (1989).

7 Rajagopal, K.R. On boundary conditions for fluids of differential type, In: *Navier-Stokes equations and related non-linear problems,* A. Sequiera (Ed.). Plenum Press , New York (1995).

8 Bandelli, R., K.R. Rajagopal, & G.P. Galdi. On some unsteady motions of fluids of second grade. *Archive Mechanics* 47 (4): 661-676 (1995).

9 Fetecau, C., & J. Zierep. On a class of exact solutions of the equations of motion of a second grade fluid. *Acta Mechanica* 150**:** 135-138 (2001).

10 Christov, I.C. & C.I. Christov. Comments on “On a class of exact solutions of the equations of motion of a second grade fluid”. *Acta Mechanica* 215: 25-28 (2010).

11 Bandelli, R. Unsteady unidirectional flows of second grade fluids in domains with heated boundaries. *International Journal of Non-Linear Mechanics* 30: 263-269 (1995).

12 Fetecau, C., & C. Fetecau. The Rayleigh-Stokes problem for heated second grade fluids. *International Journal of Non- Linear Mechanics* 37: 1011-1015 (2002).

13 Fetecau, C., & C. Fetecau. The Rayleigh-Stokes-Problem for a fluid of Maxwellian type. *International Journal of Non-Linear Mechanics* 38: 603-607 (2003).

14 Dunn, J.E. Rajagopal, K.R. Fluids of differential type: critical review and thermodynamic analysis. *International Journal of Engineering Sciences* 33: 689-728 (1995).

15 Fosdick, R.L. & K.R. Rajagopal. Anomalous features in the model of second order fluids. *Archive for Rational Mechanics and Analysis* 70: 145-152 (1980).

16 Sneddon, I.N. Functional Analysis, In: *Encyclopedia of Physics,* Vol. II. Springer, Berlin, (1955).

Proceedings of the Pakistan Academy of Sciences 49 (3): 199–207 (2012)

ISSN: 0377 - 2969

Pakistan Academy of Sciences

Original Article

Exact and Numerical Solution for Fractional Differential Equation based on Neural Network

Hamid A. Jalab[1], Rabha W. Ibrahim[2]*, Shayma A. Murad[3], Samir B. Hadid[4]

[1]Faculty of Computer Science and Information Technology, University Malaya, 50603, Malaysia
[2]Institute of Mathematical Sciences, University Malaya, 50603, Malaysia
[3]Department of Mathematics, Faculty of Science, Duhok University, Kurdistan, Iraq
[4]Department of Mathematics and Basic Sciences, College of Education and Basic Sciences, Ajman University of Science and Technology, UAE

Abstract: In this paper a fractional differential equations based on Riemann-Liouville fractional derivatives are solved exactly. The solution is obtained in terms of H-functions and it is finite for all times. Moreover, by using the neural network method, we have estimated the numerical solution for some special equations.

Keywords: Fractional calculus, Riemann-Liouville fractional operators, exact solution, fractional differential equations, neural network, hypergeometric function

1. INTRODUCTION

The class of fractional differential equations of various types plays important roles and tools not only in mathematics but also in physics, control systems, dynamical systems and engineering to create the mathematical modeling of many physical phenomena. Naturally, such equations required to be solved. Many studies on fractional calculus and fractional differential equations have appeared, involving different operators such as Riemann-Liouville operators, Erdélyi-Kober operators, Weyl-Riesz operators, Caputo operators and Grünwald-Letnikov operators. The existence of positive solution and multi-positive solutions for nonlinear fractional differential equation are established and studied [1-4]. Moreover, by using the concepts of the subordination and superordination of analytic functions, the existence of analytic solutions for fractional differential equations in complex domain are suggested and posed in [5-8]. In addition, a generalization of fractional operators in the unit disk is imposed in [9]. One of the most frequently used tools in the theory of fractional calculus is furnished by the Riemann-Liouville operators [10]. The Riemann-Liouville fractional derivative could hardly pose the physical interpretation of the initial conditions required for the initial value problems involving fractional differential equations. Moreover, this operator possesses advantages of fast convergence, higher stability and higher accuracy to derive different types of numerical algorithms [11].

Our aim is to find the exact solution for different kind of fractional differential equations in sense of Riemann-Liouville fractional derivative, in terms of H-functions. Numerical solution for some equations are introduced by using the neural network.

Received, March 2012; Accepted, September 2012
*Corresponding author: Rabha W. Ibrahim. E-mail: rabhaibrahim@yahoo.com

2. PRELIMINARIES

Definition 2.1. The fractional (arbitrary) order integral of the function f of order $\alpha > 0$ is defined by

$$I_a^\alpha f(t) = \int_a^t \frac{(t-\tau)^{\alpha-1}}{\Gamma(\alpha)} f(\tau)d\tau.$$

When $a = 0$, we write $I_a^\alpha f(t) = f(t) * \phi_\alpha(t)$, where (*) denoted the convolution product

$\phi_\alpha(t) = \dfrac{t^{\alpha-1}}{\Gamma(\alpha)}, t > 0$ and $\phi_\alpha(t) = 0, t \le 0$ and $\phi_\alpha \to \delta(t)$ as $\alpha \to 0$ where $\delta(t)$ is the delta function.

Definition 2.2. The fractional (arbitrary) order derivative of the function f of order $0 \le \alpha < 1$ is defined by

Remark 2.1. From Definition 2.1 and Definition 2.2, we have

$$D^\alpha t^\mu = \frac{\Gamma(\mu+1)}{\Gamma(\mu-\alpha+1)} t^{\mu-\alpha}, \mu > -1; 0 < \alpha < 1$$

and

$$I^\alpha t^\mu = \frac{\Gamma(\mu+1)}{\Gamma(\mu+\alpha+1)} t^{\mu+\alpha}, \mu > -1; \alpha > 0.$$

The goal of this work is to find the exact solution for different kind of fractional differential equations, in terms of H-functions. We consider the non-linear fractional differential equation

$$D_0^\alpha u(t) = f(t, u(t)), \quad (1)$$

where $0 < \alpha < 1$, subject to the initial values

$$[D_0^{\alpha-1} u(t)]_{t=0} = [D_0^{-\beta} u(t)]_{t=0} = [I_0^\beta u(t)]_{t=0} = 0, \ \beta = 1-\alpha. \quad (2)$$

Where $f(t, u(t) : [0,T] \times \mathsf{R} \to \mathsf{R}$ is a continuous function. Also the exact solution for the linear case

$$D^\alpha u(t) - \lambda u(t) = f(t).$$

Furthermore, The multi-term fractional differential equation

$$D^\alpha u(t) = f(t, u, D^{\alpha_1} u(t), ..., D^{\alpha_n} u(t)) \quad (3)$$

subject to the initial condition (2) is solved.

By using Laplace technique where $f : [0,T] \times \mathsf{R}^{n+1} \to \mathsf{R}$ is a continuous function and $0 < \alpha_i < \alpha < 1$ for all $i = 1, ..., n.$ Also, the non-constant coefficients fractional differential equation

$$D^\alpha u(t) - \sum_{i=1}^n g_i(t,u) D^{\alpha_i} u(t) = f(t,u), \quad (4)$$

subject to the initial condition (2) is solved exactly in terms of H-functions. Finally, we find the exact solution for the mixed equation

$$D^\alpha f(x,t) = c \frac{\partial^2 f(x,t)}{\partial x^2} + g(x,t), \quad (5)$$

where c denotes the fractional diffusion constant, with the integral initial condition

$$I^\beta f(x,0) = f_{0,\alpha} \delta(x). \quad (6)$$

For this purpose we need the following concepts.

Definition 2.3 The function $F(s)$ on the complex variable s defined by

$$F(s) = \angle\{f(t); s\} = \int_0^\infty e^{-st} f(t) dt$$

is called the Laplace transform of the function $f(t)$.

Definition 2.4 The Mellin transform of the function $f(t)$ is

$$M\{f(t)\}(s) = \int_0^\infty t^{s-1} f(t) dt.$$

Definition 2.5 By $Fox's\,H-$ functions we mean a generalized hypergeometric function, defined by means of the Mellin-Barnes type contour integral

$$H_{p,q}^{m,n}\left[z \,\middle|\, \begin{matrix} (a_j, A_j)_1^p \\ (b_k, B_k)_1^q \end{matrix} \right] = \frac{1}{2i\pi} \int_{c'} \frac{\prod_{k=1}^m \Gamma(b_k - sB_k) \prod_{j=1}^n \Gamma(1-a_j+sA_j)}{\prod_{k=m+1}^q \Gamma(1-b_k+sB_k) \prod_{j=n+1}^p \Gamma(a_j - sA_j)} z^s ds$$

or

$$H_{p,q}^{m,n}\left[z\,|\,\begin{matrix}(a_j,A_j)_1^p\\(b_k,B_k)_1^q\end{matrix}\right]=\frac{1}{2i\pi}\int_{c'}\frac{\prod_{k=1}^{m}\Gamma(b_k+sB_k)\prod_{j=1}^{n}\Gamma(1-a_j-sA_j)}{\prod_{k=m+1}^{q}\Gamma(1-b_k-sB_k)\prod_{j=n+1}^{p}\Gamma(a_j+sA_j)}z^{-s}ds,$$

$z\neq 0$ where c' is a suitable contour in $\mathbb{C}$, the orders (m,n,p,q) are integers such that $0\le m\le q, 0\le n\le p,$ and the parameters $a_j\in\mathbb{R}, A_j>0, j=1,...,p\; b_k\in\mathbb{R}, B_k>0, k=1,...,q$ are such that $A_j(b_k+l)\neq B_k(a_j-l'-1), l,l'=0,1,2,....$

Definition 2.6 The Fourier transformation for one dimension is defined as

$$F\{f(r)\}(q)=\int_{R^d}e^{iqr}f(r)dr.$$

3. THE EXACT SOLUTION

The Laplace transform of equation (1) yields

$$s^{\alpha}U(s)=F(s,U(s)). \tag{7}$$

To invert the Laplace transform it is convenient use the relation

$$M\{f(t)\}(s)=\frac{M\{\angle\{f(t)\}(u)\}(1-s)}{\Gamma(1-s)} \tag{8}$$

between the Laplace transform and Mellin transform of the function $f(t)$. But

$$\begin{aligned}M\{s^{\alpha}U(s)\}(1-v)&=M\{F(s,U(s))(1-v)\\&=M\{\int_0^{\infty}e^{-st}f(t,u(t))dt\}(1-v)\\&=F(v)G(1-v),\end{aligned}$$

where $F(v)$ is the Mellin transform of the function f and $G(1-v)$ is the Mellin transform of the function $g(st)=e^{-st}$. Hence

$$M\{u(t)\}(v)=\frac{F(v)G(1-v)}{\Gamma(1-v)}.$$

Now inverting Mellin transform and comparing this with the definition of general $H-$ function, allows one to identity the $H-$ function parameters for the first fraction as: $m=0, n=1, q=1, p=1, b_1=0, B_1=1, a_1=A_1=0.$

Then we obtain

$$u(t)=H_{1,1}^{0,1}\left[F(v)G(1-v)t\,|\,\begin{matrix}(0,0)\\(0,1)\end{matrix}\right]. \tag{9}$$

In the same way, we can show that the exact solution for equation (3), takes the form (9). For the equation (4), we have

$$M\{u(t)\}(v)=\frac{F(v)G(1-v)}{\Gamma(1-v)}+[G(1-v)]^2\sum_{i=1}^{n}G_i(v)\times\frac{\Gamma(v+\alpha_i)}{\Gamma(v)\Gamma(1-v)}U(1-v-\alpha_i).$$

The $H-$function parameters for the first term as $m=0, n=p=q=1, a_1=A_1=0, b_1=B_1=0,$ and for the second term as $m=n=p=1, q=2, a_1=A_1=0, b_1=\alpha_i, B_1=B_2=1, b_2=0,$ then we obtain

$$u(t)=H_{1,1}^{0,1}\left[F(v)G(1-v)t\,|\,\begin{matrix}(0,0)\\(0,1)\end{matrix}\right]+\sum_{i=1}^{n}H_{1,2}^{1,1}\left[G_i(v)[G(1-v)]^2U(1-v-\alpha_i)t\,|\,\begin{matrix}(0,0)\\(\alpha_i,1),(0,1)\end{matrix}\right].$$

4. THE MIXED PROBLEM

One of the main applications of the fractional calculus (integration and differentiation of arbitrary order)is the modeling of the processes. In this section, by applying Fourier transform with respect to x and Laplace with respect to t we shall provide the exact solution for the mixed problem (5-6). Fourier and Laplace transformation of equation (5-6) yields

$$f(q,u)=\frac{f_{0,\alpha}}{cq^2+u^{\alpha}}+G(q,u), \tag{10}$$

where q is the Fourier transform parameter and u is the Laplace transform parameter. To obtain $f(x,t)$, first invert the Fourier transform in equation(10) using the formula

$$(2\pi)^{-d/2}\int_{\mathbb{R}^d}e^{iqr}(\frac{|r|}{m})^{1-d/2}K_{(d-2)/2}(m/|r|)dr=\frac{1}{q^2+m^2}$$

where $K_{(d-2)/2}$ is a Bessel function of order $(d-2)/2,$ which leads to:

$$f(x,u)= f_{0,\alpha}(2\pi)^{-d/2}(\frac{|x|}{\sqrt{c}})^{1-(d/2)}u^{\alpha(d-2)/4}$$

$$K_{(d-2)/2}(\frac{|x|}{\sqrt{c}}u^{\alpha/2})+G(x,u).$$

Setting $\lambda=\alpha/2, \nu=(d-2)/2$ and $\mu=\alpha(d-2)/4$ and using the general relation

$$M\{x^a g(yx^b)\}(s)=\frac{1}{b}y^{-(s+a)/b}g(\frac{s+a}{b}),\ y,b>0,$$

implies

$$\mathrm{M}\{f(x,u)\}(s)=\frac{f_{0,\alpha}}{\lambda}(2\pi c)^{-d/2}(\frac{|x|}{\sqrt{c}})^{1-(d/2)-(s+\mu)/\lambda}$$

$$\mathrm{M}\{K_\nu(u)\}((s+\mu)/\lambda)+\mathrm{M}\{G(x,u)\}(s). \qquad (11)$$

The Mellin transform of the Bessel function is

$$M\{K_\nu(u)\}(s)=2^{s-2}\Gamma(\frac{s+\nu}{2})\Gamma(\frac{s-\nu}{2})$$

Substituting this in equation (11), using (8), and restoring the original variables then we have

$$\mathrm{M}\{f(x,t)\}(s)=\frac{f_{0,\alpha}}{\alpha[(|x|)^2\pi]^{d/2}}(\frac{|x|}{2\sqrt{c}})^{2(1-\frac{1+s}{\alpha})}$$

$$\frac{\Gamma(\frac{d}{2}+\frac{1-s}{\alpha}-1)\Gamma(\frac{1-s}{\alpha})}{\Gamma(1-s)}+\frac{G(1-s)}{\Gamma(1-s)},$$

where $G(1-s)$ denotes the Mellin transform of the function $G(x,u)$ Now inverting Mellin transform and comparing this with the general $H-$function allows one to identify the $H-$function parameters as $m=0, n=2, p=2, q=1, A_1=A_2=1/\alpha, a_1=2-\frac{d}{2}-\frac{1}{\alpha}, a_2=1-\frac{1}{\alpha}, b_1=0$, and $B_1=1$, if $\frac{\alpha d}{2}-\alpha+1>0$, for the first term. And for the second term , setting $m=0, n=1, q=1, p=1, b_1=0, B_1=1, a_1=A_1=0$. Then the result becomes

$$f(x,t)=\frac{f_{0,\alpha}}{\alpha[(|x|)^2\pi]^{d/2}}(\frac{|x|}{2\sqrt{c}})^{2(1-1/\alpha)}H^{0,2}_{2,1}$$

$$\left[(\frac{2\sqrt{c}}{|x|})^{2/\alpha}t\,\middle|\,\begin{matrix}((2-\frac{d}{2}-\frac{1}{\alpha}),\frac{1}{\alpha}),((1-\frac{1}{\alpha}),\frac{1}{\alpha})\\(0,1)\end{matrix}\right]$$

$$+H^{0,1}_{1,1}\left[G(1-s)t\,\middle|\,\begin{matrix}(0,0)\\(0,1)\end{matrix}\right].$$

For $g(x,t)\equiv 0$, and $\alpha=1$, equation (5) becomes the classical diffusion equation, and for $\alpha=2$ it becomes the classical wave equation, For $0<\alpha<1$, we have the so-called ultraslow diffusion, and values $1<\alpha<2$ correspond to so-called intermediate processes.

5. ARTIFICIAL NEURAL NETWORK

Neural network (NN) was first introduced by McCulloch and Pitts in 1943, since the introduction it has been widely used in different real world classification tasks in industry, business, and science [12]. Neural network emulates the functionality of human brains in which the neurons (nerves cell) communicate with each other by sending messages among them. Artificial neural network (ANN) represents the mathematical model of these biological neurons. It is a parallel distributed information processing structure consisting of a number of nonlinear processing units, which can be trained to recognize features and to identify incomplete data [13]. Neural network has great mapping capabilities or pattern association thus exhibiting generalization, robustness, high fault tolerance, and high speed parallel information processing.

In this work a standard back-propagation neural network (NN) is used to estimate the exact solution for the following mixed fractional differential equation.

$$D_t^\alpha u+6uu_x+u_{xxx}=0 \qquad t>0 \quad 0<\alpha\leq 1 \qquad (12)$$

subject to the initial condition

$$u(x,0)=\frac{1}{2}sech^2(\frac{1}{2}x)$$

The exact solution, for the special case $\alpha=1$

$$u(x,t)=\frac{1}{2}sech^2(\frac{1}{2}(x-t))$$

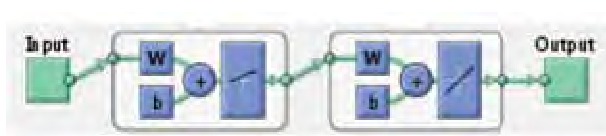

Fig. 1. Neural network structure.

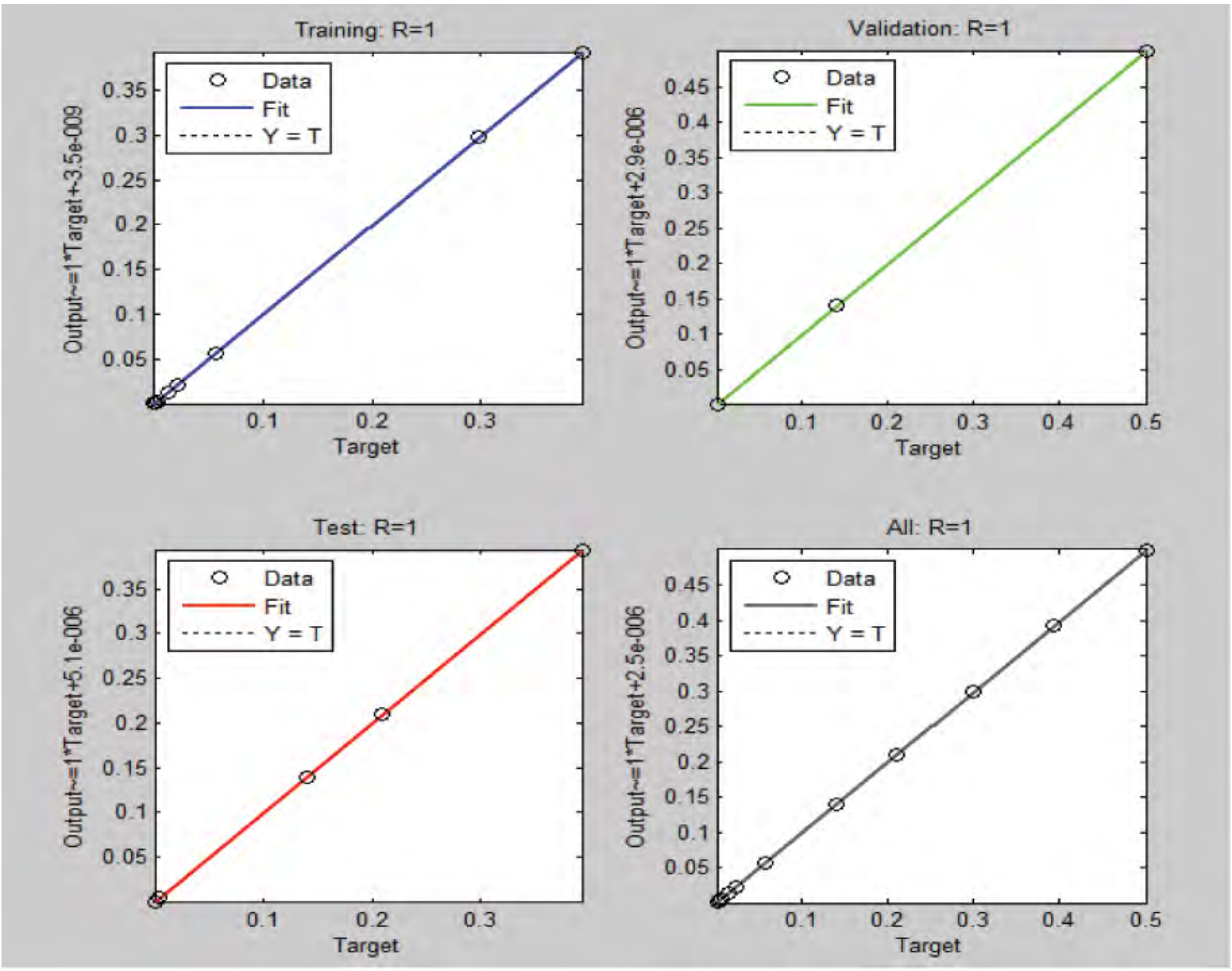

Fig. 2. Regressions analysis for t=0.

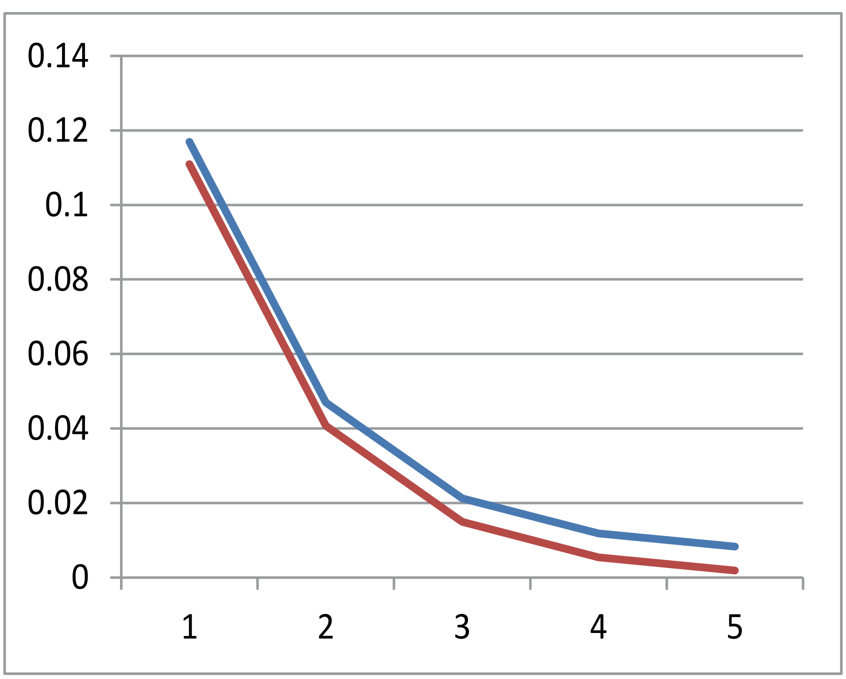

Fig. 3. Neural network estimated exact solution v. the exact solution for t=0.

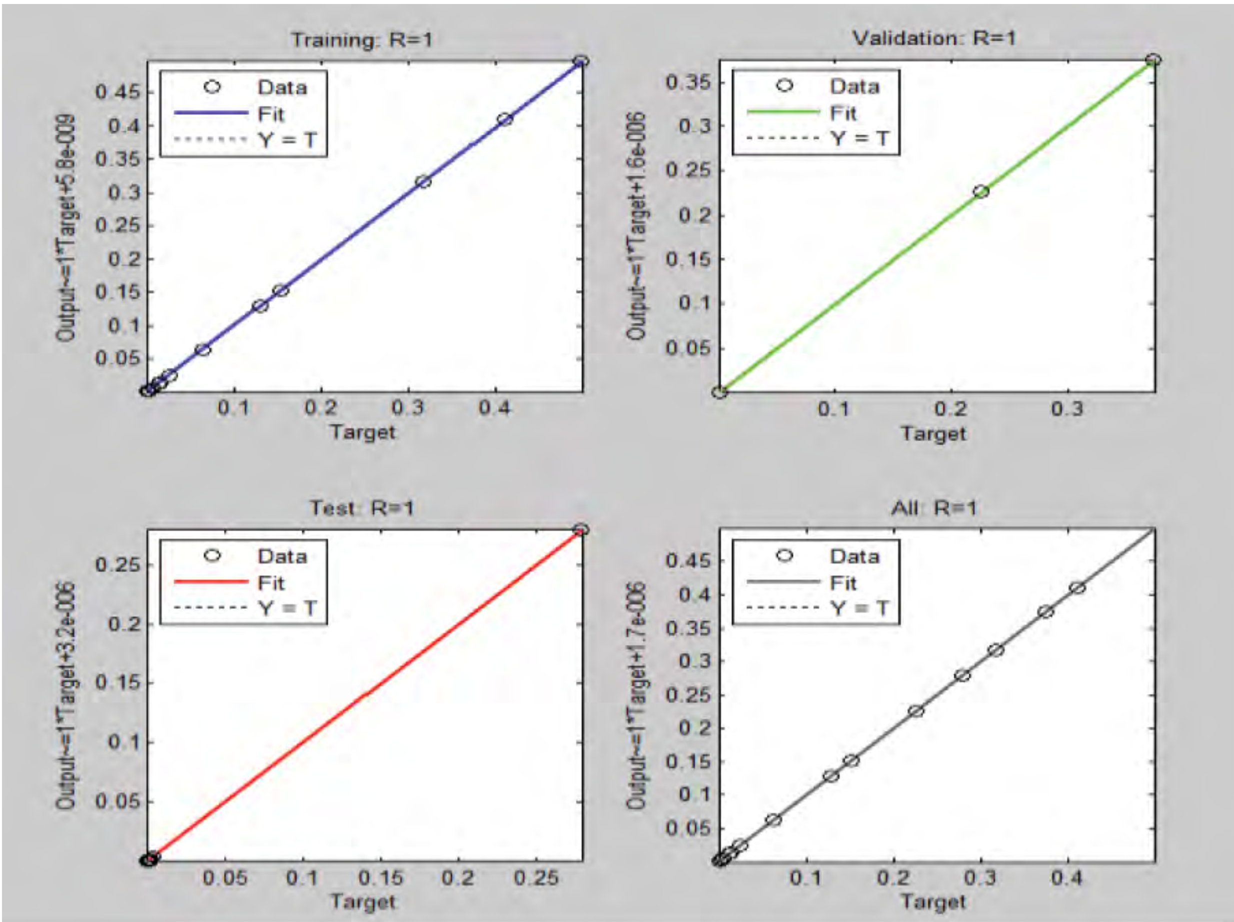

Fig. 4. Regressions analysis for t=0.1.

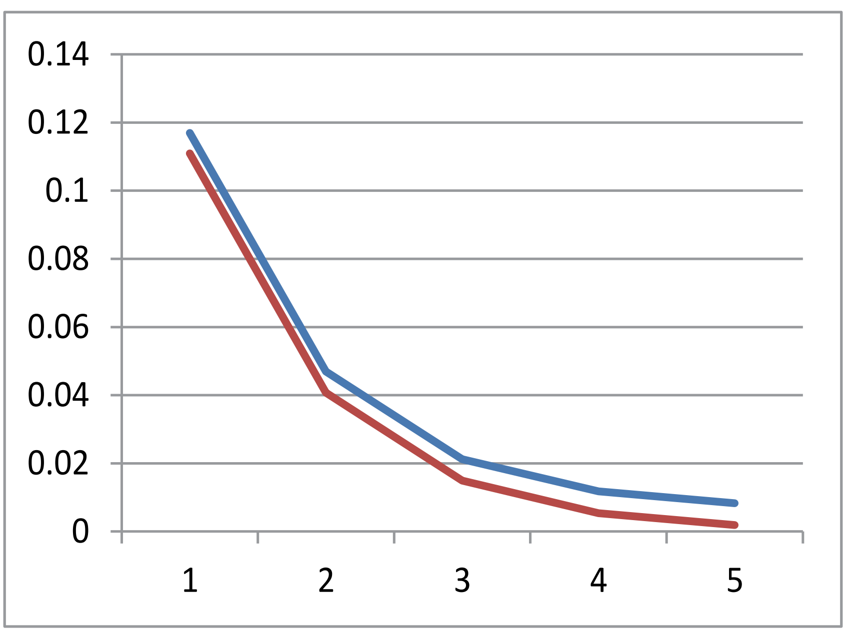

Fig. 5. Neural network estimated exact solution v. th exact solution for t=0.1.

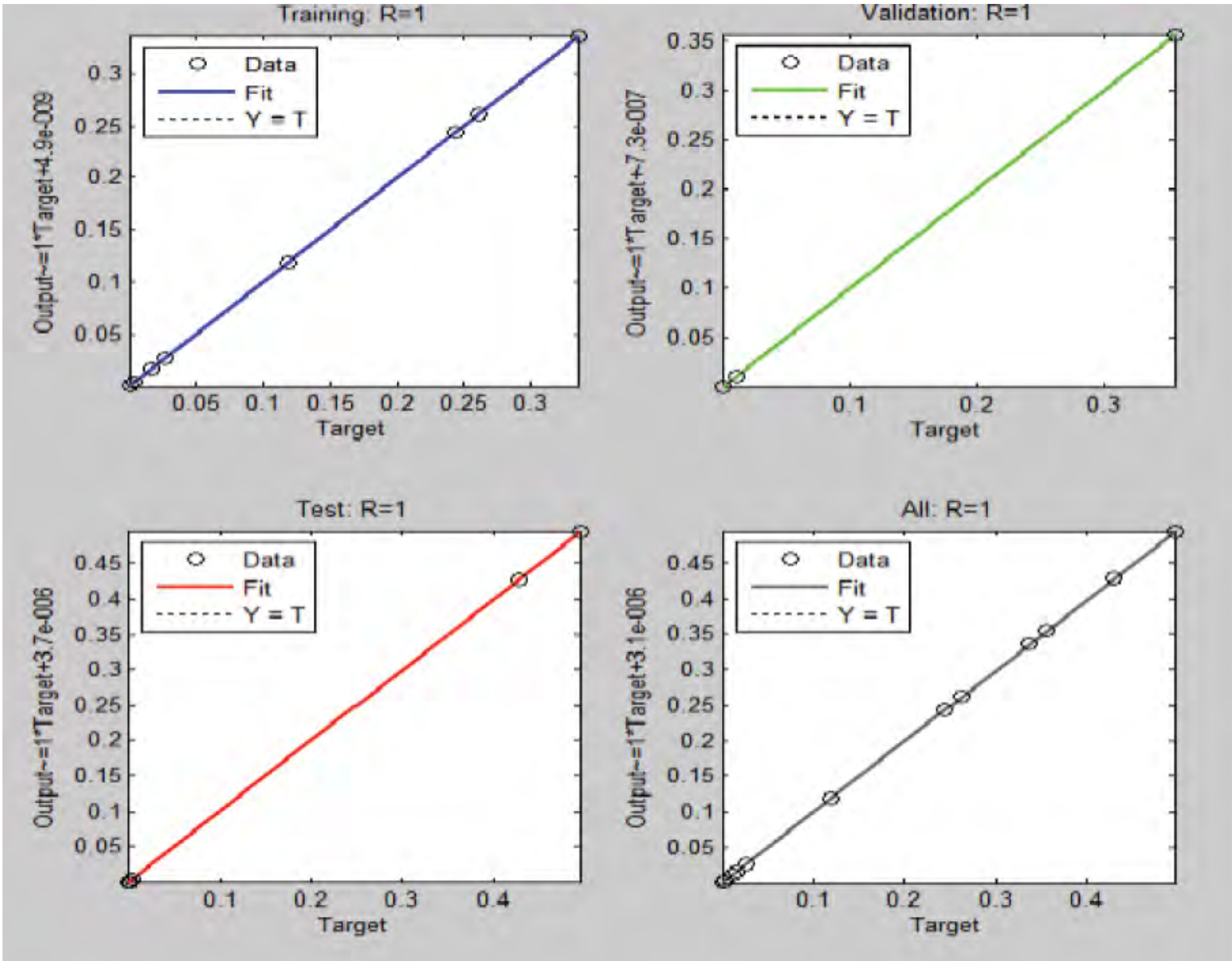

Fig. 6. Regressions analysis for t=0.1.

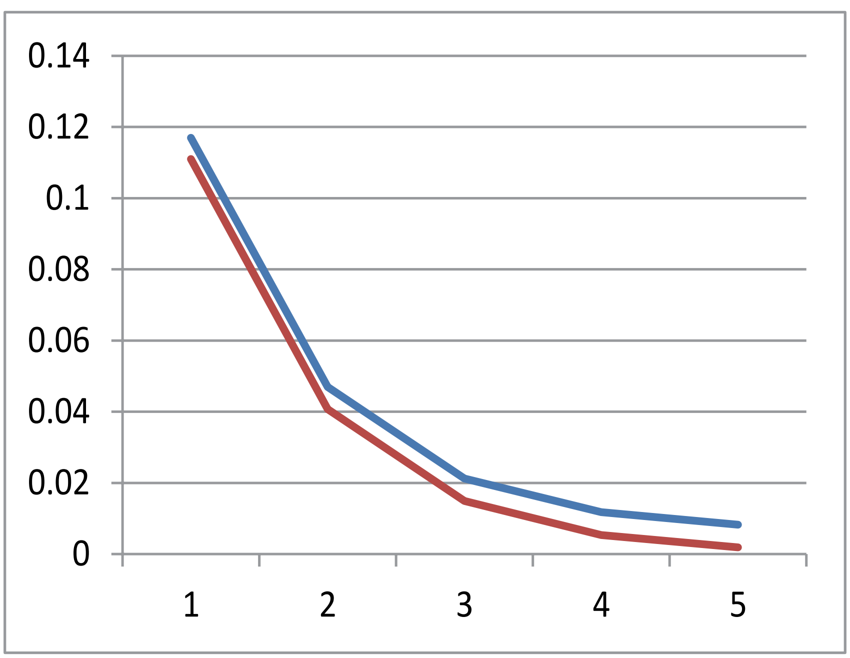

Fig. 7. Neural network estimated exact solution v. the exact solution for t=0.1.

6. TRAINING PHASE

The NN is trained to estimate the exact solution. The dataset contains 105 exact solutions for training, which are solved numerically for three values of *t* (*t*=0, *t*=0.1 and *t*=0.2), using Eq.(12). In the training phase of the NN, the weight matrices among the input and the hidden and output layers are initialized with random values. After repeatedly presenting data of the input samples and desired targets, we have compared the output with the desired outcome, followed by error measurement and weight adjustment. This pattern is repeated until the error rate of the output layer reaches a minimum value. This process is then repeated for the next input value, until all values of the input have been processed. The binary-sigmoid activation function is used. The value of this function ranges between 0 and 1. Whereas, the output layer neuron is estimated using the activation function that features the linear transfer function. The training algorithm used is Gradient descent with momentum back propagation. The exact solution is solved manually by using the giving equation and entered as training input data into the NN. The quality of the training sets that enters into the network determines efficiency of neural network. Fig. 2.4 & 6, show the regressions analysis of the trained network for different values of *t* in Eq. (12). The regressions analysis returns the correlation coefficient R. This coefficient equals to 1 between the output and the target for training; thus, both output and target are very close, which indicates good fit.

7. RESULTS AND DISCUSSION

The experimental results are presented to show the effectiveness of the proposed neural network. The training and testing phases were carried out on a 2.33 GHz Intel (R) Core TM 2Duo CPU 4 GB RAM on Windows 7 platform using MATLAB R2011a. The results of the proposed algorithm in this paper are compared with the exact solution. Fig. 3.5 and 7, show the estimated neural network exact solution (blue line) v. the exact solution (red line) for different values of *t* in Eq. (12). The figures show that for all values of *t* there are almost similar estimated exact solution.

8. CONCLUSIONS

This paper had proved that the fractional differential equations based on Riemann-Liouville fractional derivatives are solved exactly. The solution was obtained in terms of H-functions. The solution was proved to be finite for all times. Moreover, by using the neural network method, the numerical solution for some special equations has been estimated. The experimantal results have proved that for all values of *t* there are almost similar estimated exact solutions. The parallel processing property of trained neural network enabled to recognize features and to identify incomplete data, which resulted in reducing the differences between the estimated and the exact solution.

9. ACKNOWLEDGEMENTS

The authors are thankful to the referees for helpful suggestions for the improvement of this article.

10. REFERENCES

1 Ibrahim, R.W. & H.A. Jalab. Existence solution for fractional integral inclusion. *Miskolc Math. Notes* 11:139-144 (2010) .

2. Ibrahim, R.W. & S. Momani. On the existence and uniqueness of solutions of a class of fractional differential equations. *J. Math. Anal. Appl.* 334 :1-10 (2007).

3. Momani, S.M. & R.W. Ibrahim. On a fractional integral equation of periodic functions involving Weyl-Riesz operator in Banach algebras. *J. Math. Anal. Appl*. 339 :1210-1219 (2008).

4. Ibrahim, R.W. Global controllable for fractional differential equations *Miskolc Math. Notes* 12 :51-60(2011).

5. Ibrahim, R.W. & M. Darus. Subordination and superordination for analytic functions involving fractional integral operator. *Complex Variables and Elliptic Equations*. 53 :1021-1031 (2008) .

6. Ibrahim, R.W. & M. Darus. Subordination and superordination for univalent solutions for fractional differential equations. *J. Math. Anal. Appl.* 345 :871-879 (2008).

7. Ibrahim, R.W. & M. Darus. On analytic functions associated with the Dziok–Srivastava linear operator and Srivastava–Owa fractional integral operator. *Arab J. Sci. Eng.* 36 :441-450 (2011).

8. Ibrahim, R.W. Existence and uniqueness of holomorphic solutions for fractional Cauchy problem. *J. Math. Anal. Appl.* 380 :232-240 (2011).

9. Ibrahim, R.W. On generalized Srivastava-Owa fractional operators in the unit disk. *Advances in Difference Equations* 55 : 1-11 (2011).

10. Podlubny, I. *Fractional Differential Equations*

Academic Press, London (1999).
11. Kilbas, A.A., Srivastava H.M. & J.J. Trujillo. *Theory and Applications of Fractional Differential Equations*. North-Holland, Mathematics Studies. Elsevier (2006).
12. Taqa, A. & H.A. Jalab. Increasing the reliability of skin detectors. *Scientific Research and Essays*17: 2480-2490 (2010).
13. Thamarai, S., H.A. Jalab & A. Taqa. Overview of textual anti-spam filtering techniques. *International Journal of the Physical Sciences* 12 :1869-1882 (2010).

Proceedings of the Pakistan Academy of Sciences 49 (3): 209–218 (2012)

ISSN: 0377 - 2969

Pakistan Academy of Sciences

Original Article

Demographic Dependency of Aging Process in Bangladesh

M. Taj Uddin*, M. Nazrul Islam and Ahmed Kabir

Department of Statistics, Shahjalal University of Science and Technology, Sylhet, Bangladesh

Abstract: The number of old age dependent people is increasing not only in developed countries but also in developing countries. The growth rate of elderly people is higher in rich countries than in poor countries. This study was an attempt to assess the demographic dependency of aging process using census data from Bangladesh Bureau of Statistics during the period of 1951 to 2011. From the analysis, a decreasing trend of young age dependency ratio (DR) as well as an increasing trend of the old age DR was observed. Overall, a downward trend in dependency burden of Bangladesh aging process has also been observed. A variation of DR have been observed in both urban and rural areas of the country. Rural areas hasvemore dependent people than urban areas. Male dependence is higher than their female counterpart. Non-Muslim communities have more old age dependence than Muslim communities. A declining pattern of young: old ratio has also been observed; the ratio is greater in urban areas than in rural areas.

Keywords: Demographic dependency, aging process and young-old ratio

1. INTRODUCTION

The process of ageing of populations is not limited to developed (i.e., high income) countries. The ‘elderly dependency ratio’ to the economically active population is on a steady increase even in under developed and developing countries (i.e., low income countries). However, the present and future elderly dependency ratios in developing countries are quite a bit smaller than those in rich countries.

The impacts of current population trend are reflected in the total dependency ratio (DR) and old age DR. The dependency ratio has a declining trend and the old age dependency has an increasing. These increasing trends of old age DR will have severe socio economic implication for the total population, especially on the elderly population of Bangladesh in the near future [1]. The consequences of unbalanced age structure may create socio-economic problem in the developing countries and thereby the excess of dependent population. This dependent population is measured by the ‘dependency ratio’ [2]. The ‘dependency ratio’ is the proportional relationship between active population and those of children and aged taken together. The relative faster increase in the proportion of the aged population will contribute a higher dependency ratio of population [3]. As fertility levels decline, the dependency ratio falls initially because the proportion of children decreases while the proportion of the population of working age increases. The period when dependency ratio declines is known as the “window of opportunity” because the society possesses a growing number of potential producers relative to the number of consumers.

Aging is the process of growing old. It is a biological process, experienced by the mankind in all times [4]. It generally deals with the age structure of population. It is a continuous, complex, and dynamic process that begins with birth and ends with death. And unless we die in our early years, each of us will grow old and experience the effects of aging process. The overall population begins to age as society moves from a condition of high rates of birth and death, to one of low rates of birth and death. The following pyramids show how emerging the elderly people increased during 1950 to 2050 (Fig. 1, 2).

Received, April 2012; Accepted, September 2012
*Corresponding author: M. Taj Uddin; Email: mtajstat@yahoo.com

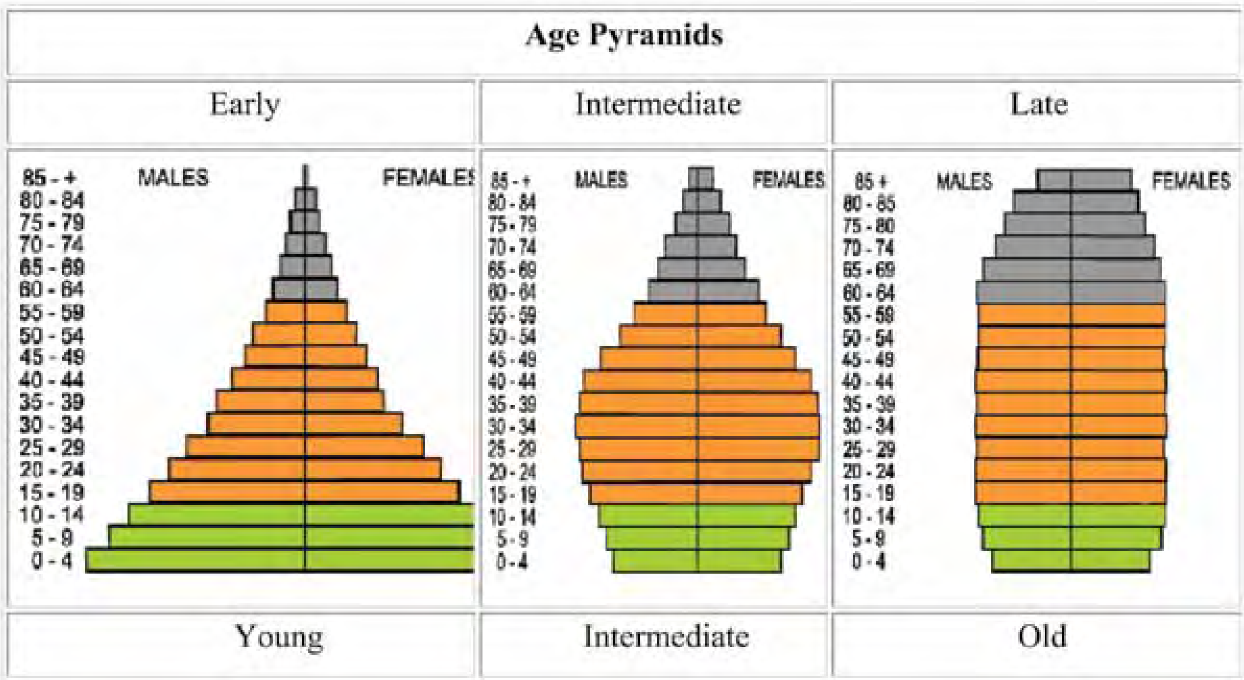

Fig. 1. The generalized age pyramids.

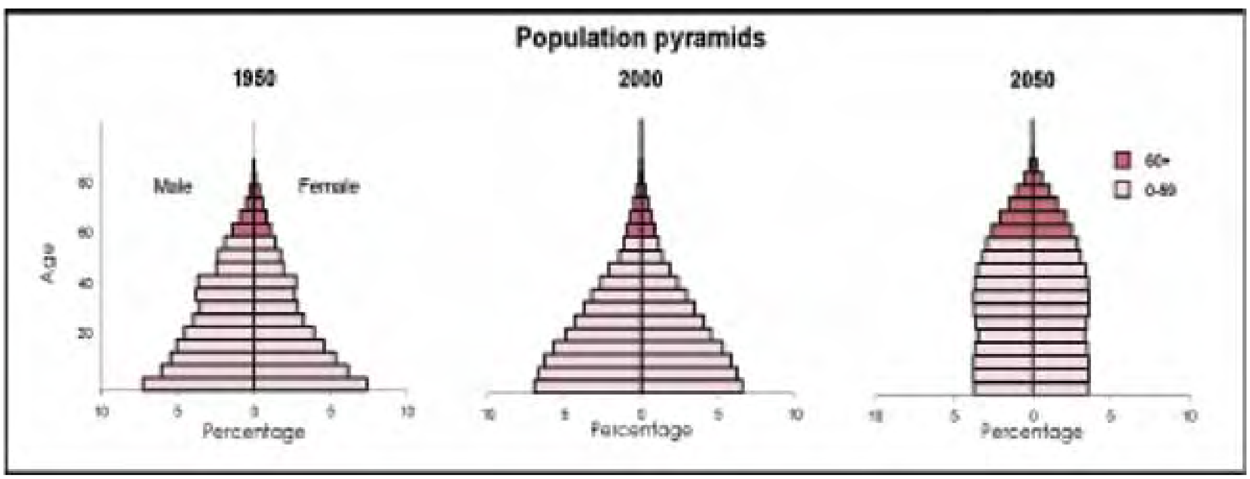

Fig. 2. Age pyramids of Bangladesh.

Source: World Population Ageing [5].

The rapid ageing of population and the growing cohorts of older persons have particular implications for the development of the country indicating increasing economic dependency and rising incidence of care giving to the aged by the traditional social unit, the family [6].

The demographic transition shows a very interesting change in the age composition of the population. These changes can be visualized using ‘age pyramids’.

From the above age pyramids, we observe that nations which are in the middle part of the demographic transition are potentially in a particularly favorable position as regards the economy, because they have a relatively large working age population. This situation however is transitory because this population will change to the type in the right pyramid: a reduced proportion of working age people and an enlarged proportion of elderly people.

Now an economy depends on those people who are in the age group 15–59 and while all members of the population are consumers, children and old people need to be supported by the working age population (economically active population). The base aging (children) and peak aging (old people) is simultaneously termed as 'dependent population' or 'demographic burden' of the aging process. However, it should be remembered that in the agrarian societies children give a lot of help to their parents, and in modern industrialized societies older people may also help the economy by looking after the children or continuing to work.

When the proportion of older persons in the total population increases dramatically in a short period of time, it becomes particularly difficult for the social and economic institutions to adjust. An increasing proportion in the older ages necessarily affects the relative importance of the other segments. These changes in age composition can dramatically affect society's political, economic and social structure [7, 8]. Due to country's poverty and under development scenario with other demographic and socio-cultural changes, the emerging aged population will have severe economic consequences. These economically dependent elderly will become a burden on major portion of the working population [9]. The overall health conditions of the elderly were not good enough. The present state of health is significantly allied with their age, level of education, monthly income and proper sanitation facilities [10]. The elderly population is growing at a considerably faster rate and the life expectancies are increased with the advancement of medical science. The state has not yet develops the mechanisms to respond to the emerging ageing challenge [11]. The government should identify and assess the size of aged people in order to improve their socio economic condition [12]. The exact figure of demographic dependency will help to formulate proper policy and take decision for the government as well as stakeholders of the country. Therefore, comprehensive research is needed to assess the size, nature and overall population aging process of Bangladesh. The present study is an attempt to measure demographic dependency of aging process in Bangladesh.

2. MATERIALS AND METHODS

This paper uses population census data mainly from Bangladesh Bureau of Statistics (BBS), Sample surveys conducted by BBS for several census years, International Data Base (IDB), US Census Bureau and other related information during the period 1951-2011. Young age DR, Old age DR, Total DR and Young-old ratio were computed to asses the trend of demographic dependency for the aging process of Bangladesh. The ratios were also calculated with respect to locality (rural and urban), sex (male and female) and religious communities (i.e., Muslim and non-Muslim) for better understanding of the dependency pattern of the country.

2.1. Young Age Dependency Ratio (YDR)

The ratio between the number of persons of 0 –14 years per 100 persons to the number of persons of 15 –59 years is known as young age DR. If $N_{0-14}(t)$ and $N_{15-59}(t)$ are the number of person age between 0 and 14 and the number of person age between 15 and 59 of a country at time t, then the child DR is defined as:

$$YDR = \frac{N_{0-14}(t)}{N_{15-59}(t)} \times 100 \tag{1}$$

It is also known as youth DR or child DR. It provides a measure of the child population that is dependent on the general working age population. Again, the lower the value, the greater the potential of the community to support the dependent children. It also gives a better sense of the component of the total dependency rate attributable to the child population.

2.2. Old-Age Dependency Ratio (OADR)

The ratio between the number of persons of 60 years and above to the per 100 persons of 15–59 years is known as old age dependency ratio. If $N_{60}(t)$ and $N_{15-59}(t)$ is the number of persons age 60 years and over and the number of person age between 15 and 59 of a country at time t, then the old-age dependency ratio is defined as"

$$OADR = \frac{N_{60}(t)}{N_{15-59}(t)} \times 100 \tag{2}$$

It is an indirect measure of population aging. For convenience, working ages may be assumed to start at age 15. The ratio of the old-age dependent population to the economically active (working) population is also known as elderly dependency ratio, age-dependency ratio or elderly dependency burden and is used to assess intergenerational transfers, taxation policies, and saving behavior [13]. As populations grow older, increases in old-age DR are indicators of the added pressures that social security and public health systems have to withstand.

2.3. Total Dependency Ratio (DR)

The ratio of the number of persons of age between 0 and 14 years plus the number of persons aged 60 and over to the per 100 persons age between 15 and 59 is known as the Total DR. If $N_{0-14}(t)$, $N_{60}(t)$ and $N_{15-59}(t)$ are the number of persons age between 0 and 14,the number of person aged 60 and over and the number of person age between 15 and 59 years in a country at time t, then the total DR is defined as:

$$DR = \frac{N_{15}(t) + N_{60}(t)}{N_{15-59}(t)} \times 100 \qquad (3)$$

i.e., $DR = YDR + OADR$

Thus, total dependency ratio is the sum of young age DR and old-age DR. The lower the percentage, the greater the theoretical potential to support the young and old.

Dependency ratio is a crude measure because a significant number of young person as well as elderly persons are engaged in labour force and not dependent where others portion of working force may not be engaged in labour force at all [14]. The dependency ratio provides at best only a rough approximation of the actual dependency burden in a society [15].

2.4. Young-Old Ratio (YOR)

The ratio of the number of person age between 0 and 14 years to the per 100 persons aged 60 years and over is known as young-old ratio. If $N_{0-14}(t)$, $N_{60}(t)$ are the number of person age between 0 and 14 years and the number of person age 60 and over of a country at time t, then the young-old ratio is defined as

$$YOR = \frac{N_{0-14}(t)}{N_{60}(t)} \times 100 \qquad (4)$$

3. RESULTS AND DISCUSSION

To study the nature and trend of demographic burden of Bangladesh population, various measures of DR have been computed and presented in Table 1-4. Some of the measures have been presented graphically for better understanding of dependent people of aging process in Bangladesh.

3.1. Demographic Dependency of Aging Process

The old age dependency ratio (OADR) shows a very slow increasing trend (Fig. 3). The OADR indicates the burden of elderly people per 100 economically active populations. The ratio was 8 in 1951 and then more or less 11 up to 2001. The child dependency ratio (CDR) shows an increasing trend from 1951 to 1974 and then a decreasing trend from 1981 to 2001 (Fig. 4). The young age dependency ratio (YDR) was 79 in 1951 and 104 in 2001. Like the YDR, the total dependency ratio (DR) shows an increasing trend from 1951 to 1974 and decreasing trend from 1981 to 2001 (Fig.4). The highest DR was 116 in 1974 and the lowest was 83 in 2001 (Table 1). Due to liberation war in 1971, active population may have died or baby boom may have happened. The decreasing trend of DR may be due to population aging at base.). A decreasing trend of the young-old ratio (YOR) has been observed over the study period except in 1991 (Fig. 5). The highest YOR was 950 in 1951 and the lowest was 481 in 2011 (Table 1).

Table 1. Trend of demographic dependency of aging process in Bangladesh**.**

Year	OADR	YDR	DR	YOR
1951	8.288328	78.77706	87.06539	950.4577
1961	10.72049	94.71855	105.439	883.5281
1974	12.27608	104.0093	116.2854	847.2517
1981	11.7869	97.56572	109.3526	827.7472
1991	11.01474	92.07012	103.0849	835.8809
2001	11.23712	72.12484	83.36196	641.8445
2011	12.15949	58.45447	70.61311	480.7311

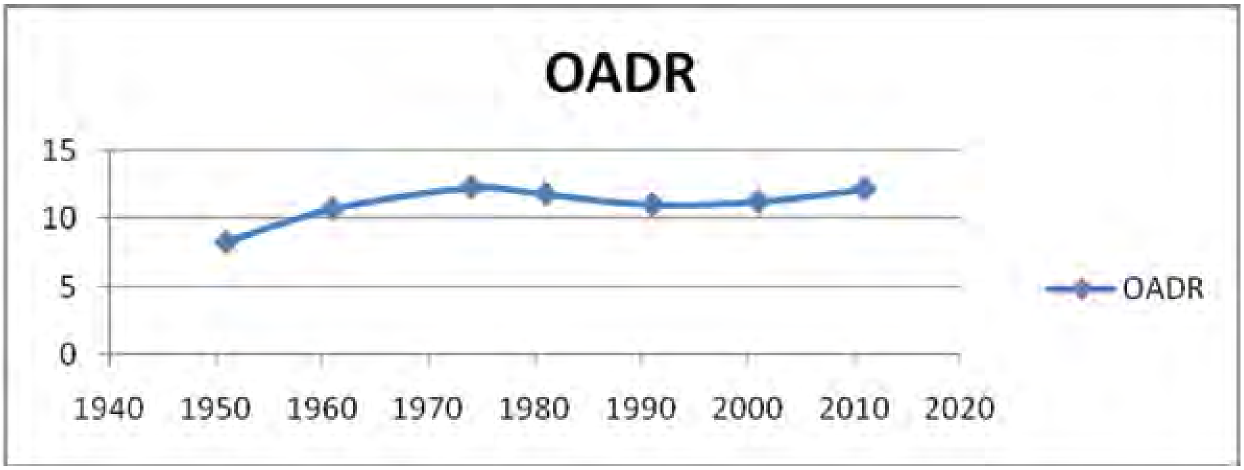

Fig. 3. Trend of OADR.

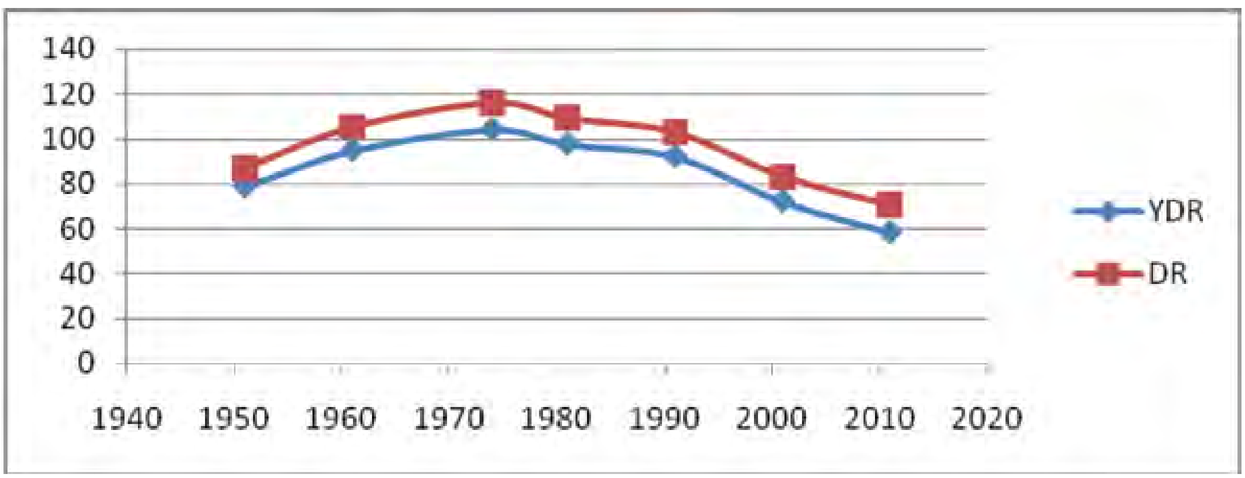

Fig. 4. Trend of YDR and DR.

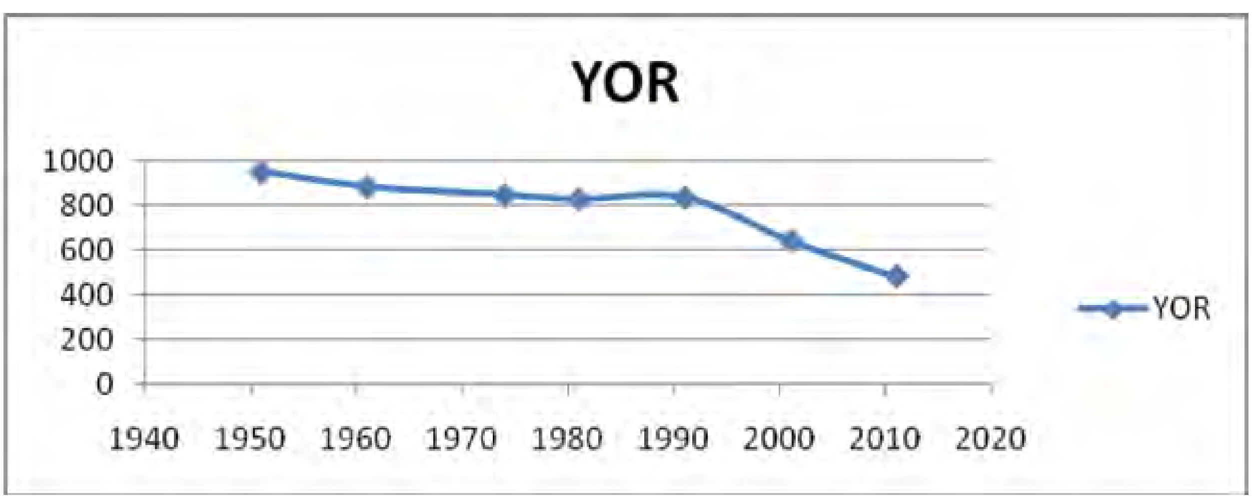

Fig. 5. Trend of young old ratio.

Table 2. Trend of demographic dependency of Bangladesh with respect to locality

Year	Locality	OADR	YDR	DR	YOR
1961	Urban	7.103064	76.81058	83.91365	1081.373
	Rural	10.94333	95.826	106.7693	875.6566
1974	Urban	7.979369	82.34223	90.3216	1031.939
	Rural	12.75166	106.4027	119.1544	834.4228
1981	Urban	9.182372	78.26272	87.44509	852.3148
	Rural	12.31553	101.5047	113.8202	824.2011
1991	Urban	6.883759	73.47073	80.35449	1067.305
	Rural	12.18685	97.34743	109.5343	798.7908
2001	Urban	7.794437	55.90592	63.70035	717.254
	Rural	12.43859	77.7851	90.22369	625.3532

The dependency ratio is likely to remain high till early in this century. This high total dependency has primarily been the result of a high proportion of children in the population and the aged population did not exert any major effect on the same [3].

3.2. Urban-rural Disparity in Dependency Ratio

Various measures of dependency with respect to locality have been presented in Table 2. Rural has more dependent people than urban over the study period according to measure OADR. Though the trend of the OADR is not clear but the urban-rural gap is significant (Fig. 6). A downward trend of the YDR has been observed in urban-rural sub population, except during 1974. Rural has more young dependent than urban (Fig. 7). This is because of higher fertility in rural than in urban areas. Like the YDR, the total dependency ratio (DR) shows a downward trend of urban-rural sub population (Fig. 8). Urban-rural gap of DR is large compared to OADR and YDR. Rural has more dependent people than urban accordingly. A decreasing trend of YOR has been observed for both urban and rural areas of the country except in 1991 (Table 2). The dependency burden is higher in rural areas than in urban areas because of latter's slightly more favourable age structure resulting from urban-rural migration of adult population [3].

3.3. Gender Disparity in Dependency Ratio

There is no specific trend of OADR of male population but shows decreasing trend of OADR of female population except before 1971. Male old age dependent is higher than female old age

Table 3. Trend of demographic dependency of Bangladesh with respect sex**.**

Year	Sex	OADR	YDR	DR	YOR
1951	Male	8.729414	78.29166	87.02108	896.8719
	Female	7.804604	79.30938	87.11398	1016.187
1961	Male	11.40563	94.01263	105.4183	824.2652
	Female	9.983221	95.47819	105.4614	956.3866
1974	Male	13.34342	102.4742	115.8177	767.9756
	Female	11.12091	105.6707	116.7916	950.1983
1981	Male	12.90943	97.87893	110.7884	758.197
	Female	10.60875	97.237	107.8457	916.5738
1991	Male	11.83989	93.9221	105.762	793.2686
	Female	10.16429	90.16133	100.3256	887.0404
2001	Male	12.34669	73.36424	85.71093	594.2015
	Female	10.10699	70.86247	80.96946	701.1236
2011	Male	12.91228	62.75462	75.66690	486.0073
	Female	11.48552	54.60450	66.09002	475.4204

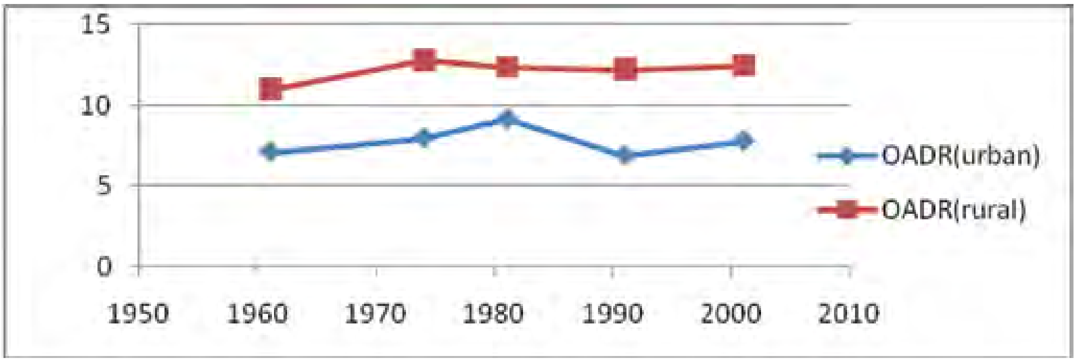

Fig. 6. Trend of OADR with respect to locality.

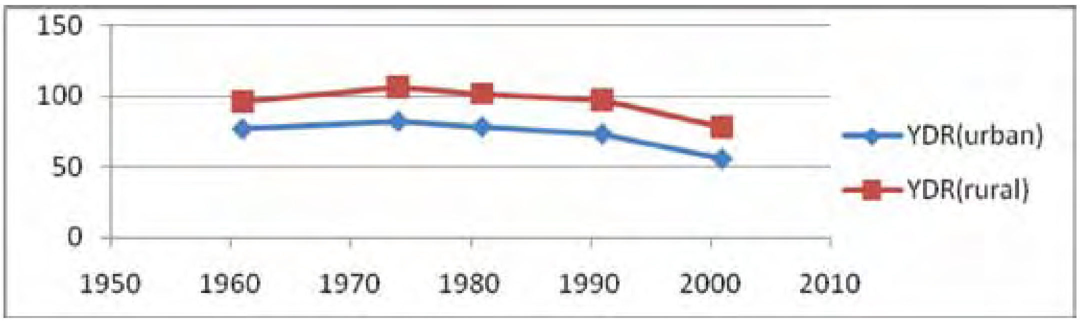

Fig. 7. Trend of YDR with respect to locality.

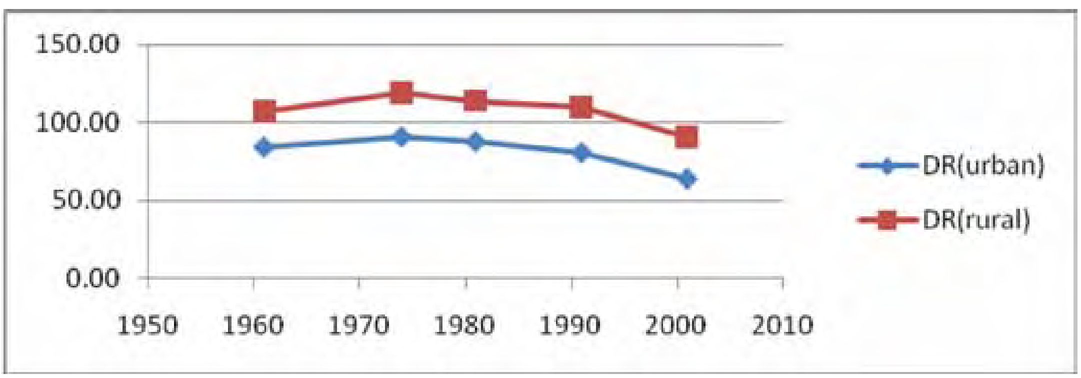

Fig. 8. Trend of DR with respect to locality.

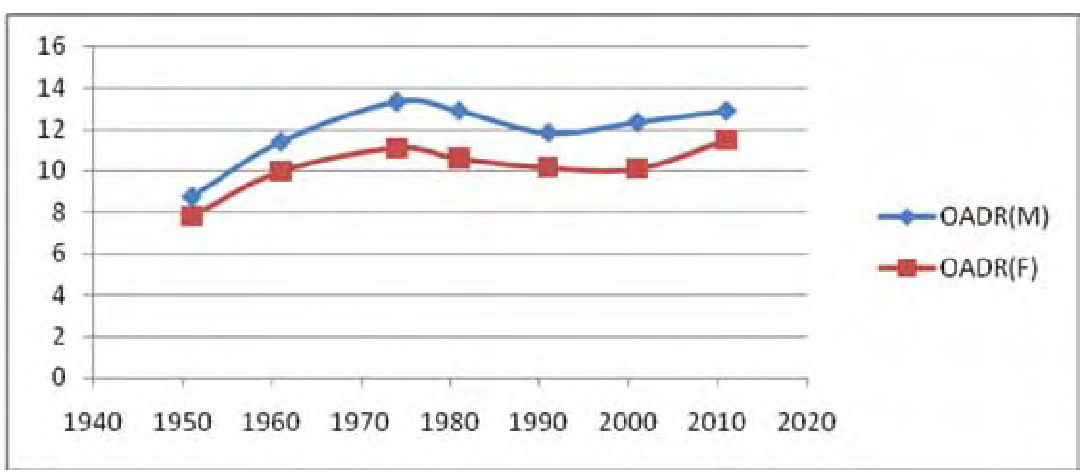

Fig. 9. Trend of OADR with respect to sex.

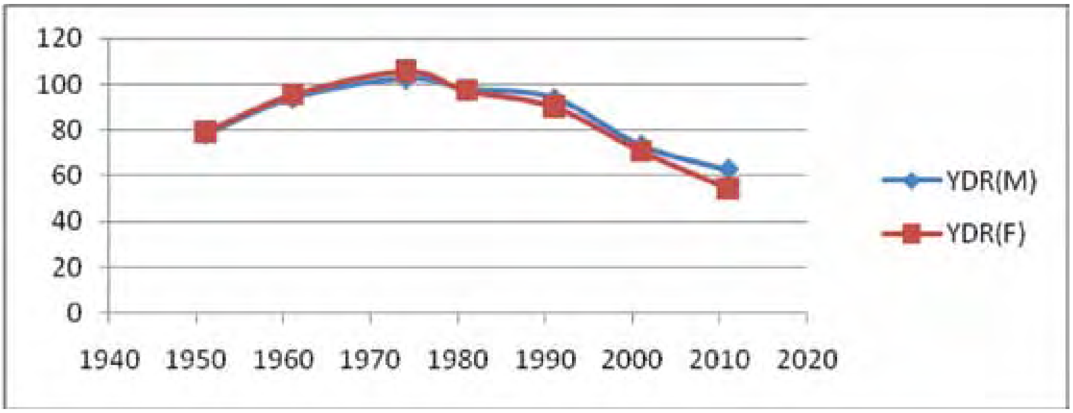

Fig. 10. Trend of YDR with respect to sex.

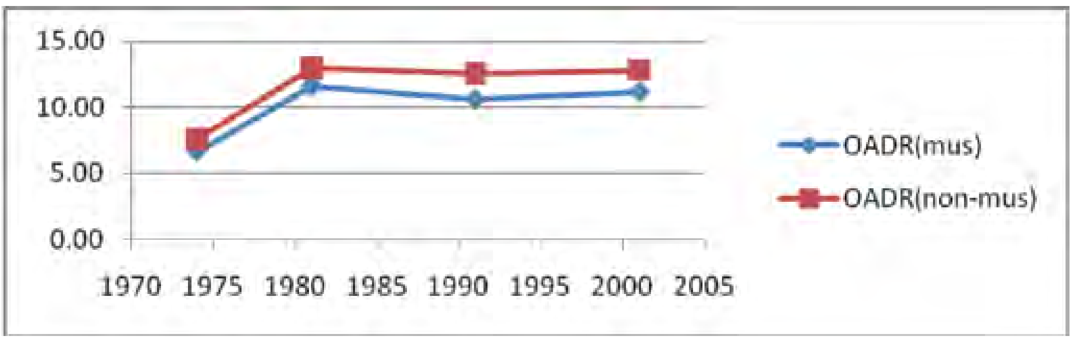

Fig. 11. Trend of OADR with respect to religious community.

dependent over the study period in Bangladesh according to measure OADR (Fig. 9). Thus male elderly needs more support than female. Like OADR, there is also a disparity in the young age dependency ratio (YDR) in male and female sub-population. A decreasing trend of both male and female YDR has been observed except in 1974 (Fig. 10). An increasing trend of total dependency ratio (DR) has been observed for both male and female sub population over the period 1951 to 1974. During this period (1951-1974) female are more dependent than male according to measure DR. On the other hand, a decreasing trend of DR has also been observed over the period 1981 to 2001 (Table 3). During this period (1981-2001), more female involved in working force than male and due to increasing female active population, the female DR is significantly decreased. A decreasing trend of YOR of male and female sub-population has been observed over the study period except in 1991 male population. Considering various measures of dependency, it can be concluded that population aging has no negative impact in Bangladesh, because Bangladesh is gaining demographic dividend from its population aging process.

3.4. Religious Disparity in Dependency Ratio

There may be a variation of demographic dependency in aging process with respect to religious communities (Muslim and non-Muslim). Our study also supports this claim. Various indicators regarding dependency have been presented in Table 4. A mentionable variation due to religious community was found in the OADR. The OADR is higher in non-Muslim community than in Muslim (Fig. 11). The dependency pattern is more or less same except in 1974. A decreasing trend of the YDR for both communities was observed in the country. The young age dependency ratio is higher in Muslim than non-Muslim community (Fig. 12). The total DR shows the similar pattern as that of CDR. The DR is greater in Muslim community than non-Muslim community. A decreasing trend of the YOR was observed for both Muslim and non-Muslim community. The YOR is higher in Muslim than non-Muslim community (Table 4). Therefore,

Table 4. Trend of demographic dependency with respect to religious community.

Year	Religious community	OADR	YDR	DR	YOR
1974	Muslim	6.693677	101.1304	107.824	1510.834
	Non-Muslim	7.61052	87.09196	94.70248	1144.363
1981	Muslim	11.58325	99.73407	111.3173	861.0198
	Non-Muslim	13.00068	84.36864	97.36931	648.9556
1991	Muslim	10.59094	93.07532	103.6663	878.8202
	Non-Muslim	12.56746	79.16731	91.73477	629.9387
2001	Muslim	11.17173	72.97494	84.14666	653.211
	Non-Muslim	12.83712	58.51401	71.35114	455.8187

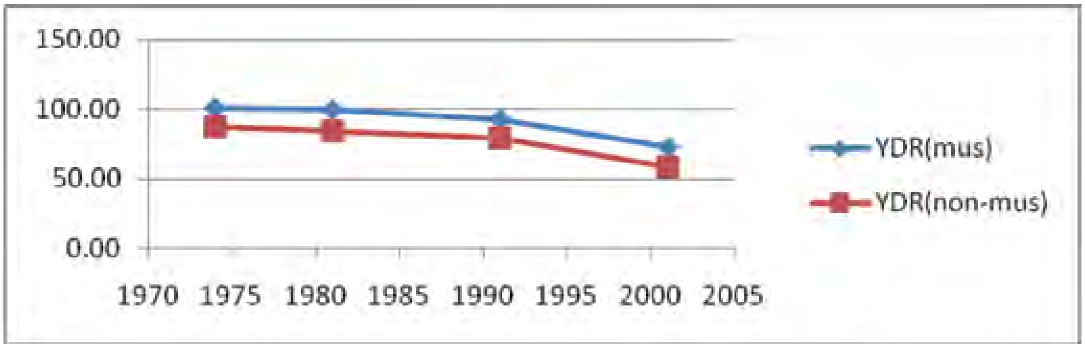

Fig. 12. Trend of YDR with respect to religious community.

from the above analysis, it can be concluded that the population aging has no negative impact on country's economy with respect to religious community.

4. CONCLUSIONS

The DR shows a decreasing trend over the studied time period. The highest dependency ratio was observed in 1974 and the lowest in 2011. This decreasing trend of DR may be due to population aging at the base. But in a developing country, like Bangladesh, many elderly people as well as children support their families. According to the old age dependency ratio, rural areas have more dependent population than urban. Non-Muslim community shows more old age dependent population than Muslim community. Therefore, it is concluded that population aging has a significant impact on demographic dependency. The Bangladesh government should take care of the situation of old age dependent people.

5. REFERENCES

1. Khan, M.M.H. The emerging aging situation in Bangladesh. *Bold* 17(2): 11-20 (2007).
2. Clarke, J. I. *Population Geography*. Pergamum, London (1968).
3. Elahi, K. M. The age structure and the aged population in Bangladesh. p. 165-179. In: *Elderly Contemporary Issues*, M. Kabir (Ed.). Bangladesh Association of Gerontology (BAG), Dhaka, Bangladesh (2003).
4. Goyal, R.S. Implications of demographic and economic transition for elderly: An illustration from India. *International Journal of Anthropology* 15(1-2): 19-34 (2000).
5. Anonymous. *World Population Ageing: 1950-2050*. Population Division, Department of Economic and Social Affairs, United Nations. doi: www.un.org/esa/population/publications/worldageing19502050/
6. Abedin, S. *Social and Health Status of the Aged Population in Bangladesh*, Paper 4. Centre for Policy Dialogue, Dhaka, Bangladesh (1999).
7. Walker, A. The economic burden of ageing and the prospect of intergenerational conflict. *Ageing and Society* 10(4): 337-396 (1990).
8. Jackson, W. A. *Political Economy of Population Ageing*. Edward Elgar Publishing, Cheltenham,

United Kingdom (1998).

9. Kabir, M.H. Local level policy development to deal with the consequences of population aging in Bangladesh. *ESCAP Asian Population Studies Series* No. 131-A (1994).
10. Uddin, M.T., M.A.I. Chowdhury, M.N. Islam, & G.U. Baher. Status of elderly people of Bangladesh: Health perspective. *Proceedings of the Pakistan Academy of Sciences* 47(3): 181-189 (2010).
11. Rahman, M.M., M.I. Tareque, & K.M.M. Rahman. Living arrangements and health status of the rural elderly of Naogaon district, Bangladesh. *Indian Journal of Gerontology* 21(4): 378-393 (2007).
12. Abedin, S. Population aging in Bangladesh: Issues and perspectives. Summary of the country paper. *ESCAP, Asian Population Studies Series* No. 145 (1996).
13. Gavrilov, L.A. & P. Heuveline. Aging of population. In: *The Encyclopedia of Population,* P. Demeny & G. McNicoll (Eds.). Macmillan Reference, New York, USA (2003).
14. Smith, G. P. Legal and health care ethics for the elderly. Chapter 1, In: *Aging as a Phenomenon*. Taylor and Francis, USA (1996).
15. Taeuber, C. M. Sixty-five plus in America, In: *Current Population Reports*: *Special Studies*, p. 3-178. United States Bureau of Census, Washington, DC (1992).

Proceedings of the Pakistan Academy of Sciences 49 (3): 219–225 (2012)

ISSN: 0377 - 2969

Pakistan Academy of Sciences

Original Article

A New Class of Harmonic p-Valent Functions of Complex Order

M. K. Aouf, A. A. Shamandy, A. O. Mostafa[3] and A. K. Wagdy*

Department of Mathematics, Faculty of Science, Mansoura University, Mansoura 35516, Egypt

Abstract: In this paper, we define a class of p-valent harmonic functions and study some results as coefficient inequality, distortion theorem, extreme points, convolution conditions and convex combination.

Keywords and phrases: Harmonic, p-valent, sense-preserving, distortion.

2000 Mathematics Subject Classification: 30C45.

1. INTRODUCTION

A continuous complex-valued function f = u + iv defined in a simply connected complex domain B is said to be harmonic in B if both u and v are real harmonic in B. Let

$f = h + \bar{g}$

be defined in any simply connected domain, where h and g are analytic in B. A necessary and sufficient condition for f to be locally univalent and sense-preserving in B is that

$$|h'(z)| > |g'(z)|, z \in B \text{ (see [2])}. \tag{1.1}$$

Let $H(p)$ denote the class of functions of the form:

$$f = h + g$$

which are harmonic p-valent in the open unit disc U={z : z ∈ ℂ ,|z| < 1}, where

$$h(z) = z^p + \sum_{k=p+1}^{\infty} a_k z^k, \qquad g(z) = \sum_{k=p}^{\infty} b_k z^k$$
$$(|b_p| < 1; p \in N = \{1,2,3,\ldots\}). \tag{1.2}$$

Let $\overline{H}(p)$ denote the class of functions of the form:

$$f = h + \bar{g}, \tag{1.3}$$

Where

$$h(z) = z^p - \sum_{k=p+1}^{\infty} |a_k| z^k, g(z) = \sum_{k=p}^{\infty} |b_k| z^k, |b_p| < 1. \tag{1.4}$$

For $0 < \beta \leq 1, p \in N, b \in \mathbb{C}^* = \mathbb{C}\backslash\{0\}, |b| \leq 1, z' = (\partial/(\partial\theta))(z = re^{i\theta})$, $0 \leq r < 1, 0 \leq \theta < 2\pi$ *and* $f'(z) = \frac{\partial}{\partial\theta}(f(z))$, let $S_H(b,p,\beta)$, let be the class of hamonic functions $f(z)$ of the form (1.2) such that

$$\left|\frac{1}{b}\left[\frac{zf'(z)}{z'f(z)} - p\right]\right| < \beta, \tag{1.5}$$

or, equivalently,

$$\text{Re}\left\{\frac{zf'(z)}{z'f(z)}\right\} > p - \beta|b|. \tag{1.6}$$

Also, let

$\bar{S}_H(b,p,\beta) = S_H(b,p,\beta) \cap \overline{H}(p)$.

We note that:

(i) $\bar{S}_H(p-\alpha,p,1) = TH(p,\alpha)$ (see Ahuja and Jahangiri [1]);

(ii) $\bar{S}_H(b,1,\beta) = \overline{H}S^*(b,\beta)$ (see Janteng [4]);

(iii) $\bar{S}_H(1-\alpha,1,1) = S_H^*(\alpha)$ $(0 \leq \alpha < 1)$ (*see Jahangiri* [3]);

(iv) $\bar{S}_H(1-\alpha,1,1) = S_H^*(0) = T_H^*$(*see Silverman* [5]).

Received, April 2012; Accepted, September 2012
* Corresponding author: A. K. Wagdy; Email: awagdyfos@yahoo.com

Also we note that:

(i) $\bar{S}_H\big((p-\alpha)cos\lambda e^{-i\lambda}, p, 1\big) = \overline{S_H^{\lambda}}(p,\alpha)$

$$= \left\{ f(z) \in \bar{H}(p): \text{Re}\left\{ e^{i\lambda} \frac{zf'(z)}{z'f(z)} \right\} \geq \alpha \cos\lambda \left(0 \leq \alpha < p; |\lambda| < \frac{\pi}{2}\right) \right\};$$

(ii) $\bar{S}_H(1, p, \beta) = \bar{S}_H(p, \beta)$

$$= \left\{ f(z) \in \bar{H}(p): \left| \frac{zf'(z)}{z'f(z)} - p \right| < \beta \right\}.$$

In this paper we introduce a new classes $S_H(b,p,\beta)$ and $\bar{S}_H(b,p,\beta)$. We obtain also the coefficient inequality, distortion theorem, extreme points, convolution conditions and convex combination for functions in the class $\bar{S}_H(b,p,\beta)$.

2. COEFFICIENT ESTIMATE

Unless otherwise mentioned, we assume throughout this paper that $0 < \beta \leq 1, p \in N, b \in \mathbb{C}^*$, $|b| \leq 1, z' = (\partial/(\partial\theta))(z = re^{i\theta})$, $0 \leq r < 1, 0 \leq \theta < 2\pi, f'(z) = (\partial/(\partial\theta))f(z), z \in U$ and $f(z)$ is given by (1.3).

In the following theorem, we obtain the coefficient inequality for functions of the class $S_H(b,p,\beta)$.

Thereom 1. Let $f = h + \bar{g}$, where h and g are given by (1.2). Furthermore, let

$$\sum_{k=p+1}^{\infty} \frac{k-p+\beta|b|}{\beta|b|} |a_k| + \sum_{k=p}^{\infty} \frac{k+p-\beta|b|}{\beta|b|} |b_k| \leq 1, \tag{2.1}$$

then $f(z) \in S_H(b,p,\beta)$.

Proof. We only need to show that if (2.1) holds then the condition (1.6) is satisfied. Since $Re\, w > \delta$ if and only if $|1-\delta+w| > |1+\delta-w|$, it suffices to show that

$$|(1-p+\beta|b|)z'f(z) + zf'(z)| - |(1+p-\beta|b|)z'f(z) - zf'(z)| > 0.$$

Substituting for $z'f(z)$ and $zf'(z)$, we obtain

$$|(1-p+\beta|b|)z'f(z) + zf'(z)| - |(1+p-\beta|b|)z'f(z) - zf'(z)|$$

$$= \left| (1+\beta|b|)z^p + \sum_{k=p+1}^{\infty} (k-p+1+\beta|b|)a_k z^k - \sum_{k=p}^{\infty} (k+p-1-\beta|b|)b_k \bar{z}^k \right|$$

$$- \left| (1-\beta|b|)z^p - \sum_{k=p+1}^{\infty} (k-p-1+\beta|b|)a_k z^k + \sum_{k=p}^{\infty} (k+p+1-\beta|b|)b_k \bar{z}^k \right|$$

$$\geq (1+\beta|b|)|z|^p - \sum_{k=p+1}^{\infty} (k-p+1+\beta|b|)|a_k||z|^k - \sum_{k=p}^{\infty} (k+p-1-\beta|b|)|b_k||z|^k$$

$$-(1-\beta|b|)|z|^p - \sum_{k=p+1}^{\infty} (k-p-1+\beta|b|)|a_k||z|^k - \sum_{k=p}^{\infty} (k+p+1-\beta|b|)|b_k||z|^k$$

$$= 2\beta|b||z|^p - 2\sum_{k=p+1}^{\infty} (k-p+\beta|b|)|a_k||z|^k - 2\sum_{k=p}^{\infty} (k+p-\beta|b|)|b_k||z|^k$$

$$> 2\beta|b| \left\{ 1 - \sum_{k=p+1}^{\infty} \frac{k-p+\beta|b|}{\beta|b|}|a_k| - \sum_{k=p}^{\infty} \frac{k+p-\beta|b|}{\beta|b|}|b_k| \right\}. \tag{2.2}$$

This last expression is non-negative by (2.1), which completes the proof of Theorem 1. The harmonic p-valent function

$$f(z)=z^p+\sum_{k=p+1}^{\infty}\frac{\beta|b|}{k-p+\beta|b|}X_k z^k+\sum_{k=p}^{\infty}\frac{\beta|b|}{k+p-\beta|b|}\overline{Y_k z^k}, \tag{2.3}$$

where $\sum_{k=p+1}^{\infty}|X_k|+\sum_{k=p}^{\infty}|Y_k|=1$, show that the coefficient bound given by (2.1) is sharp. This is because

$$\sum_{k=p+1}^{\infty}\frac{k-p+\beta|b|}{\beta|b|}|a_k|+\sum_{k=p}^{\infty}\frac{k+p-\beta|b|}{\beta|b|}|b_k|$$

$$=\sum_{k=p+1}^{\infty}\frac{k-p+\beta|b|}{\beta|b|}\cdot\frac{\beta|b|}{k-p+\beta|b|}|X_k|$$

$$+\sum_{k=p}^{\infty}\frac{k+p-\beta|b|}{\beta|b|}\cdot\frac{\beta|b|}{k+p-\beta|b|}|Y_k|$$

$$=\sum_{k=p+1}^{\infty}|X_k|+\sum_{k=p}^{\infty}|Y_k|=1.$$

Now, we need to prove that the condition (2.1) is also necessary for functions of the form (1.3) to be in the class $\bar{S}_H(b,p,\beta)$.

Thereom 2. Let $f=h+\bar{g}$, where h and g are given by (1.4). then $f(z)\in\bar{S}_H(b,p,\beta)$ if and only if

$$\sum_{k=p+1}^{\infty}\frac{k-p+\beta|b|}{\beta|b|}|a_k|+\sum_{k=p}^{\infty}\frac{k+p-\beta|b|}{\beta|b|}|b_k|\le 1. \tag{2.4}$$

Proof. Since $\bar{S}_H(b,p,\beta)\subset S_H(b,p,\beta)$, we only need to prove the "only if" part of this theorem. Let $f(z)\in\bar{S}_H(b,p,\beta)$, then

$$\operatorname{Re}\left\{\frac{zf'(z)}{z'f(z)}\right\}>p-\beta|b|,$$

that, is that

$$\operatorname{Re}\left\{\frac{zf'(z)-(p-\beta|b|)z'f(z)}{z'f(z)}\right\}$$
$$=\operatorname{Re}\left\{\frac{\beta|b|z^p-\sum_{k=p+1}^{\infty}(k-p+\beta|b|)a_k z^k-\sum_{k=p}^{\infty}(k+p-\beta|b|)b_k\bar{z}^k}{z^p-\sum_{k=p+1}^{\infty}a_k z^k+\sum_{k=p}^{\infty}b_k\bar{z}^k}\right\}>0. \tag{2.5}$$

By choosing the values of z on the positive real axis where $0\le z=r<1$, we have

$$\frac{\beta|b|-\sum_{k=p+1}^{\infty}(k-p+\beta|b|)a_k-\sum_{k=p}^{\infty}(k+p-\beta|b|)b_k}{z^p-\sum_{k=p+1}^{\infty}a_k+\sum_{k=p}^{\infty}b_k}\ge 0. \tag{2.6}$$

If the condition (2.4) does not hold, then the numerator in (2.6) is negative for $r\to 1$. This contradicts (2.6), then the proof of Theorem 2 is completed.

Putting $p=1$ in Theorem 2, we obtain the following corollary:

Corollary 1. Let $f=h+\bar{g}$, where h and g are given by (1.4). Then $f(z)\in\overline{H}S^*(b,\beta)$ if and only if

$$\sum_{k=2}^{\infty}\frac{k-1+\beta|b|}{\beta|b|}|a_k|+\sum_{k=1}^{\infty}\frac{k+1-\beta|b|}{\beta|b|}|b_k|\le 1. \tag{2.7}$$

Putting $b=(p-\alpha)\cos\lambda e^{-i\lambda}$ $(0\le\alpha<p,|\lambda|<\frac{\pi}{2})$ and $\beta=1$ in Theorem 2, we obtain the following corollary:

Corollary 2. Let $f=h+\bar{g}$, where h and g are given by (1.4). Then $f(z)\in\bar{S}_H^{\lambda}(p,\alpha)$ if and only if

$$\sum_{k=p+1}^{\infty}\frac{k-p+(p-\alpha)\cos\lambda}{(p-\alpha)\cos\lambda}|a_k|+\sum_{k=p}^{\infty}\frac{k+p-(p-\alpha)\cos\lambda}{(p-\alpha)\cos\lambda}|b_k|\le 1. \tag{2.8}$$

3. SOME PROPERTIES FOR THE CLASS $\bar{S}_H(b,p,\beta)$

Distortion bounds for the class $\bar{S}_H(b,p,\beta)$ are given in the following theorem.

Thereom 3. Let the function $f(z)$ given by (1.3) be in the class $\bar{S}_H(b,p,\beta)$. Then for $|z|=r<1$, we have

$$f(z)|\le(1+|b_p|)r^p+\left(\frac{\beta|b|}{1+\beta|b|}-\frac{2p-\beta|b|}{1+\beta|b|}|b_p|\right)r^{p+1} \tag{3.1}$$

and

$$|f(z)|\ge(1-|b_p|)r^p-\left(\frac{\beta|b|}{1+\beta|b|}-\frac{2p-\beta|b|}{1+\beta|b|}|b_p|\right)r^{p+1}. \tag{3.2}$$

The equalities in (3.1) and (3.2) are attained for the functions $f(z)$ given by

$$f(z)=(1+b_p)\bar{z}^p+\left(\frac{\beta|b|}{1+\beta|b|}-\frac{2p-\beta|b|}{1+\beta|b|}b_p\right)\bar{z}^{p+1}$$

and

$$f(z)=(1-b_p)\bar{z}^p-\left(\frac{\beta|b|}{1+\beta|b|}-\frac{2p-\beta|b|}{1+\beta|b|}b_p\right)\bar{z}^{p+1}.$$

Proof. Let $f(z)\in\overline{S}_H(b,p,\beta)$. Then we have

$$|f(z)|\le r^p+\sum_{k=p+1}^{\infty}|a_k|r^k+\sum_{k=p}^{\infty}|b_k|r^k$$

$$\le(1+|b_p|)r^p+r^{p+1}\sum_{k=p+1}^{\infty}(|a_k|+|b_k|)$$

$$=(1+|b_p|)r^p+\frac{\beta|b|}{1+\beta|b|}\sum_{k=p+1}^{\infty}\left(\frac{1+\beta|b|}{\beta|b|}|a_k|+\frac{1+\beta|b|}{\beta|b|}|b_k|\right)r^{p+1}$$

$$\le(1+|b_p|)r^p+\frac{\beta|b|}{1+\beta|b|}\sum_{k=p+1}^{\infty}\left(\frac{k-p+\beta|b|}{\beta|b|}|a_k|+\frac{k+p-\beta|b|}{\beta|b|}|b_k|\right)r^{p+1}$$

$$\le(1+|b_p|)r^p+\frac{\beta|b|}{1+\beta|b|}\left(1-\frac{2p-\beta|b|}{\beta|b|}|b_p|\right)r^{p+1}$$

$$=(1+|b_p|)r^p+\left(\frac{\beta|b|}{1+\beta|b|}-\frac{2p-\beta|b|}{1+\beta|b|}|b_p|\right)r^{p+1}.$$

Similarly, we can prove the left-hand inequality, where

$$|f(z)|\ge r^p-\sum_{k=p+1}^{\infty}|a_k|r^k-\sum_{k=p}^{\infty}|b_k|r^k. \quad (3.3)$$

This completes the proof of Theorem 3.

Putting $p=1$ in Theorem 3, we obtain the following corollary:

Corollary 3. Let the function $f(z)$ given by (1.3) be in the class $\overline{H}S^*(b,\beta)$. Then for $|z|=r<1$, we have

$$|f(z)|\le(1+|b_1|)r+\left(\frac{\beta|b|}{1+\beta|b|}-\frac{2-\beta|b|}{1+\beta|b|}|b_1|\right)r^2 \quad (3.4)$$

and

$$|f(z)|\ge(1-|b_1|)r-\left(\frac{\beta|b|}{1+\beta|b|}-\frac{2-\beta|b|}{1+\beta|b|}|b_1|\right)r^2. \quad (3.5)$$

The equalities in (3.4) and (3.5) are attained for the functions $f(z)$ given by

$$f(z)=(1+b_1)\bar{z}+\left(\frac{\beta|b|}{1+\beta|b|}-\frac{2-\beta|b|}{1+\beta|b|}b_1\right)\bar{z}^2$$

and

$$f(z)=(1-b_1)\bar{z}-\left(\frac{\beta|b|}{1+\beta|b|}-\frac{2-\beta|b|}{1+\beta|b|}b_1\right)\bar{z}^2.$$

Putting $b=(p-\alpha)\cos\lambda e^{-i\lambda}$ $(0\le\alpha<p, |\lambda|<\frac{\pi}{2})$ and $\beta=1$ in Theorem 3, we obtain the following corollary:

Corollary 4. Let the function $f(z)$ given by (1.3) be in the class $S_H^{\lambda}(p,\alpha)$. Then for $|z|=r<1$, we have

$$f(z)|\le(1+|b_p|)r^p+\left(\frac{(p-\alpha)\cos\lambda}{1+(p-\alpha)\cos\lambda}-\frac{2p-(p-\alpha)\cos\lambda}{1+(p-\alpha)\cos\lambda}|b_p|\right)r^{p+1} \quad (3.6)$$

and

$$|f(z)|\ge(1-|b_p|)r^p-\left(\frac{(p-\alpha)\cos\lambda}{1+(p-\alpha)\cos\lambda}-\frac{2p-(p-\alpha)\cos\lambda}{1+(p-\alpha)\cos\lambda}|b_p|\right)r^{p+1}. \quad (3.7)$$

The equalities in (3.6) and (3.7) are attained for the functions$f(z)$ given by

$$f(z)=(1+b_p)\bar{z}^p+\left(\frac{(p-\alpha)\cos\lambda}{1+(p-\alpha)\cos\lambda}-\frac{2p-(p-\alpha)\cos\lambda}{1+(p-\alpha)\cos\lambda}b_p\right)\bar{z}^{p+1}$$

and

$$f(z)=(1-b_p)\bar{z}^p-\left(\frac{(p-\alpha)\cos\lambda}{1+(p-\alpha)\cos\lambda}-\frac{2p-(p-\alpha)\cos\lambda}{1+(p-\alpha)\cos\lambda}b_p\right)\bar{z}^{p+1}.$$

Our next theorem is on the extreme points of convex hulls of the class $\overline{S}_H(b,p,\beta)$ denoted by $clco\,\overline{S}_H(b,p,\beta)$.

Thereom 4. Let $f(z)$ be given by (1.3). Then $f\in\overline{S}_H(b,p,\beta)$ if and only if $f(z)=\sum_{k=p}^{\infty}(X_kh_k+Y_kg_k)$, where

$$h_p(z)=z^p, h_k(z)=z^p-\frac{\beta|b|}{k-p+\beta|b|}z^k\ (k=p+1,p+2,\dots), \quad (3.8)$$

and

$$g_k(z) = z^p + \frac{\beta|b|}{k+p-\beta|b|}\bar{z}^k \ (k = p, p+1, \ldots)$$

$$\left(X_k \geq 0; Y_k \geq 0; \sum_{k=p}^{\infty}(X_k + Y_k) = 1\right). \quad (3.9)$$

Proof. Let

$$f(z) = \sum_{k=p}^{\infty}(X_k h_k + Y_k g_k)$$

$$= \sum_{k=p}^{\infty}(X_k + Y_k)z^p - \sum_{k=p+1}^{\infty}\frac{\beta|b|}{k-p+\beta|b|}X_k z^k$$

$$+ \sum_{k=p}^{\infty}\frac{\beta|b|}{k+p-\beta|b|}\overline{Y_k z^k}$$

$$= z^p - \sum_{k=p+1}^{\infty}\frac{\beta|b|}{k-p+\beta|b|}X_k z^k$$

$$+ \sum_{k=p}^{\infty}\frac{\beta|b|}{k+p-\beta|b|}Y_k \bar{z}^k. \quad (3.10)$$

Using (2.4), we get

$$\sum_{k=p+1}^{\infty}\frac{k-p+\beta|b|}{\beta|b|}|a_k| + \sum_{k=p}^{\infty}\frac{k+p-\beta|b|}{\beta|b|}|b_k|$$

$$= \sum_{k=p+1}^{\infty}\frac{k-p+\beta|b|}{\beta|b|}\cdot\frac{\beta|b|}{k-p+\beta|b|}X_k$$

$$+ \sum_{k=p}^{\infty}\frac{k+p-\beta|b|}{\beta|b|}\cdot\frac{\beta|b|}{k+p-\beta|b|}Y_k$$

$$= \sum_{k=p+1}^{\infty}X_k + \sum_{k=p}^{\infty}Y_k = \sum_{k=p}^{\infty}(X_k + Y_k) - X_p \leq 1,$$

then $f \in \overline{S}_H(b, p, \beta)$.

Conversely, if $f \in \overline{S}_H(b, p, \beta)$, let

$$|a_k| = \frac{\beta|b|}{k-p+\beta|b|}X_k \ (k = p+1, p+2, \ldots) \quad (3.11)$$

and

$$|b_k| = \frac{\beta|b|}{k+p-\beta|b|}Y_k \ (k = p, p+1, \ldots), \quad (3.12)$$

where $\sum_{k=p}^{\infty}(X_k + Y_k) = 1$.. Then, we have

$$f(z) = z^p - \sum_{k=p+1}^{\infty}|a_k| z^k + \sum_{k=p}^{\infty}|b_k| \bar{z}^k;$$

$$= z^p - \sum_{k=p+1}^{\infty}\frac{\beta|b|}{k-p+\beta|b|}X_k z^k + \sum_{k=p}^{\infty}\frac{\beta|b|}{k+p-\beta|b|}Y_k \bar{z}^k$$

$$= z^p + \sum_{k=p+1}^{\infty}(h_k(z) - z^p)X_k + \sum_{k=p}^{\infty}(g_k(z) - z^p)Y_k$$

$$= \sum_{k=p}^{\infty}(X_k h_k + Y_k g_k).$$

This completes the proof of Theorem 4.

Putting $p = 1$ in Theorem 4, we obtain the following corollary:

Corollary 5. Let t $f(z)$ be given by (1.3) with $p = 1$. Then $f \in \overline{\mathrm{H}}\mathrm{S}^*(\mathrm{b}, \beta)$ if and only if $f(z) = \sum_{k=1}^{\infty}(X_k h_k + Y_k g_k)$, where

$$h_1(z) = z, h_k(z) = z - \frac{\beta|b|}{k-1+\beta|b|}z^k \ (k = 2, 3, \ldots), \quad (3.13)$$

and

$$g_k(z) = z + \frac{\beta|b|}{k+1-\beta|b|}\bar{z}^k \ (k = 1, 2, \ldots)$$

$$\left(X_k \geq 0; Y_k \geq 0; \sum_{k=1}^{\infty}(X_k + Y_k) = 1\right). \quad (3.14)$$

Putting $b = (p-\alpha)cos\lambda e^{-i\lambda}$ $(0 \leq \alpha < p, |\lambda| < \frac{\pi}{2})$ and $\beta = 1$ in Theorem 4, we obtain the following corollary:

Corollary 6. Let $f(z)$ be given by (1.3). Then $f \in \overline{S}_H^{\lambda}(p, \alpha)$ if and only if $f(z) = \sum_{k=p}^{\infty}(X_k h_k + Y_k g_k)$, where

$h_p(z) = z^p, h_k(z)$

$$= z^p - \frac{(p-\alpha)\cos\lambda}{k-p+(p-\alpha)\cos\lambda} z^k \ (k = p+1, p+2, \ldots), \quad (3.15)$$

and

$$g_k(z) = z^p + \frac{(p-\alpha)\cos\lambda}{k+p-(p-\alpha)\cos\lambda} \bar{z}^k \ (k = p, p+1, \ldots)$$

$$\left(X_k \geq 0; Y_k \geq 0; \sum_{k=p}^{\infty} (X_k + Y_k) = 1 \right). \quad (3.16)$$

For harmonic functions of the form:

$$f(z) = z^p - \sum_{k=p+1}^{\infty} |a_k| z^k + \sum_{k=p}^{\infty} |b_k| \bar{z}^k \quad (3.17)$$

and

$$F(z) = z^p - \sum_{k=p+1}^{\infty} |A_k| z^k + \sum_{k=p}^{\infty} |B_k| \bar{z}^k, \quad (3.18)$$

we define the convolution of two harmonic functions f and F by

$$(f * F)(z) = z^p - \sum_{k=p+1}^{\infty} |a_k A_k| z^k + \sum_{k=p}^{\infty} |b_k B_k| \bar{z}^k. \quad (3.19)$$

Thereom 5. For $0 < \gamma \leq \beta \leq 1$, let $f \in \overline{S}_H(b,p,\beta)$ and $F \in \overline{S}_H(b,p,\gamma)$. Then $f * F \in \overline{S}_H(b,p,\beta) \subset \overline{S}_H(b,p,\gamma)$.

Proof. Let the convolution $f * F$ be of the form (3.19), then we want to prove that the coefficient of $f * F$ satisfy the condition of Theorem 2. Since $F \in \overline{S}_H(b,p,\gamma)$ we note that $|A_k| \leq 1$ and $|B_k| \leq 1$. Then we have

$$\sum_{k=p+1}^{\infty} \frac{k-p+\gamma|b|}{\gamma|b|} |a_k A_k| + \sum_{k=p}^{\infty} \frac{k+p-\gamma|b|}{\gamma|b|} |b_k B_k|$$

$$\leq \sum_{k=p+1}^{\infty} \frac{k-p+\gamma|b|}{\gamma|b|} |a_k| + \sum_{k=p}^{\infty} \frac{k+p-\gamma|b|}{\gamma|b|} |b_k|$$

$$\leq \sum_{k=p+1}^{\infty} \frac{k-p+\beta|b|}{\beta|b|} |a_k| + \sum_{k=p}^{\infty} \frac{k+p-\beta|b|}{\beta|b|} |b_k| \leq 1,$$

since $0 < \gamma \leq \beta \leq 1$ and $f \in \overline{S}_H(b,p,\beta)$. Therefore $f * F \in \overline{S}_H(b,p,\beta) \subset \overline{S}_H(b,p,\gamma)$, which completes the proof of Theorem 5.

Now we want to prove that the class $\bar{S}_H(b,p,\beta)$ is closed under convex combinations.

Thereom 6. Let $0 \leq c_i \leq 1$ for $i = 1,2,\ldots$ and $\sum_{i=1}^{\infty} c_i = 1$. If the functions $f_i(z)$ defined by

$$f_i(z) = z^p - \sum_{k=p+1}^{\infty} |a_{k,i}| z^k$$

$$+ \sum_{k=p}^{\infty} |b_{k,i}| \bar{z}^k \ (z \in U; i = 1,2,3,\ldots), \quad (3.20)$$

are in the class $\bar{S}_H(b,p,\beta)$ for every $i = 1,2,3,\ldots$, then $\sum_{i=1}^{\infty} c_i f_i(z)$ of the form

$$\sum_{i=1}^{\infty} c_i f_i(z) = z^p - \sum_{k=p+1}^{\infty} \left(\sum_{i=1}^{\infty} c_i |a_{k,i}| \right) z^k$$

$$+ \sum_{k=p}^{\infty} \left(\sum_{i=1}^{\infty} c_i |b_{k,i}| \right) \bar{z}^k \quad (3.21)$$

is in the class $\bar{S}_H(b,p,\beta)$.

Proof. Since $f_i(z) \in \overline{S}_H(b,p,\beta)$, it follows from Theorem 2 that

$$\sum_{k=p+1}^{\infty} \frac{k-p+\beta|b|}{\beta|b|} |a_{k,i}|$$

$$+ \sum_{k=p}^{\infty} \frac{k+p-\beta|b|}{\beta|b|} |b_{k,i}| \leq 1, \quad (3.22)$$

for every $i = 1,2,3,\ldots$. Hence

$$\sum_{k=p+1}^{\infty} \left(\frac{k-p+\beta|b|}{\beta|b|} \sum_{i=1}^{\infty} c_i |a_{k,i}| \right)$$

$$+ \sum_{k=p}^{\infty} \left(\frac{k+p-\beta|b|}{\beta|b|} \sum_{i=1}^{\infty} c_i |b_{k,i}| \right)$$

$$= \sum_{i=1}^{\infty} c_i \left(\sum_{k=p+1}^{\infty} \frac{k-p+\beta|b|}{\beta|b|} |a_{k,i}| \right.$$

$$\left. + \sum_{k=p}^{\infty} \frac{k+p-\beta|b|}{\beta|b|} |b_{k,i}| \right) \leq \sum_{i=1}^{\infty} c_i \leq 1.$$

By Theorem 2, it follows that $\sum_{i=1}^{\infty} c_i f_i(z) \in \bar{S}_H(b,p,\beta)$. This proves that $\bar{S}_H(b,p,\beta)$ is closed under convex combinations.

Remarks. (i) The results in Corollaries 1, 3 and 5, respectively, correct the results obtained by Janteng [4, Theorem 2.1, 2.2 and 2.3, respectively];

(ii) Putting $b = 1$ in the above results, we obtain the corresponding results for the class $\bar{S}_H(p, \beta)$.

4. REFERENCES

1. Ahuja O. P. & J. M. Jahangiri. Multivalent harmonic starlike functions. *Ann. Univ. Mariae Curie-Sklodowska, Sect. A 55* (no. 1): 1-13 (2001).
2. Clunie, J. & T. Shell-Small. Harmonic univalent functions. *Ann. Acad. Sci. Fenn. Ser. A. I. Math*. 9: 3-25 (1984).
3. Jahangiri, J. M. Harmonic functions starlike in the unit disc. *J. Math. Anal. Appl.* 235: 470-477 (1999).
4. Janteng, A. Starlike functions of complex order. *Appl. Math. Sci*. 3 (no. 12): 557-564 (2009).
5. Silverman, H. Harmonic univalent functions with negative coefficients. *J. Math. Anal. Appl*. 220 (no. 1): 283-289 (1998).

Proceedings of the Pakistan Academy of Sciences 49 (3): 227–232 (2012)

ISSN: 0377 - 2969

Pakistan Academy of Sciences

Original Article

Stability for Univalent Solutions of Complex Fractional Differential Equations

Rabha W. Ibrahim*

Institute of Mathematical Sciences
University Malaya, 50603
Kuala Lumpur, Malaysia

Abstract: In this paper, we consider the Hyers-Ulam stability for the following fractional differential equations in sense of Srivastava-Owa fractional operators (derivative and integral) defined in the unit disk:

$$D_z^{\beta} f(z) = G(f(z), D_z^{\alpha} f(z), z), \quad 0 < \alpha < 1 < \beta \leq 2,$$

in a complex Banach space. Furthermore, a generalization of the admissible functions in complex Banach spaces is imposed and applications are illustrated.

Keywords: Analytic function; unit disk; Hyers-Ulam stability; admissible functions; fractional calculus; fractional differential equation; univalent function; convex function.

1. INTRODUCTION

A classical problem in the theory of functional equations is that: If a function f approximately satisfies functional equation E when does there exists an exact solution of E which f approximates. In 1940, S. M. Ulam [1] imposed the question of the stability of Cauchy equation and in 1941, D. H. Hyers solved it [2]. In 1978, Th. M. Rassias [3] provided a generalization of Hyers theorem by proving the existence of unique linear mappings near approximate additive mappings. The problem has been considered for many different types of spaces (see [4-6]). Recently, Li and Hua [7] discussed and proved the Hyers-Ulam stability of spacial type of finite polynomial equation, and Bidkham, Mezerji and Gordji [8] introduced the Hyers-Ulam stability of generalized finite polynomial equation. Finally, M.J. Rassias [9] imposed a Cauchy type additive functional equation and investigated the generalised Hyers-Ulam "product-sum" stability of this equation.

Fractional calculus can be considered as a generalization of classical calculus. Fractional differential equations have many applications in various area not only in mathematics but also in physics, computer sciences, mechanics and others. Stability analysis of the solution for these equations is a main central task in the study of fractional analysis. The authors and researchers investigated the stability for different kind of fractional derivatives such as Caputo derivatives, Miller-Ross sequential derivative and Riemann-Liouville derivative.

In this note, we shall study the stability of complex differential equation in sense of the Srivastava-Owa fractional operators (derivative and integral). The solutions are univalent in the unit disk. Recently, the author suggested and introduced the generalized Ulam stability for various types of fractional differential equations in the complex domain [10-14]. Furthermore, Ulam stability for fractional differential equations can be found in [15-17].

Received, July 2012; Accepted, September 2012
*E-mail: rabhaibrahim@yahoo.com

2. METHODS

Let $U := \{z \in \mathbb{C} : |z| < 1\}$ be the open unit disk in the complex plane $\mathbb{C}$ and $\mathbb{H}$ denote the space of all analytic functions on U. Here we suppose that $\mathbb{H}$ as a topological vector space endowed with the topology of uniform convergence over compact subsets of U. Also for $a \in \mathbb{C}$ and $m \in \mathbb{N}$, let $\mathbb{H}[a,m]$ be the subspace of $\mathbb{H}$ consisting of functions of the form

$$f(z) = a + a_m z^m + a_{m+1} z^{m+1} + \ldots, \quad z \in U.$$

Let $\mathbb{A}$ be the class of functions f, analytic in U and normalized by the conditions $f(0) = f'(0) - 1 = 0$ A function $f \in \mathbb{A}$ is called univalent $(\mathbb{S})$ if it is one-one in U. A function $f \in \mathbb{A}$ is called convex if it satisfies the following inequality

$$\Re\{\frac{zf''(z)}{f'(z)} + 1\} > 0, (z \in U).$$

We denoted this class $\mathbb{C}$.

In [18], Srivastava and Owa, posed definitions for fractional operators (derivative and integral) in the complex z-plane $\mathbb{C}$ as follows:

Definition 2.1. The fractional derivative of order α is defined, for a function $f(z)$ by

$$D_z^\alpha f(z) := \frac{1}{\Gamma(1-\alpha)} \frac{d}{dz} \int_0^z \frac{f(\zeta)}{(z-\zeta)^\alpha} d\zeta,$$

where the function $f(z)$ is analytic in simply-connected region of the complex z-plane $\mathbb{C}$ containing the origin and the multiplicity of $(z-\zeta)^{-\alpha}$ is removed by requiring $log(z-\zeta)$ to be real when $(z-\zeta) > 0$

Definition 2.2 The fractional integral of order $\alpha > 0$ is defined, for a function $f(z)$ by

$$I_z^\alpha f(z) := \frac{1}{\Gamma(\alpha)} \int_0^z f(\zeta)(z-\zeta)^{\alpha-1} d\zeta; \alpha > 0,$$

where the function $f(z)$ is analytic in simply-connected region of the complex z-plane $(\mathbb{C})$ containing the origin and the multiplicity of $(z-\zeta)^{\alpha-1}$ is removed by requiring $log(z-\zeta)$ to be real when $(z-\zeta) > 0$

Remark 2.1

$$D_z^\alpha z^\mu = \frac{\Gamma(\mu+1)}{\Gamma(\mu-\alpha+1)} z^{\mu-\alpha}, \mu > -1$$

and

$$I_z^\alpha z^\mu = \frac{\Gamma(\mu+1)}{\Gamma(\mu+\alpha+1)} z^{\mu+\alpha}, \mu > -1.$$

More details on fractional derivatives and their properties and applications can be found in [19,20].

We next introduce the generalized Hyers-Ulam stability depending on the properties of the fractional operators.

Definition 2.3 Let p be a real number. We say that

$$\sum_{n=0}^{\infty} a_n z^{n+\alpha} = f(z) \qquad (1)$$

has the generalized Hyers-Ulam stability if there exists a constant $K > 0$ with the following property:

for every $\varepsilon > 0, w \in \overline{U} = U \bigcup \partial U$, if

$$|\sum_{n=0}^{\infty} a_n w^{n+\alpha}| \leq \varepsilon(\sum_{n=0}^{\infty} \frac{|a_n|^p}{2^n})$$

then there exists some $z \in \overline{U}$ that satisfies equation (1) such that

$$|z^i - w^i| \leq \varepsilon K,$$

$$(z, w \in \overline{U}, \quad i \in \mathbb{N})$$

In the present paper, we study the generalized Hyers-Ulam stability for holomorphic solutions of the fractional differential equation in complex Banach spaces X and Y

$$D_z^\beta f(z) = G(f(z), D_z^\alpha f(z); z), \quad 0 < \alpha < 1 < \beta \leq 2, \qquad (2)$$

where $G : X^2 \times U \to Y$ and $f : U \to X$ are holomorphic functions such that $f(0) = \Theta$ (Θ is the zero vector in X).

3. RESULTS

In this section we present extensions of the generalized Hyers-Ulam stability to holomorphic vector-valued functions. Let X, Y represent complex Banach space. The class of admissible functions $\mathsf{G}(X,Y)$, consists of those functions $g: X^2 \times U \to Y$ that satisfy the admissibility conditions:

$$\| \; g(r,ks;z) \; \| \geq 1, when \quad \| \; r \; \| = 1, \| \; s \; \| = 1, \tag{3}$$

$(\quad z \in U, k \geq 1)$.

We need the following results:

Lemma 3.1. [21] If $f: D \to X$ is holomorphic, then $\| \; f \; \|$ is a subharmonic of $z \in D \subset \mathsf{C}$. It follows that $\| \; f \; \|$ can have no maximum in D unless $\| \; f \; \|$ is of constant value throughout D.

Lemma 3.2. [22, p. 88] If the function $f(z)$ is in the class S, then

$$| D_z^{\alpha+n} f(z) | \leq \frac{(n+\alpha+|z|)\Gamma(n+\alpha+1)}{(1-|z|)^{n+\alpha+2}},$$

$(z \in U; n \in \mathsf{N}_0 = \mathsf{N} \cup \{0\}; 0 \leq \alpha < 1)$.

Lemma 3.3. [18, p. 225] If the function $f(z)$ is in the class C, then

$$| D_z^{\alpha+n} f(z) | \leq \frac{\Gamma(n+\alpha+1)}{(1-|z|)^{n+\alpha+1}},$$

$(z \in U; n \in \mathsf{N}_0 0 \leq \alpha < 1)$.

Theorem 3.1. Let $G \in \mathsf{G}(X,Y)$ and $f: U \to X$ be a holomorphic vector-valued function defined in the unit disk U, with $f(0) = \Theta$. If $f \in \mathsf{S}$, then

$$\| \; G(f(z), D_z^{\alpha} f(z); z) \; \| < 1 \Rightarrow \| \; f(z) \; \| < 1. \tag{4}$$

Proof. Since $f \in \mathsf{S}$, then from Lemma 3.2, we observe that

$$| D_z^{\alpha} f(z) | \leq \frac{(\alpha+|z|)\Gamma(\alpha+1)}{(1-|z|)^{\alpha+2}}.$$

Assume that f dose not satisfie $\| \; f(z) \; \| < 1$ for $z \in U$. Thus, there exists a point $z_0 \in U$ for which $\| \; f(z_0) \; \| = 1$ According to Lemma 3.1, we have

$$\max_{|z| \leq |z_0|} \| \; f(z) \; \| = \| \; f(z_0) \; \| = 1.$$

and

$$\max_{|z| \leq |z_0|} \| \; f(z) \; \| = \| \; f(z_0) \; \| = 1.$$

Consequently, we obtain

$$\| \; f(z_0) \; \| = \frac{(1-|z|)^{\alpha+2}}{(\alpha+|z|)\Gamma(\alpha+1)} \| \; D_{z_0}^{\alpha} f(z_0) \; \| = 1.$$

We put $k := \frac{(\alpha+|z|)\Gamma(\alpha+1)}{(1-|z|)^{\alpha+2}} \geq 1$, for some $0 < \alpha < 1$ and $z \in U$; hence from equation (3), we deduce

$$\| \; G(f(z_0), D_{z_0}^{\alpha} f(z_0); z_0) \; \| = \| \; G(f(z_0), k[D_{z_0}^{\alpha} f(z_0)/k]; z_0) \; \| \geq 1,$$

which contradicts the hypothesis in (4), we must have $\| \; f \; \| < 1$.

Corollary 3.1. Assume the problem (2). If $G \in \mathsf{G}(X,Y)$ is a holomorphic univalent vector-valued function defined in the unit disk U then

$$\| \; G(f(z), D_z^{\alpha} f(z); z) \; \| < 1 \Rightarrow \| \; I_z^{\beta} G(f(z), D_z^{\alpha} f(z); z) \; \| < 1. \tag{5}$$

Proof. By univalency of G, the fractional differential equation (2) has at least one holomorphic univalent solution f. Thus according to Remark 1.1, the solution $f(z)$ of the problem (2) takes the form

$$f(z) = I_z^{\beta} G(f(z), D_z^{\alpha} f(z); z).$$

Therefore, in virtue of Theorem 3.1, we obtain the assertion (5).

Theorem 3.2. Let $G \in \mathsf{G}(X,Y)$ be holomorphic univalent vector-valued functions defined in the unit disk U then the equation (2) has the generalized Hyers-Ulam stability for $z \to \partial U$.

Proof. Assume that

$$G(z) := \sum_{n=0}^{\infty} \varphi_n z^n, \quad z \in U$$

therefore, by Remark 1.2, we have

$$G(z) := \sum_{n=0}^{\infty} \varphi_n z^n, \quad z \in U$$

Also, $z \to \partial U$ and thus $|z| \to 1$ According to Theorem 3.1, we have

$$\| f(z) \| < 1 = |z|.$$

Let $\varepsilon > 0$ and $w \in \overline{U}$ be such that

$$|\sum_{n=1}^{\infty} a_n w^{n+\beta}| \le \varepsilon (\sum_{n=1}^{\infty} \frac{|a_n|^p}{2^n}).$$

We will show that there exists a constant K independent of ε such that

$$|w^i - u^i| \le \varepsilon K, \quad w \in \overline{U}, u \in U$$

and satisfies (1). We put the function

$$f(w) = \frac{-1}{\lambda a_i} \sum_{n=1, n\neq i}^{\infty} a_n w^{n+\beta}, \qquad (6)$$
$$a_i \neq 0, 0 < \lambda < 1,$$

thus, for $w \in \partial U$, we obtain

$$\begin{aligned} |w^i - u^i| &= |w^i - \lambda f(w) + \lambda f(w) - u^i| \\ &\le |w^i - \lambda f(w)| + \lambda |f(w) - u^i| \\ &< |w^i - \lambda f(w)| + \lambda |w^i - u^i| \\ &= |w^i + \frac{1}{a_i} \sum_{n=1, n\neq i}^{\infty} a_n w^{n+\beta}| + \lambda |w^i - u^i| \\ &= \frac{1}{|a_i|} |\sum_{n=1}^{\infty} a_n w^{n+\beta}| + \lambda |w^i - u^i|. \end{aligned}$$

Without loss of generality, we consider $|a_i| = \max_{n\ge 1}(|a_n|)$ yielding

$$\begin{aligned} |w^i - u^i| &\le \frac{1}{|a_i|(1-\lambda)} |\sum_{n=1}^{\infty} a_n w^{n+\beta}| \\ &\le \frac{\varepsilon}{|a_i|(1-\lambda)} (\sum_{n=0}^{\infty} \frac{|a_n|^p}{2^n}) \\ &\le \frac{\varepsilon |a_i|^{p-1}}{(1-\lambda)} (\sum_{n=0}^{\infty} \frac{1}{2^n}) \\ &\le \frac{2\varepsilon |a_i|^{p-1}}{(1-\lambda)} \\ &:= K\varepsilon. \end{aligned}$$

This completes the proof.

In the same manner of Theorem 3.1, and by using Lemma 3.3, we have the following result:

Theorem 3.3. Let $G \in \mathsf{G}(X, Y)$ and $f : U \to X$ be a holomorphic vector-valued function defined in the unit disk U, with $f(0) = \Theta$. If $f \in \mathsf{C}$, then

$$\| G(f(z), D_z^{\alpha} f(z); z) \| < 1 \Rightarrow \| f(z) \| < 1. \qquad (7)$$

4. APPLICATIONS

In this section, we introduce some applications of functions to achieve the generalized Hyers-Ulam stability.

Example 4.1. Consider the function

$$G : X^2 \times U \to \mathsf{R}$$

by

$$G(r, s; z) = a(\| r \| + \| s \|)^n + b|z|^2, \quad n \in \mathsf{R}_+$$

with $a \ge 0.5$, $b \ge 0$ and $G(\Theta, \Theta, 0) = 0$ Our aim is to employ Theorem 3.1, this holds because

$$\| G(r, ks; z) \| = a(\| r \| + k\| s \|)^n + b|z|^2$$
$$= a(1+k)^n + b|z|^2 \ge 1,$$

when $\| r \| = \| s \| = 1, z \in U$. Thus by Theorem 3.1, yields : If $a \ge 0.5$, $b \ge 0$ and $f : U \to X$ is a holomorphic univalent vector-valued function defined in U, with $f(0) = \Theta$, then

$$a(\| f(z) \| + \| D_z^{\alpha} f(z) \|)^n + b|z|^2 < 1$$
$$\Rightarrow \| f(z) \| < 1.$$

Consequently, $\| I_z^{\alpha} G(f(z), D_z^{\alpha} f(z); z) \| < 1$, thus in view of Theorem 3.2, f has the generalized Hyers-Ulam stability.

Example 4.2. Assume the function $G : X^2 \to X$ by

$$G(r, s; z) = G(r, s) = re^{\| s \|^m - 1}, \quad m \ge 1$$

with $G(\Theta, \Theta) = \Theta$. By applying Theorem 3.1, we need to show that $G \in \mathsf{G}(X, X)$. Since

$$\| G(r, ks) \| = \| re^{\| ks \|^m - 1} \| = e^{k^m - 1} \ge 1,$$

when $\| r \| = \| s \| = 1, z \in U$. Therefore by Theorem 3.1 implies : For $f : U \to X$ is a holomorphic univalent vector-valued function defined in U, with $f(0) = \Theta$, then,

$$\| f(z)e^{\| D_z^\alpha f(z) \|^m - 1} \| < 1 \Rightarrow$$
$$\| f(z) \| < 1$$

Consequently, $\| I_z^\alpha G(f(z), D_z^\alpha f(z); z) \| < 1$; thus in view of Theorem 3.2, f has the generalized Hyers-Ulam stability.

Example 4.3. Let $a, b : U \to \mathbb{C}$ satisfy

$$| a(z) + \mu b(z) | \geq 1,$$

for every $\mu \geq 1$, $\nu > 1$ and $z \in U$. Consider the function $G : X^2 \to Y$ by

$$G(r, s; z) = a(z)r + \mu b(z)s,$$

with $G(\Theta, \Theta) = \Theta$. Now for $\| r \| = \| s \| = 1$, we have

$$\| G(r, \mu s; z) \| = | a(z) + \mu b(z) | \geq 1$$

and thus $G \in \mathcal{G}(X, Y)$. If $f : U \to X$ is a holomorphic univalent vector-valued function defined in U, with $f(0) = \Theta$, then

$$\| a(z) f(z) + b(z) D_z^\alpha f(z) \| < 1$$
$$\Rightarrow \| f(z) \| < 1.$$

According to Theorem 3.2, f has the generalized Hyers-Ulam stability.

Example 4.4. Let $\lambda : U \to \mathbb{C}$ be a function such that

$$\Re\left(\frac{1}{\lambda(z)}\right) > 0,$$

for every $z \in U$. Consider the function $G : X^2 \to Y$ by

$$G(r, s; z) = r + \frac{s}{\lambda(z)},$$

with $G(\Theta, \Theta) = \Theta$. Now for $\| r \| = \| s \| =$ we have

$$\| G(r, ks; z) \| = \left| 1 + \frac{k}{\lambda(z)} \right| \geq 1, \quad k \geq 1$$

and thus $G \in \mathcal{G}(X, Y)$. If $f : U \to X$ is a holomorphic univalent vector-valued function defined in U, with $f(0) = \Theta$, then

$$\left\| f(z) + \frac{D_z^\alpha f(z)}{\lambda(z)} \right\| < 1 \Rightarrow \| f(z) \| < 1.$$

Hence in view of Theorem 3.2, f has the generalized Hyers-Ulam stability.

5. CONCLUSIONS

Ulam stability of fractional differential equation is defined and studied. The applications are imposed by employing the concept of addimisible functions in the unit disk. This class of functions is generalized to include the fractional differential operator in sense of the Srivastaava-Owa operators.

6. ACKNOWLEDGEMENTS

The author is thankful to the referees for helpful suggestions for the improvement of this article.

7. REFERENCES

1. Ulam, S. M. *A Collection of Mathematical Problems.* Interscience Publ., New York (1961).
2. Hyers, D. H. On the stability of linear functional equation. *Proceedings National Academy Sciences* 27: 222-224 (1941).
3. Rassias, Th. M. On the stability of the linear mapping in Banach space. *American Mathematical Society* 72: 297-300 (1978).
4. Hyers, D.H. The stability of homomorphisms and related topics, in Global Analysis-Analysis on Manifolds. *Teubner-Texte Math*. 75: 140-153 (1983).
5. Hyers, D.H. & Th. M. Rassias. Approximate homomorphisms, *Aequationes Mathematics* 44: 125-153 (1992).
6. Hyers, D.H., G.I. Isac & Th. M. Rassias. *Stability of Functional Equations in Several Variables*. Birkhauser, Basel. (1998).
7. Li, Y. & L. Hua. Hyers-Ulam stability of a polynomial equation. *Banach Journal of Mathematical Analysis* 3: 86-90 (2009).
8. Bidkham, M., H.A. Mezerji & M. E. Gordji, Hyers-Ulam stability of polynomial equations. *Abstract and Applied Analysis* 1-7 (2010).
9. Rassias, M.J. Generalised Hyers-Ulam product-sum stability of a Cauchy type additive functional equation. *European Journal of Pure and Appllied Mathathematics* 4: 50-58 (2011).
10. Ibrahim, R.W. On generalized Hyers-Ulam stability of admissible functions. *Abstract and Applied Analysis* 1-10 (2012).
11. Ibrahim, R.W. Generalized Ulam-Hyers stability for fractional differential equations. *International*

Journal of Mathematics 23: 1-9 (2012).

12. Ibrahim, R.W. On stability of a class of fractional differential equations. *Proceedings of the Pakistan Academy of Sciences* 49 (1): 37-41 (2012).
13. Ibrahim, R.W. Ulam stability for fractional differential equation in complex domain. *Abstract and Applied Analysis* 1-8 (2012).
14. Ibrahim, R.W. Ulam-Hyers stability for Cauchy fractional differential equation in the unit disk. *Abstract and Applied Analysis* 1-10 (2012).
15. Wang, J.R., Lv L. & Y. Zhou. Ulam stability and data dependence for fractional differential equations with Caputo derivative. *Electronic Journal of Qualitative Theory of Differential Equations* 63: 1-10 (2011).
16. Wang, J.R. & Y. Zhou. Mittag-Leffler-Ulam stabilities of fractional evolution equations. *Applied Mathematics Letters* 25: 723–728 (2012).
17. Wang, J.R., Dong X. & Y. Zhou. Existence, attractiveness and stability of solutions for quadratic Urysohn fractional integral equations. *Communications in Nonlinear Science and Numerical Simulation* 17: 545–554 (2012).

18 Srivastava, H.M. & S. Owa. *Univalent Functions, Fractional Calculus, and Their Applications.* Halsted Press, John Wiley and Sons, New York (1989).

19. Kilbas, A.A., Srivastava H.M. & J.J. Trujillo. Theory and Applications of Fractional Differential Equations. In: *North-Holland Mathematics Studies*, 204, Elsevier Science B.V, Amsterdam (2006).
20. Sabatier, J., O. P. Agrawal & J.A. Tenreiro Machado. *Advances in Fractional Calculus: Theoretical Developments and Applications in Physics and Engineering.* Springer (2007).
21. Hill, E. & R.S. Phillips. *Functional Analysis and Semi-group. American Mathematical Society* (1957).

22 Owa, S., K. Nishimoto, S.K. Lee & N.E. Cho. A note on certain fractional operator. *Bulletin Calcutta Mathematical Society* 83: 87-90 (1991).

Proceedings of the Pakistan Academy of Sciences

Instructions for Authors

Purpose and Scope: *Proceedings of the Pakistan Academy of Sciences* is official journal of the *Pakistan Academy of Sciences,* published quarterly, in English. It publishes original research papers in *Engineering Sciences & Technology, Life Sciences, Medical Sciences***,** *and Physical Sciences*. State-of-the-art reviews (~ 20 pages, supported by recent references) summarizing R&D in a particular area of science, especially in the context of Pakistan, and suggesting further R&D are also considered for publication. Manuscripts undergo double-blind review. Authors are not required to be Fellows or Members of the *Pakistan Academy of Sciences* or citizens of Pakistan.

Manuscript Format:
Manuscripts, in *Times New Roman*, double-spaced (but single-space the Tables), with line numbering and one-inch margins on all sides on A-4 size paper, should not exceed 20 pages, including Tables, Figures and illustrations. *To conserve space, the Instructions are not double spaced and are in font size 10.*

The manuscripts may contain **Abstract, Keywords, INTRODUCTION, MATERIALS AND METHODS, RESULTS, DISCUSSION (or RESULTS AND DISCUSSION), CONCLUSIONS, ACKNOWLEDGEMENTS and REFERENCES** *and any other information that the author(s) may consider necessary.* The Manuscript sections must be numbered, starting with **1. INTRODUCTION**. The text (in **Font Size 10** for **Abstract, Keywords, ACKNOWLEDGEMENTS and REFERENCES,** and in **Font Size 11 for all other sections)** must be typed in a single column across the paper width; all Tables and Figures must be placed after REFERENCES.

Title Page: Should carry: (a) Concise **Title** of the article **(**in Initial Capital and then lower case letters for each main word; font size 16; **bold**), $\leq$ 160 characters, depicting its contents. Do not use abbreviations or acronyms; (b) Author(s)' first name, middle initial and last name (font size 12, **bold**), and professional affiliation(s) [i.e., each author's Department, Institution, Mailing address and Email; but no position titles]; (c) Indicate the corresponding author with *; (d) **Short running title** of $\leq$ 50 characters (in font size 10).

Second Page should start with **Title** of the Article, followed by entire manuscript.

Headings and Subheadings: All flush left

LEVEL-1: **ALL CAPITAL LETTERS; bold**

Level-2: **Initial Capital and then lower case letters for each main word; bold**

Level-3: Initial Capital and then lower case letters for all words; bold, Italic

Level-4: *Run-in head*; *Italics*, in the normal paragraph position with only an Initial Capital and ending in a colon (i.e., **:**)

Abstract: Must be self-explanatory**,** 200–250 words (in font size 10), stating rationale, objective(s), methodology, main results and conclusions of the study. Abbreviations, if used, must be defined on first mention in the Abstract as well as in the main text. Abstract of review articles may have variable format.

Keywords: Three to eight keywords**,** depicting the article.

INTRODUCTION: Provide a clear and concise statement of the problem, citing relevant recent literature, and objectives of the investigation.

MATERIALS AND METHODS: Provide an adequate account of the procedures or experimental details, including statistical tests (if any), in a concise manner but sufficient enough to replicate the study.

RESULTS: Be clear and concise with the help of appropriate Tables, Figures and other illustrations. Data should not be repeated in Tables and Figures, but must be supported with statistics.

DISCUSSION: Provide interpretation of the RESULTS in the light of previous relevant studies, citing published references.

ACKNOWLEDGEMENTS: In a brief statement, acknowledge financial support and other assistance.

REFERENCES: Cite references in the text (in font size 10) **by number only** in **square brackets**, e.g. "Brown et al [2] reported ..." or "... as previously described [3, 6-8]", and list them in REFERENCES section, in the order of citation in the text, Tables and Figures (not alphabetically). Only published (and accepted for publication) journal articles, books, and book chapters qualify for REFERENCES. List of REFERENCES must be prepared as under:

a. **Journal Articles** *(Name of journals must be stated in full)*

1. Golding, I. Real time kinetics of gene activity in individual bacteria. *Cell* 123**:** 1025–1036 (2005).
2. Bialek, W. & S. Setayeshgar. Cooperative sensitivity and noise in biochemical signaling. *Physical Review Letters* 100**:** 258–263 (2008).
3. Kay, R.R. & C.R.L. Thompson. Forming patterns in development without morphogen gradients: scattered differentiation and sorting out. *Cold Spring Harbor Perspectives in Biology* 1: doi: 10.1101/cshperspect.a001503 (2009).

b. **Books**

4. Luellen, W.R. *Fine-Tuning Your Writing*. Wise Owl Publishing Company, Madison, WI, USA (2001).
5. Alon, U. & D.N. Wegner (Eds.). *An Introduction to Systems Biology: Design Principles of Biological Circuits*. Chapman & Hall/CRC, Boca Raton, FL, USA (2006).

c. **Book Chapters**

6. Sarnthein, M.S. & J.D. Stanford. Basal sauropodomorpha: historical and recent phylogenetic developments. In: *The Northern North Atlantic: A Changing Environment.* Schafer, P.R. & W. Schluter (Eds.), Springer, Berlin, Germany, p. 365–410 (2000).
7. Smolen, J.E. & L.A. Boxer. Functions of Europhiles. In: *Hematology, 4^{th} ed*. Williams, W.J., E. Butler, & M.A. Litchman (Eds.), McGraw Hill, New York, USA, p. 103–101 (1991).

Tables, with concise but comprehensive headings, on separate sheets, must be numbered according to the order of citation (like **Table 1.**, **Table 2.**). Round off data to the nearest three significant digits. Provide essential explanatory footnotes, with superscript letters or symbols keyed to the data. Do not use vertical or horizontal lines, except for separating column heads from the data and at end of the **Table**.

Figures may be printed in two sizes: (i) column width of 8.0 cm; or (ii) entire page width of 16.5 cm; number them as **Fig. 1.**, **Fig. 2.**, … in the order of citation in the text. Captions to Figures must be concise nut self-explanatory. Computer generated, laser printed line drawings are acceptable. Do not use lettering smaller than 9 points or unnecessarily large. **Photographs**, digital or glossy prints, must be of high quality. A scale bar should be provided on all photomicrographs.

Declaration: Provide a declaration that the results are original; the same material is neither 'in press' nor under consideration elsewhere; approval of all authors has been obtained to submit the manuscript; and, in case the article is accepted for publication, its copyright will be assigned to *Pakistan Academy of Sciences*. Authors must obtain permission to reproduce copyrighted material from other sources.

Reviewers: Authors may suggest four prospective reviewers, two Pakistani and two from a scientifically advanced country.

For detailed information, visit **website** of the *Pakistan Academy of Sciences*, i.e., www.paspk.org

Manuscript Submission: Soft copy of the manuscript in **Microsoft (MS) Word** (**pdf** files not acceptable)**,** as Email attachment or on a CD, may be submitted to**:**

Editor-in-Chief
Pakistan Academy of Sciences
3-Constitution Avenue, G-5/2, Islamabad, Pakistan
E-mail: pas.editor@gmail.com
Tel: +92-51-9207140
Website: www.paspk.org

Proceedings

OF THE PAKISTAN ACADEMY OF SCIENCES

C O N T E N T S

Volume 49, No. 3, September 2012 **Page**

Research Articles

Engineering Sciences

Green Processing of Coal to Liquid Fuels: Pakistan's Perspective 165
— *Zeeshan Nawaz, Naveed Ramzan, Saad Nawaz, Shahid Naveed and M. Bilal Khan*

Possibility of Control of Transition of Switching Arc Dc into Glowing 173
— *B. Miedzinski, G. Wisniewski, S.N. Kharin and H. Nouri*

Life Sciences

Taxonomic Study of Some *Cosmarium* Species from North-Eastern Areas of Pakistan 181
— *Waqar-ul-Haq, Zarina Ali, Masud-ul-Hasan and Mustafa Shameel*

A New Chewing Louse (Phthiraptera: Amblycera: Menoponidae) of *Anas platyrhynchos* (L.)
from Karachi, Pakistan, having Parasitic Impact 187
— *Saima Naz and Syed A. Rizvi*

Physical Sciences

Hall Effects on Rayleigh-Stokes Problem for Heated Second Grade Fluid 193
— *Masud Ahmad and Muhammad Yaseen*

Exact and Numerical Solution for Fractional Differential Equation based on Neural Network 199
— *Hamid A. Jalab, Rabha W. Ibrahim, Shayma A. Murad and Samir B. Hadid*

Demographic Dependency of Aging Process in Bangladesh 209
— *M.Taj Uddin, M. Nazrul Islam and Ahmed Kabir*

New Class of Harmonic p-Valent Functions of Complex Order 219
— *M. K. Aouf, A. A. Shamandy, A.O. Mostafa and A. K. Wagdy*

Stability for Univalent Solutions of Complex Fractional Differential Equations 227
— *Rabha W. Ibrahim*

Instructions for Authors
233

PAKISTAN ACADEMY OF SCIENCES, ISLAMABAD, PAKISTAN

HEC Recognized, Category X; PM&DC Recognized